GEOMETRICAL AND GROUP CHARACTERIZATION OF SIC-POVMS ON GENERALIZED BLOCH SPHERE

by
SOLOMON BIRHANU SAMUEL

Submitted to the Graduate School of Natural Sciences and Enigneering
in partial fulfilment of
the requirements for the degree of Doctor of Philosophy

Sabancı University
June 2024

ABSTRACT

GEOMETRICAL AND GROUP CHARACTERIZATION OF SIC-POVMS ON GENERALISED BLOCH SPHERE

SOLOMON BIRHANU SAMUEL

PHYSICS Ph.D DISSERTATION, June 2024

Dissertation Supervisor: Prof. Mehmet Zafer Gedik

Keywords: Gell-Mann matrices, density matrix, Gram matrix, Bloch sphere

The Symmetric Informationally Complete Positive Operator-Valued Measures (SIC-POVMs) are a generalized quantum measurements ideal for quantum state tomography of finite dimensional quantum systems. In n-dimensional complex space, the SIC-POVMs are represented by a set of n^2 normalized vectors satisfying the condition $|\langle\psi_j|\psi_k\rangle|^2 = \frac{1}{n+1}$. In this thesis, we classify SIC-POVMs up to a unitary and anti-unitary equivalence without the restriction of group covariance. First, the general geometric properties of SIC-POVMs on the generalized Bloch sphere is explored. We prove the existence of a simplex implied by the modified version of Kakutani theorem, and we restate the existence of SIC-POVMs as a geometrical problems associated with a special polynomial function. Analysis of the Bloch sphere shows that, solely from geometrical considerations and properties of $SU(n)$ on the Bloch sphere, simplexes satisfying the criteria stated in the modified Kakutani theorem form continuous set of solutions, creating path connected generalized equiangular POVMs. Further classification requires numerical analysis due to the non-linear nature of the problem. For this reason, a numerical method of construction for general SIC-POVMs is generated, which shows that the SIC-POVMs form disjoint islands of Gram matrices each corresponding to a distinct class of SIC-POVM. The islands of Gram matrices are connected though permutation matrices, and have a symmetry group of size $3n^2$. The symmetry group contains order-3 and order-n unitaries for all $O(10^5)$ and $O(10^4)$ solutions constructed in dimensions 4 and 5, respectively. The large number of solutions show that the generating set of the triple products of the SIC-POVMs is unique in dimensions 4 and 5, and that all SIC-POVMs in these dimensions are group covariant.

ÖZET

GENELLEŞTIRILMIŞ BLOCH KÜRESI ÜZERINDE SİTE-PODÖ'LERIN GEOMETRIK VE GRUP KARAKTERIZASYONU

SOLOMON B. SAMUEL

FİZİK DOKTORA TEZİ, HAZİRAN 2024

Tez Danışmanı: Prof. Dr. Mehmet Zafer Gedik

Anahtar Kelimeler: STE-PODÖ, Yoğunluk matrisi, Gram matrisi, Bloch küresi

Simetrik Tam Enformasyonlu Pozitif Operatör Değerli Ölçüm'ler (STE-PODÖ'ler), sonlu boyutlu kuantum sistemlerinin kuantum durum tomografisi için ideal kuantum ölçümleridir. n-boyutlu kompleks uzayda, STE-PODÖ'ler, $|\langle\psi_j|\psi_k\rangle|^2 = \frac{1}{n+1}$ koşulunu sağlayan n^2 birlenmiş normalize vektör kümesi tarafından temsil edilir. Bu tezde, grup kovaryans kısıtlaması olmaksızın, STE-PODÖ'leri üniter ve anti-üniter denklik gözeterek sınıflandırdık. İlk olarak, STE-PODÖ'lerin "genelleştirilmiş" Bloch küresi üzerindeki genel geometrik özeliklerini inceledik. Değiştirilmiş Kakutani teoremini kulanarak bir simpleksin varlığını ispatladık. Ardından, STE-PODÖ'lerin varlıklarını özel bir polinom fonksiyonuyla belirlenen geometrik problemle eşileştirdik. Bloch küresinin incelenmesi, geometrik çıkarımlar ve $SU(n)$ grubunun Bloch küresi üzerindeki özellikleri, göstermektedir ki değiştirilmiş Kakutani teoremini sağlayan bir simpleks vardır ki, genelleştirilmiş eşaçılı PODÖ'ler oluşturan, sürekli bir çözüm verir. Problemin doğrusal olmaması nedeniyle, daha ileri bir sınıflandırma nümerik analiz gerektirir. Bu nedenle, genel STE-PODÖ'leri için bir sayısal çözüm yöntemi oluşturduk. Bu yöntemle STE-PODÖ'lerin, her biri ayrı bir sınıfa ait, ayrık Gram matrisi adaları öluşturduğunu gösterdik. 4 boyutta $O(10^5)$ ve 5 boyutta $O(10^4)$ inşa edilen matrislerin tamamı için simetri gruba mertebe-3 ve mertebe-n üniter matrislerinden oluşur. Yüksek sayıdaki çözümler göstermektedir ki STE-PODÖ'lerin üçlü çarpımlarının üreteç kümeleri 4 ve 5 boyutta tektir ve bu boyutlardaki tüm STE-PODÖ'lerin grup kovaryant oldukları görülmektedir.

ACKNOWLEDGEMENTS

I like to thank my parents, whose unwavering support and guidance have driven me toward higher education throughout my life. Even amid a devastating civil conflict that disrupted their livelihood, they encouraged me to persevere and pursue my dreams. This thesis stands as a testament to their enduring love and determination, their tireless efforts in raising me and my sisters, and the incredible life they've provided for us.

I would also like to thank Professor Durmuş Ali Demir, my thesis jury member, who inspired me throughout my PhD and was an exceptional teacher from whom I learned a great deal. May he rest in peace.

Last but not least, I want to express my deepest gratitude to my supervisor, Professor Zafer Gedik, for his guidance throughout my PhD. He embraced my passion and determination, providing me with all the time and support needed to complete my research to my satisfaction.

Dedicated to my father, Birhanu Samuel, and my mother, Letebrhan Birhane.

TABLE OF CONTENTS

LIST OF TABLES

LIST OF FIGURES

LIST OF ABBREVIATIONS

1. INTRODUCTION

Measurements in quantum mechanics are mathematically represented by a set of positive operators known as the positive operator-valued measures (POVMs). The elements of a POVM E_k satisfy the condition $\sum E_k = \mathbb{I}$. For a density matrix ρ, the corresponding probability that the k^{th} measurement is obtained is given by $Tr(E_k\rho)$. An informationally complete POVM allows us to reconstruct an arbitrary density matrix from the probabilities of the measurement Busch (1991); Nielsen & Chuang (2010); Prugovečki (1977). The most symmetric type of POVM is the Symmetric Informationally Complete POVM, or the SIC-POVM. The Symmetry in its name refers to the property that the all element of the SIC-POVM are equidistant from one another, i.e., $Tr(E_jE_k) = \frac{n\delta_{jk}+1}{n^2(n+1)}$. This property makes the SIC-POVMs ideal for quantum state tomography by minimizing the total number of measurements needed Scott (2006). In addition to tomography SIC-POVMs have applications in Quantum cryptography Durt, Kurtsiefer, Lamas-Linares & Ling (2008) and the foundational study of QBism Fuchs (2010); Fuchs, Hoang & Stacey (2017).

We can perceive the SIC-POVMs as a geometric object to make their structure more intuitive. This involves mapping the set of operators onto the Bloch sphere, which allows us to form a geometric description of the density operators. Through a bit of calculation, one can see that the properties of the SIC-POVMs form a regular simplex on the Bloch sphere. Each vector of the simplex corresponds to a pure or separable density matrix, which becomes very intricate for dimensions greater than 2. The Bloch sphere is generated using the generalizations of the Pauli matrices, known as the Gell-Mann matrices Bertlmann & Krammer (2008). The Gell-Mann matrices are the generators of the special unitary group $SU(n)$, and for dimensions larger than 2, the special orthogonal group $SO(n^2-1)$ is larger than $SU(n)$.

The problem of SIC-POVMs from a purely mathematical motivation has been studied for more than half a century under the study of equiangular vectors, Haantjes (1948); van Lint & Seidel (1966). The maximum number of equiangular complex vectors that can be constructed in an n-dimensional complex projective plane is n^2. Whether this bound can be achieved in all dimensions is still an open problem.

The SIC-POVMs have been constructed in many dimensions using both analytic and numerical methods. The analytic method was first proposed by Zauner in 1999. Zauner showed that a group covariant SIC-POVM can be constructed by using the Weyl-Heisenberg group Zauner (2011) and constructed solutions in dimensions 2-7. In the same work, Zauner conjectured that a fiducial vector exists in all dimensions, where it is an eigenvector of a special matrix known as the Zauner matrix. A few years later, Renes Renes et al. (2004) independently proposed the Weyl-Heisenberg group for construction of a fiducial vector and explored numerical solutions and computed the complete list of Weyl-Heisenberg group covariant SIC-POVMs in dimensions ≤ 7. Through further researches on the extended Clifford group, Appleby Appleby, Flammia & Fuchs (2011); Appleby (2005) and Zhu Zhu (2010) showed more symmetries of fiducial vectors which simplified the search further.

To explore Zauner's conjecture in the most general form, we start by asking the following question. Are there SIC-POVMs that are not group covariant to the Weyl-Heisenberg group? This question is answered for dimensions 2 and 3. In dimension 2, the proof is trivial since $SU(2)/\{\pm\mathbb{I}\} \cong SO(3)$, i.e., for every unitary matrix in $SU(2)$, we can write a rotation matrix on the Bloch sphere.In dimension 3, a proof was given by Hughston Hughston & Salamon (2016). In these dimensions, all SIC-POVMs are unitarily equivalent to a Weyl-Heisenberg covariant SIC-POVM. The only dimension where we know solutions not covariant to the Weyl-Heisenberg group is dimension 8, where we have the Hoggar solutions. The Hoggar SICs are generated using the Hadamard matrix, Hoggar (1981). The question can be answered by classifying all unitarily and anti-unitarily equivalent SIC-POVMs. In general, the equivalence classes can be identified through the symmetries of the Bloch sphere. We explore the geometry of the Bloch sphere in detail and prove fundamental geometric properties associated with the SIC-POVMs.

Further classification of the symmetry of the Bloch sphere requires numerical analysis because the characteristic equations defining the problem are non-linear. To generate a numerical method of constructing general SIC-POVMs, we use the concept of frames. The term frame is most commonly used in mathematics and signal processing. By definition, the SIC-POVMs form tight frames. Tight frames in general are best described using their Gram matrices Waldron (2018). For a SIC-POVM, the Gram matrix is formed from the inner products of the vector elements of the SIC-POVM. The Gram matrix allows for the representation of SIC-POVMs up to a unitary equivalence, making it ideal for the study of general solutions. The Gram matrix of SIC-POVMs is a projective matrix having a trace value of n. We use this property to generate Gram matrices of SIC-POVM without the restriction of group covariance. By not considering the Weyl-Heisenberg group covariance, the

number of free parameters becomes of the order of n^4 which is much larger compared to the Welch bound, but it converges to a solution faster in dimensions 4-7.

We derive two functions of the Gram matrix with which we will construct numerical SIC-POVM Gram matrices. In order to characterize the different solutions, we explore symmetries in the functions both analytically and numerically. Analytically, we describe the two trivial symmetries of the equations. Numerically, we show that the functions only have no symmetry other than the trivial symmetries. The functions allow us to treat the SIC-POVM Gram matrices as intersections of two surfaces. We use these to show that SIC-POVMs exist on critical points of both functions and by using the Hessian matrix of the functions, show that all generated solutions are isolated in dimensions 4-7, in agreement with Bruzda, Goyeneche & Życzkowski (2017). Lastly, we characterize the Gram matrices using the generating set (see 4.1) associated with the Gram matrix and present the unique generating sets found in dimensions 4 and 5. In dimensions 6 and 7, the number of numerical solutions we generate is not large enough to make the same claim as the former, but the results in these dimensions share properties with the SICs in dimensions 4 and 5.

Before proceeding with the more involved calculations, we will provide an overview of quantum measurements and the generalized Bloch sphere. Subsequently, we will establish general properties of equiangular vectors on the Bloch sphere and formulate the problem of constructing equivalent classes. To facilitate numerical analysis, it is vital to present known solutions and their properties along with numerical methods used in the construction of group covariant SIC-POVMs. Chapter 3 is dedicated to illustrating Zauner's conjecture and order-3 symmetry of the fiducial vector. In the last chapter, we introduce an alternative method of numerical construction. We examine general solutions in dimensions 4-7 and supply all necessary derivations.

2. Geometrical Properties of SIC-POVMs

An isolated quantum mechanical system is described by using a wave function, which is a complex vector in the Hilbert space. Physically, the wave function of a system gives us information about the statistics of measured values, i.e., $|\psi|^2 \propto$ Probability. In practical scenarios, however, making a completely isolated system is impossible, and all systems we wish to study are subsystems of a much larger quantum system that includes the environment. Such systems cannot be described using a complex vector; instead, we describe the system using the density matrix. Another case where the vector description of a quantum mechanical system fails is when we want to describe an ensemble of quantum systems. In such a case, the correct predication of measurements is achieved by using the density operator. For a discrete system, the density operator is given as follows:

$$\hat{\rho} = \sum_{jk} \rho_{jk} |\phi_j\rangle\langle\phi_k|. \tag{2.1}$$

where $|\phi_k\rangle$ are orthogonal basis vectors. The density operator of an ensemble of states is simply the sum of the density operators of every individual elements.

$$\hat{\rho} = \sum_{n} p_n \hat{\rho}_n \tag{2.2}$$

where p_n is the statistical probability of finding the n-th state in the ensemble.

By definition, the density operator is a Hermitian operator, meaning all its eigenvalues are real. This follows from the fact that the coefficients p_n are real and $\hat{\rho}_n$'s are pure states, i.e., $\hat{\rho}_n = |\psi_n\rangle\langle\psi_n|$. We can then show that the trace of a density matrix is one.

$$Tr(\hat{\rho}) = \sum_k p_k Tr(|\phi_k\rangle\langle\phi_k|) = \sum_k p_k = 1 \tag{2.3}$$

The density matrix may also be written using the wave function $\psi_k(x)$ as $\rho(x,x') = \sum_k p_k \psi_k^*(x')\psi_k(x)$. Trace of the operator corresponds to integrating $\rho(x,x)$ over all values of x, which gives us unity.

For a pure state, the density matrix is pure, i.e., $|\psi\rangle\langle\psi|$ for some state ψ. Thus, the density operator of a pure state is a rank one projector, $\rho^2 = \rho$. To identify the density operator of a pure state, we can simply check the trace since $Tr(\hat{\rho}^2) = 1$ if and only if $\hat{\rho}$ is pure (Nielsen & Chuang (2010); Sakurai & Commins (1995)).

A density matrix, being the most general description of a quantum system, requires a number of linearly independent measurements to be constructed. For a finite quantum systems, the number of measurements needed for a complete characterization of the system is determined by the number of free parameters of the density operator. The density matrix for an n-dimensional system has n^2 entries, but since the matrix is symmetric all diagonal entries are real and only half of the off-diagonal terms are free. Thus, in total, a finite quantum system requires $n^2 - 1$ linearly independent measurements for a complete state tomography.

Now that we have introduced the general properties of the density operator, we are ready to represent the free variables in a geometrically intuitive form by mapping the operators onto the Bloch sphere.

2.1 Generalized Bloch Sphere

The Bloch sphere is a representation of a 2-dimensional density operators in a 3-dimensional real space (Bertlmann & Krammer (2008); Bloch (1946)). The Bloch sphere was first used to visualize the polarization of electromagnetic waves, where it was referred to as the Poincare sphere. The Bloch sphere representation of quantum state is generated by using the Pauli matrices $\sigma_x, \sigma_y, \sigma_z$ and the identity matrix $\mathbb{I}$ (2.4). In the Bloch sphere, the pure state density operators are mapped to the surface of the sphere and the all mixed state density matrices are mapped to the interior volume of the sphere.

$$\hat{\rho} = \frac{1}{2}\mathbb{I} + a_x\sigma_x + a_y\sigma_y + a_z\sigma_z \tag{2.4}$$

where $a_k = Tr(\sigma_k\hat{\rho}) : k \in (x, y, z)$, and the Pauli matrices are the following 2×2 trace-less matrices.

$$\sigma_x = \begin{pmatrix} 0 & 1 \\ 1 & 0 \end{pmatrix}, \sigma_y = \begin{pmatrix} 0 & -i \\ i & 0 \end{pmatrix}, \sigma_z = \begin{pmatrix} 1 & 0 \\ 0 & -1 \end{pmatrix} \tag{2.5}$$

The Pauli matrices are involuntary matrices, meaning the square of the matrices gives the identity, and they are orthogonal to each other,$Tr(\sigma_j\sigma_k) = 2\delta_{jk}$. The coefficient $\frac{1}{2}$ comes from the trace condition of the density matrix, since $Tr(\hat{\rho}) = a_0$. Furthermore, a pure state density operator is a rank-1 projector and consequently $Tr(\hat{\rho}^2) = 1$. On the Bloch sphere the condition is mapped to $a_x^2 + a_y^2 + a_z^2 = \frac{1}{4}$. Where as mixed state density operators satisfy the bound $Tr(\hat{\rho}^2) < 1 \rightarrow a_x^2 + a_y^2 + a_z^2 < \frac{1}{4}$, meaning the mixed states are mapped to the interior of the Bloch sphere.

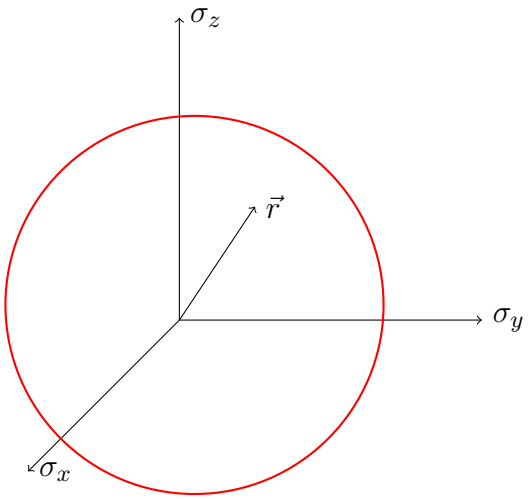

Figure 2.1 The figure depicts the Bloch sphere, where the vector $\vec{r}$ corresponds to the density operator $\hat{\rho}$, while the (x, y, z) axes correspond to the three Pauli matrices $(\sigma_x, \sigma_y, \sigma_z)$ respectively. The interior of the sphere is where mixed states are mapped to and the surface of the Bloch sphere contains all pure state density operators.

As can be seen, the Bloch sphere allows us to represent the quantum states in a geometrical manner. Special Unitary operations, which are norm preserving operators, can intuitively be described as rotations on the Bloch sphere. This follows from the 2-to-1 homeomorphism of the $SU(2)$ and $SO(3)$ groups. In simple words, the unitary evolution of a 2-dimensional system can be reduced to 3-dimensional rotations on the Bloch sphere, where the vector of the rotations corresponds to the

generator of the evolution. For a unitary operator $\hat{V} \in SU(2)$ given below,

$$\hat{V} = e^{i\frac{\phi}{2}\hat{n}\vec{\sigma}} \tag{2.6}$$

the unit vector $\hat{n}$ corresponds to the axis of rotation in the Bloch sphere representation.

The Bloch sphere can be generalized to higher dimensions using different choices of basis. To study the SIC-POVMs and other frames in a geometrically simpler way, we will use basis matrices that we map the density operators onto the real space. The basis of choice for these, are the symmetric trace-less generalizations of the Pauli matrices known as the Gell-Mann matrices.

2.1.1 The Gell-Mann Matrices

The Gell-Mann matrices are a set of 8 trace-less matrices spanning the space of 3×3 trace-less symmetric complex matrices. Before we generalize the matrices to higher dimensions, let's look at the Gell-Mann matrices in dimension 3 in more detail.

$$\begin{aligned}\Lambda = \{ &\begin{pmatrix} 0 & 1 & 0 \\ 1 & 0 & 0 \\ 0 & 0 & 0 \end{pmatrix}, \begin{pmatrix} 0 & 0 & 1 \\ 0 & 0 & 0 \\ 1 & 0 & 0 \end{pmatrix}, \begin{pmatrix} 0 & 0 & 0 \\ 0 & 0 & 1 \\ 0 & 1 & 0 \end{pmatrix}, \\ &\begin{pmatrix} 0 & -i & 0 \\ i & 0 & 0 \\ 0 & 0 & 0 \end{pmatrix}, \begin{pmatrix} 0 & 0 & -i \\ 0 & 0 & 0 \\ i & 0 & 0 \end{pmatrix}, \begin{pmatrix} 0 & 0 & 0 \\ 0 & 0 & -i \\ 0 & i & 0 \end{pmatrix}, \\ &\begin{pmatrix} 1 & 0 & 0 \\ 0 & -1 & 0 \\ 0 & 0 & 0 \end{pmatrix}, \begin{pmatrix} \frac{1}{\sqrt{3}} & 0 & 0 \\ 0 & \frac{1}{\sqrt{3}} & 0 \\ 0 & 0 & -\frac{2}{\sqrt{3}} \end{pmatrix} \}.\end{aligned} \tag{2.7}$$

The matrices can be split into three subsets based on the entries: the real terms, the complex terms and diagonal terms. In literature, these are also referred to as the symmetric, anti-symmetric and diagonal Gell-Mann matrices. Just like the 2-dimensional case, 3-dimensional density operators can be represented using the Gell-Mann matrices as,

$$\hat{\rho} = \frac{1}{3}\mathbb{I} + \sum_{k=1}^{8} r_k \lambda_k. \tag{2.8}$$

Where $\vec{r} \in \mathbb{R}^8$, and $r_k = \frac{1}{2}Tr(\lambda_k \hat{\rho})$. By applying the constraints on the density operator, we find that the vector $|\vec{r}|^2 \leq \frac{1}{\sqrt{3}}$ where the equality holds if and only if the $\hat{\rho}$ is a pure state density matrix. We will prove this for the generalized Gell-Mann matrices. The similarities to with the 2-dimensional case don't go further than this, as the $SU(3) \ncong SO(8)$, the implication of which is, that not all vectors in the Bloch sphere correspond to physical states. We can visualize the states in the diagonal subspace of the Bloch sphere.

** Let $\hat{\rho}$ be an arbitrary diagonal density matrix, and the vector $\vec{r}$ be the image of its on the Bloch sphere. For the Gell-Mann matrices given in (2.7), the image of a diagonal matrix $\vec{r}$ only has 2 none zero elements. These are the coefficients of the last two matrices in (2.7).

$$\vec{r} = \{0, \ldots, 0, r_7, r_8\} \tag{2.9}$$

The three basis vectors,i.e.,$\{|0\rangle, |1\rangle, |2\rangle\}$, are mapped to three vectors of length $\frac{1}{3}$ forming the edges of a equilateral triangle. The last two elements of which are, $\vec{v}_0 \to \{0, -1\}, \vec{v}_1 \to \{\frac{\sqrt{3}}{2}\frac{1}{2}\}, \vec{v}_2 \to \{-\frac{\sqrt{3}}{2}, \frac{1}{2}\}$. To visualize the entire diagonal density matrices, note that we write arbitrary diagonal density operator as a linear combination of pure states as shown in (2.2). This means, we can write all images of the density operators on the Gell-Mann sphere as a linear combination of the three vector listed above, with the condition that the coefficient is always positive.

$$\vec{r} = p_1\vec{v}_1 + p_2\vec{v}_2 + p_3\vec{v}_3, \text{ where} p_1 + p_2 + p_3 = 1 \tag{2.10}$$

The vector $\vec{r}$ lies with in the triangle formed by the images of the basis vectors as shown in 2.2. Note that, in the diagonal subspace, the only pure states on the surface of the Bloch sphere are the three basis vectors. This shows that, the surface of the Bloch sphere in dimension 3 contains nonphysical density operators.

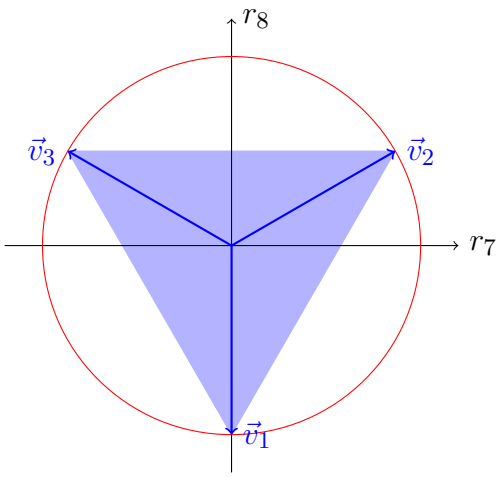

Figure 2.2 The circle depicts the diagonal subsurface of the Bloch sphere, where The image of all physical diagonal density operators lie in the shaded area. Only the three orthogonal basis vector exist on the surface of the Bloch sphere.

** We now define the generalized Bloch sphere by using the generalized Gell-Mann matrices, Bertlmann & Krammer (2008).

Definition 2.1 (Generalized Gell-Mann matrices)**.** *Let the matrices $\lambda_s, \lambda_a, \lambda_d$ be the symmetric, anti-symmetric and diagonal Gell-Mann matrices respectively in the n-dimensional complex space, where*

$$\lambda_s^{jk} = |j\rangle\langle k| + |k\rangle\langle j| : 0 \leq j < k \leq n-1 \tag{2.11}$$

$$\lambda_a^{jk} = -i(|j\rangle\langle k| - |k\rangle\langle j|) : 0 \leq j < k \leq n-1 \tag{2.12}$$

$$\lambda_d^{l} = \sqrt{\frac{2}{l(l+1)}} \sum_{k=0}^{l-1} |j\rangle\langle j| - l|l\rangle\langle l| : 1 \leq l \leq n-1 \tag{2.13}$$

The n^2-1 matrices are linearly independent, which is obvious in their matrix form. consequently, the generalized Gell-Mann matrices form a basis for the $n \times n$ symmetric matrices. From this point on, we will refer to the basis formed as a set $\{\lambda_k\}$ where the order we use is $\{\lambda_s, \lambda_a, \lambda_d\}$.(This is the same order of the set given for 3-dimensional case in (2.7)).

Using the n^2-1 symmetric trace-less matrices defined, we generate a map from the density operator to the real vector space which forms the generalized Bloch sphere as $\mathbb{C}^n \times \mathbb{C}^n \mapsto \mathbb{R}^{n^2-1}$, where

$$\vec{r}_{\hat{\rho}} = \frac{1}{2} \sum_{k=1}^{n^2-1} Tr(\lambda_k \hat{\rho}) \vec{e}_k \tag{2.14}$$

and unit vectors $\vec{e}_k$ is the images of λ_k on the Gell-Mann sphere. The density operator is then expanded as $\hat{\rho} = \mathbb{I}/n + \vec{\lambda} \cdot \vec{r}_{\hat{\rho}}$.

Consider the image of a pure state density operator $\hat{\rho}$ on the real vector space. Since the operator is pure, $Tr(\hat{\rho}^2) = 1$.

$$\begin{aligned} Tr(\hat{\rho}^2) &= Tr\Big(\big(\frac{\mathbb{I}}{n} + \sum_j \lambda_j r_j\big)\big(\frac{\mathbb{I}}{n} + \sum_k \lambda_j r_k\big)\Big) \\ &= Tr\big(\frac{\mathbb{I}}{n^2} + \sum_{jk} \lambda_j \lambda_k r_j r_k\big) \\ &= \frac{1}{n} + \sum_{jk} \underbrace{Tr(\lambda_j \lambda_k)}_{\delta_{jk}} r_j r_k = \frac{1}{n} + 2|\vec{r}|^2 \end{aligned} \tag{2.15}$$

Therefore, pure states are mapped to points on a sphere of radius $|\vec{r}| = \sqrt{\frac{n-1}{2n}}$, which we define as the generalized Bloch sphere. The free parameters of a quantum state once we apply normalization and remove global phase is $2n-2$, but the surface of the Bloch sphere is a n^2-2 dimensional manifold. Thus, for $n > 2$, the surface of the Bloch sphere contains points which are not density operators to a physical state. In the next section we will look at the manifold formed by the pure states and mixed states.

2.1.2 Density Matrices in the Generalized Bloch Sphere

Each density operator is mapped to the real space using the Gell-Mann matrices 2.1. As briefly stated in previous section, not all vectors on Bloch sphere correspond to physical density operators. The reason because not all density operators on the Bloch sphere are positive definite,i.e., some operators on the Bloch sphere have negative eigenvalue. To fully characterize and identify physical density operators on the Bloch sphere, we must classify the operators based on their eigenvalues. Mixed state density operators are mapped to the interior of the Bloch sphere as the dimension 3 case shown in figure 2.2, and in general, mixed state density operator are mapped to vectors $\vec{r}$ where $|\vec{r}| < \sqrt{\frac{n-1}{2n}}$. We will now generate a set of equations that define the image of all states on the real vector space.

We start by the pure state, which satisfies the condition $\hat{\rho}^2 = \hat{\rho}$. Comparing the density operators in this manner does not tell us much about the image of the states. For that we need equations that we can transform to the real space. These

equations are the trace of power of the density operator.

Definition 2.2. *For a given density operator $\hat{\rho}$, define the functions $\mathcal{F}_k$ where $\mathcal{F}_k = Tr(\hat{\rho}^k)$.*

The functions $\mathcal{F}_k$ are mapped to the Bloch sphere as follows:

$$\mathcal{F}_k = Tr\left(\left(\frac{\mathbb{I}}{n} + \sum_j \lambda_j r_j\right)^k\right) \tag{2.16}$$

The functions are equivalent to $\sum_j x_j^k$ in terms of the eigenvalues of the density operators and in general, we can identify a density operator up to a unitary transformation by using the functions $\{f\mathcal{F}_1, \ldots, \mathcal{F}_n\}$ as shown in the Appendix A. The number of necessary equations decreases with degeneracy's of the operator.

Theorem 2.1. *A density matrix $\hat{\rho}$ is pure if and only if $\mathcal{F}_1 = 1$, $\mathcal{F}_2 = 1$ and $\mathcal{F}_3 = 1$.*

The theorem was proved by Appleby (2007) and can be found in Appendix A.1 .

The function $\mathcal{F}_1 = 1$ is satisfied by definition for all matrices on the Bloch sphere. The function $\mathcal{F}_2 = 1$ maps to $|\vec{r}|^2 = \frac{n-1}{2n}$ which corresponds to the entirety of the Bloch sphere. The third function $\mathcal{F}_3 = 1$ is the characteristic function that determines the geometry of pure states on the Bloch sphere. In the real space, the function can be reduced to,

$$\begin{aligned} \mathcal{F}_3 &= \frac{1}{n^2} + \frac{6}{n}\frac{n-1}{2n} + \sum_{ijk} d_{ijk} r_i r_j r_k \\ \frac{n^2 - 3n + 2}{n^2} &= \sum_{ijk} d_{ijk} r_i r_j r_k \end{aligned} \tag{2.17}$$

where $d_{ijk} = Tr(\lambda_i \lambda_j \lambda_k)$ and $1 \leq i, j, k \leq n^2 - 1$.

2.1.3 $SU(n)$ in the Real Vector Sphere

The Pauli matrices allows us to map the special unitary group on to the special orthogonal group as shown in equation (2.6), where we have the isomorphism $SU(2)/\{\pm\mathbb{I}\} \cong SO(3)$. We don't have similar isomorphism between $SU(n)$ and $SO(n^2-1)$ in higher dimensions. A given unitary operator $U \in SU(n)$ is mapped

to the orthogonal transformation $M \in SO(n)$ where the matrix elements are given by $M_{jk} = \frac{1}{2}Tr(U^\dagger \lambda_j U \lambda_k)$. We can write any U as an exponential transformation $e^{i\Omega}$ where $\Omega^\dagger = \Omega$ and $Tr(\Omega) = 0$. To derive the exponential form of the orthıgonal transformations, we break down U into infinitesimal transformations.

$$e^{i\Omega} = \lim_{N\to\infty}(\mathbb{I} + \frac{i}{N}\Omega)^N \tag{2.18}$$

We first transform the infinitesimal transformations on to the real space by using the Gell-Mann matrices $\Lambda = \{\lambda_k\}$. For a given density matrix ρ we write the transformation to ρ' as $\rho' = u^\dagger \rho u$. If u is an infinitesimal transformation,

$$\rho' = (\mathbb{I} - i\delta\Omega)\rho(\mathbb{I} + i\delta\Omega), \delta \ll 1 \tag{2.19}$$

We can now expand all the symmetric matrices as $\rho' = \frac{\mathbb{I}}{n} + \Lambda \cdot \vec{r'}$, $\rho = \frac{\mathbb{I}}{n} + \Lambda \cdot \vec{r}$ and $\Omega = \Lambda \cdot \vec{c}$.

$$\frac{\mathbb{I}}{n} + \Lambda \cdot \vec{r'} = (\mathbb{I} - i\delta\Lambda \cdot \vec{c})(\frac{\mathbb{I}}{n} + \Lambda \cdot \vec{r})(\mathbb{I} + i\delta\Lambda \cdot \vec{c}) \tag{2.20}$$

$$\Lambda \cdot \vec{r'} = \Lambda \cdot \vec{r} - i\delta(\lambda_j\lambda_k - \lambda_k\lambda_j)c_j r_k + O(\delta^2) \tag{2.21}$$

define $[\lambda_j\lambda_k - \lambda_k\lambda_j] = -if_{jkp}\lambda_p$ where $f_{jkp} = \frac{d_{jkp} - d_{kjp}}{2i}$,

$$\Lambda.\vec{r'} = \Lambda.\vec{r} - i\delta(-if_{jkp}\lambda_p)c_j r_k + O(\delta^2) \tag{2.22}$$

$$r'_p = r_p - \delta(f_{jkp}c_j)r_k + O(\delta^2) \tag{2.23}$$

$$r'_p = r_p + \delta(f_{pkj}c_j)r_k + O(\delta^2) \tag{2.24}$$

We can now define an orthogonal matrix (to the first order of δ) $M_{ij}(\delta) = \mathbb{I} + \delta\sum_k f_{ijk}c_k$. Then the unitary $e^{i\Omega}$ corresponds to the product of the infinitesimal transformations M_{ij}.

$$M = \exp(\sum_k f_{ijk}c_k) \tag{2.25}$$

We can also write the matrix element using the unitary operation U as $M_{ik}(U) = tr(U^{\dagger}\Lambda_i U \Lambda_k)$. In dimension 3, the corresponding generator of the orthogonal transformation is shown below, for an arbitrary vectors $\vec{c} \in \mathbb{R}^8$.

(2.26)

$$\begin{pmatrix} 0 & 2c_7 & c_6 & -c_5 & c_4 & -c_3 & -2c_2 & 0 \\ -2c_7 & 0 & c_5 & c_6 & -c_3 & -c_4 & 2c_1 & 0 \\ -c_6 & -c_5 & 0 & c_7+\sqrt{3}c_8 & c_2 & c_1 & -c_4 & -\sqrt{3}c_4 \\ c_5 & -c_6 & -c_7-\sqrt{3}c_8 & 0 & -c_1 & c_2 & c_3 & \sqrt{3}c_3 \\ -c_4 & c_3 & -c_2 & c_1 & 0 & \sqrt{3}c_8-c_7 & c_6 & -\sqrt{3}c_6 \\ c_3 & c_4 & -c_1 & -c_2 & c_7-\sqrt{3}c_8 & 0 & -c_5 & \sqrt{3}c_5 \\ 2c_2 & -2c_1 & c_4 & -c_3 & -c_6 & c_5 & 0 & 0 \\ 0 & 0 & \sqrt{3}c_4 & -\sqrt{3}c_3 & \sqrt{3}c_6 & -\sqrt{3}c_5 & 0 & 0 \end{pmatrix}$$

The orthogonal matrix allows us to construct the entire Bloch sphere by applying it to the diagonal subspace, which has a simple geometry. The diagonal subspace is a n-simplex where the pure states form the vertices of the simplex. We can then immediately see that there exists a radius (the distance to the center of the base of the simplex) beyond which all vectors correspond to physical density operators.

2.2 Generalized Quantum Measurements

Measurement in quantum mechanics is performed by interaction of a system with a classical measurement apparatus. At a given time, the classical apparatus is found in one of its' eigenvectors and the system being measured also gets projected on to a state determined by the measurements process, Landau & Lifshitz (1977). Mathematically we write the measurement process thought the set of operators $\{E_k\}$. Each E_k corresponds to a measurement operator where k is the measurement outcome. These measurement operators project an arbitrary initial state $|\psi\rangle$ to the non-normalized post measurement state $|\phi_k\rangle$ and the probability that the system is projected to the post measurement state is $p_k = \langle\phi_k|\phi_k\rangle$. A complete measurement must account for all the possible measurement outcomes, which is given by the completeness condition,

$$\sum_k E_k^\dagger E_k = \mathbb{I} \ . \tag{2.27}$$

The normalized post measurement state is given by the following, Nielsen & Chuang (2010).

$$\frac{E_k|\psi\rangle}{\sqrt{\langle\psi|E_k^\dagger E_k|\psi\rangle}} \tag{2.28}$$

When applied to the density operator, the probability simply becomes $Tr(E_k \rho E_k^\dagger)$ and the post measurement state

$$\rho' = \frac{E_k \rho E_k^\dagger}{Tr(E_k \rho E_k^\dagger)} \ . \tag{2.29}$$

A familiar measurement is the Von-Neumann measurement, also known as the projective valued measure, where the measurement operators are orthogonal projective operators. The maximum number of the Von-Neumann measurements in n-dimensional Hilbert space is n, in which case we can write the projectors using the measurements basis vectors as $|\phi_k\rangle\langle\phi_k|$. For example, in dimension 2, the two measurement operators $P_0 = |0\rangle\langle 0|$ and $P_1 = |1\rangle\langle 1|$ form a projective value measure. These two measurements are not enough to reconstruct a density matrix, since the two operators correspond to two opposite vectors along the z axis of the Bloch sphere. Obviously, the vectors do not span the entire Bloch sphere and therefor does not allow for the unique representation of a density matrix. For a complete description of a 2-dimensional density matrix, we need at least 3 linearly independent measurement operators.

The generalized quantum measurement formalism is the positive operator-valued measure, which is abbreviated as POVM. For a set of measurement operators $\{E_k\}$ satisfying the completeness conditions, (2.27). The POVM is defined as the set of positive operators $\{\Pi_k\}$ where $\Pi_k = E_k^\dagger E_k$, satisfying (2.30). The probability of observing k is then $\langle\psi|\Pi_k|\psi\rangle$. In general, the POVM elements are not rank-1 or projective operators. If the measurement operators are rank-1 operators, we can write $E_k = |\phi_k\rangle\langle\psi_k|$ where $|\psi_k\rangle$ is the post measurement state.In such a case, we can

write the POVM elements as $|\psi_k\rangle\langle\psi_k|$.

$$\sum_k \Pi_k = \mathbb{I} \tag{2.30}$$

In general, POVM operators can be mapped onto the real vectors space by the Gell-Mann matrices. Since the POVM elements are Hermitian, one can represent them with a density matrix up to some multiplicative factor. This allows for a simplified geometric representation of many POVMs as we will see in later sections. In this picture, the probability of the measurement outcomes is correlated to the dot product of vectors corresponding to the state being measured and the POVM element. For a complete reconstruction of a density matrix, the image of the POVM elements must span the entire Bloch sphere. In other words, in n-dimensional Hilbert space, the vectors representing the operators must be linearly independent and must have at least $n^2 - 1$ elements. There are two special POVMs that are the subject of research in quantum computation and information for their efficiency. These are the symmetric informationally complete POVM and the mutually unbiased bases abbreviated as SIC-POVM and MUB respectively. The focus for this thesis is the SIC-POVMs but we shall give a brief definition of the MUBs as well for general discussion.

2.2.1 Symmetric Informationally Complete POVMs

The SIC-POVMs are a type of generalized measurements consisting of n^2 elements in n-dimensional Hilbert space. The SIC-POVM that minimize the number of measurements required for a complete state tomography Scott (2006).

Definition 2.3 (**SIC-POVM).** *Let the set of positive Hermitian operators* $\{\Pi_k\}$ *be SIC-POVMs for* n*-dimensional Hilbert space, where* $\Pi_k = \frac{|\phi_k\rangle\langle\phi_k|}{n}$ *and*

$$Tr(\Pi_j \Pi_k) = \frac{\delta_{jk} n + 1}{n^2(n+1)} \tag{2.31}$$

The density operator can be expressed using the SIC-POVM and probabilities of each measurement, $p_k = Tr(\Pi_k \rho)$.

$$\rho = \sum_{k=1}^{n^2} \Big(p_k n(n+1) - 1\Big)\Pi_k \tag{2.32}$$

Since every operator of the SIC-POVM is a rank-1 projector, it is common to represent it using normalized vectors $\{|\phi_k\rangle\}$ where $\Pi_k = \frac{1}{n}|\phi_k\rangle\langle\phi_k|$. We will use both representations interchangeably throughout the thesis. The vectors forming the SIC-POVMs are equidistant by definition, and they are also known as equiangular or equidistant complex vectors in mathematics literature Waldron (2018). For example, in 2-dimensional Hilbert space, the following 4 vectors form a SIC-POVM.

$$\begin{aligned}
|\psi_1\rangle &= |0\rangle \\
|\psi_2\rangle &= \frac{1}{\sqrt{3}}|0\rangle + \sqrt{\frac{2}{3}}|1\rangle \\
|\psi_3\rangle &= \frac{1}{\sqrt{3}}|0\rangle + \sqrt{\frac{2}{3}}e^{i2\pi/3}|1\rangle \\
|\psi_4\rangle &= \frac{1}{\sqrt{3}}|0\rangle + \sqrt{\frac{2}{3}}e^{i4\pi/3}|1\rangle
\end{aligned} \tag{2.33}$$

2.2.2 Mutually Unbiased Bases

Another interesting measurement is the Mutually unbiased bases which consists of $n(n+1)$ positive operators.

Definition 2.4 (MUB). *Let the set of operators Π_{jk} be a set of rank-1 projectors where*

$$Tr(\Pi_{jk}\Pi_{j'k'}) = (1-\delta_{jj'})\frac{1}{(n+1)n} + \delta_{jj'}\delta_{kk'}\frac{1}{n+1} \tag{2.34}$$

and the two indices j and k correspond to the basis index and the basis element index respectively.

Similar to the SIC-POVMs, we can represent the operators forming a MUB by normalized states, where $\Pi_{jk} = \frac{1}{n+1}|\phi_{jk}\rangle\langle\phi_{jk}|$. The mutually unbiased bases can be constructed in all prime power dimensions where all $n+1$ bases are known. In other dimensions how ever it is not known if $n+1$ bases exist. The smallest of such

dimensions is dimension 6, where no complete set of bases is known. For example, in 2-dimensional Hilbert space, the eigenbasis of the Pauli matrices form a MUB.

$$\begin{aligned} \Pi_{0k} &= \{|0\rangle, |1\rangle\} \\ \Pi_{1k} &= \Big\{\frac{|0\rangle + |1\rangle}{\sqrt{2}}, \frac{|0\rangle - |1\rangle}{\sqrt{2}}\Big\} \\ \Pi_{1k} &= \Big\{\frac{|0\rangle + i|1\rangle}{\sqrt{2}}, \frac{|0\rangle - i|1\rangle}{\sqrt{2}}\Big\} \end{aligned} \tag{2.35}$$

2.3 Geometry of SIC-POVMs in the Generalized Bloch Sphere

We know have the necessary tools to explore the geometry formed by the SIC-POVMs in the Bloch sphere. Let's start with the SIC-POVM given in (2.33). We can map each vector given to the Bloch sphere by using the Pauli matrices as follows. Let $\vec{r}_k$ be the image of the state $|\phi_k\rangle$. Then, $\vec{r}_k$ is given by $\frac{1}{2}Tr(\vec{\sigma}|\phi_k\rangle\langle\phi_k|)$. The corresponding 4 vectors are as follows:

$$\begin{aligned} \vec{r}_1 = \{0, 0, \frac{1}{2}\}, \vec{r}_2 = \{\frac{\sqrt{2}}{3}, 0, -\frac{1}{6}\} \\ \vec{r}_3 = \{-\frac{1}{3\sqrt{2}}, -\frac{1}{\sqrt{6}}, -\frac{1}{6}\}, \vec{r}_4 = \{-\frac{1}{3\sqrt{2}}, \frac{1}{\sqrt{6}}, -\frac{1}{6}\} \end{aligned} \tag{2.36}$$

Plotting the vectors on the Bloch sphere, the 4 vectors form the vertices of a simplex as shown in figure 2.3.

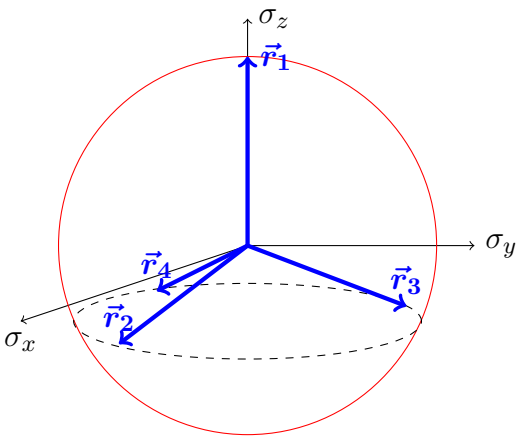

Figure 2.3 The 4 vectors span the entire Bloch sphere and an arbitrary state can be written as a linear combination of the 4-vectors with only positive expansion coefficients.

In general the condition $Tr(\Pi_j\Pi_k) = \frac{1}{n+1}$ for $j \neq k$ is equivalent to the condition $\vec{r}_j \cdot \vec{r}_k = -\frac{1}{2n(n+1)}$ as shown below (2.37). Since the norm of the vectors $\vec{r}_j = \sqrt{\frac{n-1}{2n}}$, the angle between the vectors is such that $\cos(\theta_{jk}) = -\frac{1}{n^2-1}$. This shows that the SIC-POVM form the vertices of an (n^2-1)-simplex on the Bloch sphere.

$$
\begin{aligned}
Tr(\Pi_j\Pi_k) &= Tr\Big(\Big(\frac{\mathbb{I}}{n} + \vec{r}_j \cdot \vec{\Lambda}\Big)\Big(\frac{\mathbb{I}}{n} + \vec{r}_k \cdot \vec{\Lambda}\Big)\Big) \\
\frac{1}{n+1} &= Tr\Big(\frac{\mathbb{I}}{n^2} + 2\vec{r}_j \cdot \vec{r}_k\Big) \\
\frac{1}{2}\left(\frac{1}{n+1} - \frac{1}{n}\right) &= \vec{r}_j \cdot \vec{r}_k \\
-\frac{1}{2n(n+1)} &= \vec{r}_j \cdot \vec{r}_k
\end{aligned}
\tag{2.37}
$$

While, in 2-dimensional Hilbert space, the 4 vectors can be rotated arbitrarily to form a new SIC-POVM, in higher dimensions this is not the case. The rank-1 operators are mapped to the surface of the Bloch sphere and the pure states on the surface are determined by the equation $Tr(\rho^3) = 1$. Therefore, the SIC-POVMs do not form an arbitrary simplex, rather the orientation is restricted in a complicated way. To explore the restriction on the orientation, we go back to the condition of purity A.1. Restricting our selves to states who's image is on the surface of the Bloch sphere, the defining characteristic for a density operator to be pure is the trace cub condition, which we can equivalently map to the Bloch sphere as follows. Let $\rho_k = |\phi_k\rangle\langle\phi_k|$ be an element of a SIC-POVM.

$$
\begin{aligned}
Tr(\rho_k^3) &= Tr\Big(\frac{\mathbb{I}}{n^3} + 3\frac{1}{n^2}\vec{r}\cdot\Lambda + 3\frac{1}{n}(\vec{r}\cdot\vec{\Lambda})^2 + (\vec{r}\cdot\vec{\Lambda})^3\Big) \\
1 &= \frac{1}{n^2} + 6\frac{1}{n}\vec{r}_j\cdot\vec{r}_k + \sum_{abc} r_a r_c r_c Tr(\Lambda_a\Lambda_b\Lambda_c) \\
1 - \frac{1}{n^2} - 6\frac{n-1}{2n^2} &= \sum_{abc} r_a r_c r_c d_{abc} \\
\frac{(n-1)(n-2)}{n^2} &= \sum_{abc} r_a r_c r_c d_{abc}
\end{aligned}
\tag{2.38}
$$

The tensor $d_{ijk} = Tr(\lambda_i\lambda_j\lambda_k)$ is zero for most of the indices. For example, the equation in for Bloch sphere of the 3-dimensional Hilbert space is shown in (2.64) (see Appendix A).

(2.39)

$$
\begin{aligned}
&\sum_{a_1a_2a_3} d^3_{a_1a_2a_3} r_{a_1} r_{a_2} r_{a_3} = 2\sqrt{3}r_1^2 r_8 + 6r_1r_2r_3 + 6r_1r_5r_6 + 3r_2^2r_7 - \sqrt{3}r_2^2r_8 - 6r_2r_4r_6 - 3r_3^2r_7 \\
&-\sqrt{3}r_3^2r_8 + 6r_3r_4r_5 + 2\sqrt{3}r_4^2r_8 + 3r_5^2r_7 - \sqrt{3}r_5^2r_8 - 3r_6^2r_7 - \sqrt{3}r_6^2r_8 + 2\sqrt{3}r_7^2r_8 - \frac{2r_8^3}{\sqrt{3}} = \frac{2}{9}
\end{aligned}
$$

In general, a pure state density operators is identified through the homogeneous polynomial (2.38). We can now define the SIC-POVM vectors as the vertices of (n^2-1)-simplex such that each vector satisfied the condition (2.38). In other word the function polynomial function maps the points on the surface of the Bloch sphere to the real space, $f : \vec{r} \mapsto \mathbb{R}, f(\vec{r}) = \sum_{a_1a_2a_3} d^3_{a_1a_2a_3} r_{a_1} r_{a_2} r_{a_3}$ where $-\frac{(n-1)(n-2)}{n^2} \leq f(\vec{r}) \leq \frac{(n-1)(n-2)}{n^2}$. The polynomials Boundary is maximized for pure states, which can easily be deduced from the diagonal subspace where the pure states are n points. on the other limit, since the function is odd, the minimum has to be $-\frac{(n-1)(n-2)}{n^2}$. At this point, we can draw a parallel between the construction of SIC-POVMs and a well known problem in geometry called Kakutani's theorem (see theorem 2.2). This will help us lay the ground work for a generalized understanding of the SIC-POVM existence problem and possible direction of a general proof. In 1947, Bronislaw Knaster posed the following problem in the Colloquium Mathematicae Col (1947), which was originally in French and presented in English in the "Life and Work of Bronislaw Knaster" in Duda (1987) as follows. *"Given three points p_1, p_2, p_3 on a 2-dimensional sphere and a continuous mapping of S^2 into the $\mathbb{R}$. Do there exist points q_1, q_2, q_3 on S^2 which are equivalent to rotation to p_1, p_2, p_3 that have the common image on $\mathbb{R}$, i.e.,*

$$f(q_1) = f(q_2) = f(q_3) \ ? \tag{2.40}$$

More generally, For any given k points $(p_1, \cdots, p_k)$ *on* S^n *and any continuous mapping of* S^n *into* $\mathbb{R}^{n-k+2}$*, where* $k \in \{2, \cdots, n+1\}$*, is there a set of points* $(q_1, \cdots, q_k)$ *which has the same image in* $\mathbb{R}^{n-k+2}$ *?"* The problem has been answered for various special sets of vectors. One of the most notable examples is Kakutani's theorem. Kakutani proved the conjecture for orthogonal vectors on a 3-dimensional sphere in Kakutani (1942). Later, Yamebe and Yujobo (1950) generalized the theorem to orthogonal vectors in arbitrary dimensions. Other examples are the Borsuk-Ulam theorem, which corresponds to antipodal points on an n-sphere Borsuk (1933) and Dyson's theorem, which corresponds to 2 orthogonal lines crossing through the origin of an n-sphere Dyson (1951).

The Kakutani's theorem, originally inspired by the geometric problem of a convex body circumscribed in a cube, states that given a continuous function on a sphere, there exists 3 orthogonal vectors such that all vectors map to a constant value of the function Kakutani (1942). Later, the theorem was generalized to higher dimensions by H. Yamabe et.al. Yamabe & Yujobô (1950). The generalized Kakutani's theorem is stated as follows: given a continuous map $f : S^{n-1} \to \mathbb{R}$, there exists a set of orthonormal vectors $\{\vec{p}_j\}$ such that,

$$f(\vec{p}_1) = f(\vec{p}_2) = \ldots = f(\vec{p}_n) \tag{2.41}$$

As shown in equation (2.38), the SIC-POVM is a set of n^2 equi-norm vectors forming the vertices of an (n^2-1)-simplex such that $\sum d_{abc} r_a r_b r_c =$ constant for all the vectors. We can not directly apply the Kakutani's theorem since the vectors forming the SIC-POVM are not orthogonal. Thus,we will first prove a modified version of the Kakutani's theorem for the vertices of a simplex in the next section.

2.3.1 Modified Kakutani's Theorem

We start by constructing a regular simplex in the n^2-1 dimensional real space. This can be done using the Gram-Schmidt process. Start with the one dimensional

vectors $V_1 = \{(1), (-1)\}$, which is the equiangular vector in the 1-dimensional vector space. Then, by applying the algorithm $V_n = \{\{\frac{\sqrt{n^2-1}}{n} V_{n-1}, \frac{1}{n}\}, \{0, ..., 0, -1\}\}$, we construct $n+1$ equiangular unit vectors. For example, in the 2-dimensional vectors space, the set of equiangular vectors is $V_2 = \{(\frac{\sqrt{3}}{2}, \frac{1}{2}), (-\frac{\sqrt{3}}{2}, \frac{1}{2}), (0, -1)\}$ and in the 3-dimensional vector space, the corresponding set is $V_3 = \{(\frac{\sqrt{8}}{3} V_2, \frac{1}{3}), (0, 0, -1)\}$. By plugging the vectors of V_2, we generate the four vectors in V_3, which gives the vectors

$$\{(\frac{\sqrt{6}}{3}, \frac{\sqrt{2}}{3}, \frac{1}{3}), (-\frac{\sqrt{6}}{3}, \frac{\sqrt{2}}{3}, \frac{1}{3}), (0, -\frac{\sqrt{8}}{3}, \frac{1}{3}), (0, 0, -1)\} \ . \tag{2.42}$$

The vertices of a regular simplex and a set orthonormal basis vectors have geometric similarities which simplify the proof of Knaster's conjecture. In both cases, orthogonal transformations can be constructed such that any number of chosen vectors in the set are fixed by the transformations and the rest of the vectors form a connected subspace as shown in lemma 2.1.

Lemma 2.1. *Consider a set of vectors $P = \{\vec{p}_1, ..., \vec{p}_n\}$ on S^{n-1} where $\vec{p}_i . \vec{p}_j = -\frac{1}{n}$, then there exists a sets of matrices $\{U_1, ..., U_{n-1}\}$ where $U_i \in SO(n)$ such that*

$$\begin{aligned}
&U_1 \vec{p}_1 && = \vec{p}_1 \ , \\
&U_2 \vec{p}_2 && = \vec{p}_2, U_2 \vec{p}_1 = \vec{p}_1 \ , \\
&U_3 \vec{p}_3 && = \vec{p}_3, U_3 \vec{p}_2 = \vec{p}_2, U_3 \vec{p}_1 = \vec{p}_1 \ , \\
&\vdots && \\
&U_{n-1} \vec{p}_{n-1} && = \vec{p}_{n-1}, ..., U_{n-1} \vec{p}_2 = \vec{p}_2, U_{n-1} \vec{p}_1 = \vec{p}_1 \ .
\end{aligned} \tag{2.43}$$

Proof. Let's take the mutually orthogonal vectors $\{\vec{v}_1, ..., \vec{v}_n\}$ constructed from the elements of P using the Gram-Schmidt algorithm. Then the elements of P take the following form,

$$\begin{aligned}
&\vec{v}_1 = \vec{p}_1 \ , \\
&\vec{v}_2 + \tfrac{(\vec{v}_1 . \vec{p}_2)}{|\vec{v}_1|^2} \vec{v}_1 = \vec{p}_2 \ , \\
&\vec{v}_3 + \tfrac{(\vec{v}_2 . \vec{p}_3)}{|\vec{v}_2|^2} \vec{v}_2 + \tfrac{(\vec{v}_1 . \vec{p}_3)}{|\vec{v}_1|^2} \vec{v}_1 = \vec{p}_3 \ , \\
&\vdots \\
&\vec{v}_n + \tfrac{(\vec{v}_{n-1} . \vec{p}_n)}{|\vec{v}_{n-1}|^2} \vec{v}_{n-1} + ... + \tfrac{(\vec{v}_2 . \vec{p}_n)}{|\vec{v}_2|^2} \vec{v}_2 + \tfrac{(\vec{v}_1 . \vec{p}_n)}{|\vec{v}_1|^2} \vec{v}_1 = \vec{p}_n \ .
\end{aligned} \tag{2.44}$$

By using vector set $\{\hat{v}_1, ..., \hat{v}_n\}$ as our basis, we construct the set of matrices U_i as

$$U_i = \{ \begin{bmatrix} I & 0 \\ 0 & u_k \end{bmatrix} : \forall u_i \in SO(n-i) \} \ . \tag{2.45}$$

where I is a k-dimensional identity matrix. The action of the matrices U_k on the equiangular vectors P fixes the first k vectors. In addition, matrices of the form U_k exist which map each of the remaining vectors to each other. This shows that the orbits of these vectors are equivalent.

□

Given the equiangular vectors, V_{n^2-1}, and the corresponding orthogonal matrices U_k which fixed the first k vectors, the orbit of the remaining $(n-k)$ vectors is defined as the collection of points having a fixed inner product with all the k vectors. The subspaces can be defined as the intersection of the subspaces with a fixed inner product to each vector of index 1 up to k. Before defining these subspaces, let us define a representation for a surface. A surface defined by a function $g(\vec{x}) - g_0 = 0$ is represented as $\mathcal{S} = \{\vec{x} \in \mathbb{R}^N | g(\vec{x}) - g_0 = 0\}$. we will represent such surface in a slightly shorter form $\{g(\vec{x}) - g_0 = 0\}_N$.

Definition 2.5. *Given the set of equiangular vectors* $\{\vec{p}_1, \vec{p}_2, ..., \vec{p}_n\}$ *on* S^{n-1} *where* $\vec{p}_i.\vec{p}_j = -\frac{1}{n}$, *define the subspace* $J_i = S^{n-1} \bigcap_{j=1}^{i-1} \{\vec{x}.\vec{p}_j + \frac{1}{n} = 0\}_n$ *and* $J_1 = S^{n-1}$.

The subspaces J_i correspond to the orbits formed by the matrices U_{i-1}. This can be understood from the fact that the inner product of any vector in J_i and the vectors $\{\vec{p}_1, \cdots, \vec{p}_{i-1}\}$ is $\frac{1}{n}$. A key point to note from the definition is that $J_1 \supset J_2 \supset ... \supset J_n$, which will be important in the proof of theorem 2.2. Next, we show that each of the surfaces J_i is isomorphic to the sphere S^{n-i} using proof by induction.

Lemma 2.2. $J_i \cong S^{n-i} : 1 \leq i \leq n$

Proof. For $i = 1$, by definition $J_1 = S^{n-1}$.

For $i = 2$, the set is given by,

$$J_2 = S^{n-1} \cap \{\vec{x}.\vec{p}_1 + \frac{1}{n} = 0\}_n \ . \tag{2.46}$$

Let $\{\hat{e}_1, \ldots, \hat{e}_{n-1}\}$ be a set of orthogonal vectors such that $\hat{e}_i.\vec{p}_1 = 0$. Then, we can write the vector $\vec{x}$ as,

$$\vec{x} = \sum_{i=1}^{n-1} \alpha_i \hat{e}_i - \frac{\vec{p}_1}{n}, \alpha_i \in \mathbb{R} \ . \tag{2.47}$$

This form of $\vec{x}$ satisfies the equation $\vec{x}.\vec{p}_1 + \frac{1}{n} = 0$. The vector $\vec{x}$ is also an element of S^{n-1}, meaning $|\vec{x}|^2 = 1$. Using the normalization conditions of $\vec{x}$ and $\vec{p}_1$ in

$$|\vec{x}|^2 = \sum_{i=1}^{n-1} \alpha_i^2 + \frac{|\vec{p}_1|^2}{n^2} \ , \tag{2.48}$$

we calculate the sum of α_i^2 as

$$\sum_{i=1}^{n-1} \alpha_i^2 = \Big(\frac{n^2-1}{n^2}\Big) \ . \tag{2.49}$$

Clearly, 2.49 defines a sphere S^{n-2}, and we can form a homeomorphism between the subspace J_2 and S^{n-2} defined as $\phi_2 : J_2 \mapsto S^{n-2}, \phi_2(\vec{x}) = \vec{x} + \frac{\vec{p}_1}{n}$ which proves $J_2 \cong S^{n-2}$.

For $i = 3$, we start by writing the subspace J_3 and an intersection of J_2 and $\{\vec{x}.\vec{p}_2 + \frac{1}{n} = 0\}$, which becomes

$$J_3 = J_2 \cap \{\vec{x}.\vec{p}_2 + \frac{1}{n} = 0\} \ . \tag{2.50}$$

By applying the map ϕ_2 on the subspace J_3, we generate the subspace $\phi_2(J_3)$ which is homeomorphic to the original space J_3. The resulting subspace of S^{n-1} is $\phi_2(J_3) = \phi_2(J_2 \cap \{\vec{x}.\vec{p}_2 + \frac{1}{n} = 0\}) = \phi_2(J_2) \cap \phi_2(\{\vec{x}.\vec{p}_2 + \frac{1}{n} = 0\})$. The subspace $\phi_2(J_2)$ is a $n-1$ dimensional sphere of radius $\sqrt{\frac{n^2-1}{n^2}}$. Next, we need to write J_3 in the same form as J_2, specifically, as an intersection of a sphere and a surface defined by some continuous equation. This is done by applying the map ϕ_2 on the vectors $\vec{x}$ and $\vec{p}_2$. Let's define $\vec{x}' = \vec{x} + \frac{\vec{p}_1}{n}$ and $\vec{p'}_2 = \vec{p}_2 + \frac{\vec{p}_1}{n}$. By replacing the vectors in the surface equation $\vec{x}.\vec{p}_2 + \frac{1}{n} = 0$ by the vectors $\vec{x}'$ and $\vec{p'}_2$, we form the subspace $\phi_2(J_3)$ as

$$
\begin{aligned}
\phi_2(J_3) &= \phi_2(J_2) \cap \left\{ (\vec{x'} - \tfrac{\vec{p}_1}{n}) \cdot (\vec{p'}_2 - \tfrac{\vec{p}_1}{n}) + \tfrac{1}{n} = 0 \right\} \\
&= \phi_2(J_2) \cap \left\{ (\vec{x'} \cdot \vec{p'}_2 - \tfrac{\vec{p}_1}{n} \cdot \vec{p'}_2 - \vec{x'} \cdot \tfrac{\vec{p}_1}{n} + \tfrac{\vec{p}_1}{n} \cdot \tfrac{\vec{p}_1}{n}) + \tfrac{1}{n} = 0 \right\} .
\end{aligned} \tag{2.51}
$$

Since $\vec{p}_1.\vec{p'}_2 = 0$ and for $\vec{x} \in J_2$ we have $\vec{p}_1.\vec{x'} = 0$, 2.51 simplifies to

$$
\begin{aligned}
\phi_2(J_3) &= \phi_2(J_2) \cap \left\{ \vec{x'}.\vec{p'}_2 + \tfrac{1}{n^2} + \tfrac{1}{n} = 0 \right\} \\
&= \phi_2(J_2) \cap \left\{ \vec{x'}.\vec{p'}_2 + \left(\tfrac{n+1}{n^2} \right) = 0 \right\} \\
&= \phi_2(J_2) \cap \left\{ \vec{x'}.\vec{p'}_2 + \left(\tfrac{n^2-1}{n^2} \right) \tfrac{1}{n-1} = 0 \right\} .
\end{aligned} \tag{2.52}
$$

The magnitude of the vectors $\vec{x'}$ and $\vec{p'}_2$ is $\sqrt{\frac{n^2-1}{n^2}}$ as is the radius of the sphere $\phi_2(J_2)$. Thus, we define a normalization map $r_2 : R^{n-1} \mapsto R^{n-1}, r_2(\vec{x'}) = \sqrt{\frac{n^2}{n^2-1}}\vec{x'}$ and apply it on $\phi_2(J_3)$. The map $r_2(\phi_2(J_2))$ simply gives S^{n-2} and for the equation of the surface, we replace $\vec{x'}$ and $\vec{p'}_2$ by $r(\vec{x'})\sqrt{\frac{n^2-1}{n^2}}$ and $r(\vec{p'}_2)\sqrt{\frac{n^2-1}{n^2}}$, respectively. The resulting subspace is,

$$
(r_2 \circ \phi_2)(J_3) = S^{n-2} \cap \left\{ r(\vec{x'}) \cdot r(\vec{p'}_2) + \frac{1}{n-1} = 0 \right\} . \tag{2.53}
$$

Since r_2 is a homeomorphism, the map $r_2 \circ \phi_2$ is also a homeomorphism. Note that $(r_2 \circ \phi_2)(J_3)$ has the same form as J_2 with one less dimension. Therefore, we can go through the same steps as J_2 to form a homeomorphism $\phi_3 : (r_2 \circ \phi_2)(J_3) \mapsto S^{n-3}, \phi_3(x) = \vec{x} + \frac{\vec{p'}_2}{n-1}$, thereby showing $J_3 \cong S^{n-3}$. Finally, we repeat the process for each surface J_i to prove that $J_i \cong S^{n-i}$ for all $1 \leq i \leq n$.

□

Finally, we are ready to show that, given any continuous function on S^n, there exists a regular simplex for which at least n of its vertices are mapped to a unique value by the function.

Theorem 2.2. *Let f be a continuous function defined on the unit sphere S^{n-1} such that $f : S^{n-1} \mapsto \mathbb{R}$. There exists a set of points $\{p_1, p_2, ..., p_n\}$ on S^{n-1} such that,*

$$
\vec{p}_i.\vec{p}_j = -\frac{1}{n} \tag{2.54}
$$

and

$$f(p_1) = f(p_2) = ... = f(p_n) = f_0 \ , \ f_0 \in \mathbb{R} \ , \tag{2.55}$$

where $\vec{p}_i$ represents the vector from the origin to the point p_i.

Proof. We start by noting that, since f is a continuous function and S^{n-1} is a compact space, the value of $f(p)$, $\forall p \in S^{n-1}$ is continuous and bounded, i.e. $a \leq f(p) \leq b$. Let's take two points p_a and p_b where $p_a, p_b \in S^{n-1}$, such that $f(p_a) = a$ and $f(p_b) = b$ and define a set of matrices $\mu(\theta) = \{\mu(\theta) \in SO(n), \mu(1)\vec{p_a} = \vec{p_b}, \theta \in [0,1]\}$. We then construct a set of equiangular vectors $\Psi = \{p_1, p_2, ..., p_n\}$ on S^{n-1} by using the method shown in beginning of this section, such that $\vec{p}_i.\vec{p}_j = -\frac{1}{n}$ and $p_1 = p_a$. When we apply $\mu(\theta)$ on Ψ we get the set $\Psi(\theta) = \{p_1(\theta), p_2(\theta), ..., p_n(\theta)\}$ and since $\mu(\theta) \in SO(n)$ the angle between the vectors $\vec{p}_i(\theta)$ are invariants.

First, let's assume that the theorem holds for any continuous function defined on S^{n-2}. Then we can construct a set of $n-1$ points $\{r_1, ..., r_{n-1}\}$ where $\vec{x}_i.\vec{x}_j = -\frac{1}{n-1}$, such that $\forall k, f(\vec{r}_k) = f_0$. For a given $p_1(\theta)$, we construct a subspace J_2 defined in def 2.5. As shown in lemma 2.2, $J_2 \cong S^{n-2}$. By using the map ϕ_2 introduced in the proof of lemma 2.2, we can map the vectors $p_k, 2 \leq k \leq n$, to unit length vectors in $(n-1)$-dimensional sphere, where

$$\phi_2(\vec{p}_j) \cdot \phi_2(\vec{p}_k) = \left(-\frac{1}{n-1} \right) |\phi_2(\vec{p}_j)||\phi_2(\vec{p}_k)| \ . \tag{2.56}$$

The corresponding function on the subspace becomes $f(\vec{p}_k) \mapsto f \circ \phi^{-1}(\vec{p'}_k)$, where $\vec{p'}_k = \phi_2(\vec{p}_k)$. Based on our assumption, there exists an orthogonal matrix $u_1 \in SO(n-2)$ such that $f \circ \phi^{-1}(u_1 \vec{p'}_k) = f_0$ is a constant for all $k \neq 1$. The orthogonal matrix u_1 can be used to form an orthogonal matrix U_1 in $SU(n-1)$ as shown in 2.45. In other words, by taking $\mu(\theta) = U_1$, we construct a set of vectors $\Psi(\theta) = \{p_1(\theta), p_2(\theta), ..., p_n(\theta)\}$, where $f(p_2(\theta)) = f(p_3(\theta)) = ... = f(p_n(\theta)) = f_\theta$. Since $f(p_1(\theta))$ goes from a to b continuously as θ goes from 0 to 1 and $\forall \theta \ a \leq f_\theta \leq b$, there must exist a point θ for which $f(p_1(\theta)) = f(p_2(\theta)) = ... = f(p_n(\theta)) = f_\theta$. We can then conclude that, if the theorem holds for an arbitrary continuous function on S^{n-2}, it must also be true for an arbitrary function on S^{n-1}.

Finally, we need to show the theorem holds for S^1 to complete the proof. For S^1, we define the set of points $\Psi(\theta) = \{p_1(\theta), p_2(\theta)\}$ where $f(p_1(0)) = a$ and $f(p_1(1)) = b$ and $a \leq f(p_2(\theta)) \leq b$. Since f is a continuous function, there exists a point θ where

$f(p_1(\theta)) = f(p_2(\theta))$.

This concludes the proof that for any continuous function on S^{n-1}, there exists a set of equiangular vectors $\{\vec{p}_1, \vec{p}_2, ..., \vec{p}_n\}$ on S^{n-1} where $\vec{p}_i.\vec{p}_j = -\frac{1}{n}$ and $f(\vec{p}_1) = f(\vec{p}_2) = ... = f(\vec{p}_n)$. □

Extending the theorem to all of the $n+1$ vertices of the simplex requires further analysis of the specific function in question. One simple example is the function $f(\vec{r}) = 3x^2y - y^3$ on S^1. Since the function has D_6 symmetry group, we can generate a 2-simplex where all 3 vertices map to the same value of $f(\vec{r})$. Another general class of functions are ones where f_0 takes discrete values. Such functions necessarily form a subspace J_n where all the vectors map to f_0. As a result, $n+1$ of the vertices will map to the same value f_0.

2.3.2 The Existence Problem of SIC-POVMs in the Bloch Sphere

As shown in 2.3, a vector $\vec{r}$ on the surface of the Bloch sphere corresponds to a pure state density matrix if and only if $\sum_{ijk} d_{ijk} r_i r_j r_k = \frac{(n-1)(n-2)}{n^2}$. Let the function $f(\vec{r})$ be the polynomial function $\sum_{ijk} d_{ijk} r_i r_j r_k$. Since the function is continuous, theorem 2.2 shows that in the Bloch sphere of the n-dimensional Hilbert space, a regular (n^2-1)-simplex exists such that all but one of its vertices satisfy $f(\vec{p}_k) = f_0$ for some constant $f_0 \in [-\frac{(n-1)(n-2)}{n^2}, \frac{(n-1)(n-2)}{n^2}]$. A SIC-POVM on the other hand corresponds to a set of n^2 vectors $\vec{r}_k$ on the Bloch sphere, where $f(\vec{r}_k) = \frac{(n-1)(n-2)}{n^2}$ for all n^2 vectors. Consequently, the SIC existence problem can be equivalently stated as the following two questions. First, can the value f_0 take the maximum value of $\frac{(n-1)(n-2)}{n^2}$? Second, is the last vertex of the simplex, which can be written in its matrix form as

$$\Pi_{n^2} = n\mathbb{I} - \sum_{k}^{n^2-1} \Pi_k, \text{ where } \Pi_k = \frac{1}{n}\mathbb{I} + \vec{\Lambda} \cdot \vec{p}_k \ , \tag{2.57}$$

a pure state?

Regarding the first question, the function $f(\vec{r})$ was chosen to be the simplest among all the functions derived from $Tr(\rho^k)$. In principle, the question can be expressed for any of the $\{Tr(\rho^k), k > 2\}$ functions, which has the maximum value if ρ is a pure state density matrix.

In general, theorem 2.2 shows that some orientation of the simplex exists where all the vertices correspond to density matrices with the same $Tr(\rho^k)$ value. In dimensions greater than 3, the existence of SIC-POVMs requires that the theorem 2.2 be valid for continuous values of f_0. This result is particularly interesting in the 3-dimensional Hilbert space, where $Tr(\rho^2)$ and $Tr(\rho^3)$ uniquely identify a density matrix up to a unitary transformation. If the value of f_0 is a maximum value of the trace functions, then there exist continuous orientations of the simplex for continuous values of f_0, as shown in theorem 2.3. In dimension 3, the continuous value of f_0 means that a set of 8 density matrices, which are equivalent up to unitary transformations can be constructed. We confirmed the results numerically and found that, in dimensions 3 and 4, simplexes exist such that all the n^2 vertices are mapped to some values f_0 on the functions $Tr(\rho^3)$ and $Tr(\rho^4)$.

Theorem 2.3. *Let V be a set of (n^2-1) vectors $\{\vec{p}_k\}$ on the Bloch sphere of an n-dimensional Hilbert space where $n \geq 3$, such that $\vec{p}_j \cdot \vec{p}_k = -\frac{1}{n^2-1}|\vec{p}_j||\vec{p}_k|$ and $\forall k, f(\vec{p}_k) = f_0$, for the continuous function f given in A.36. Then, a SIC-POVM exists in n-dimensional Hilbert space only if the set of vectors V exists for a continuous value of f_0.*

Proof. We start by assuming that theorem 2.2 holds for a discrete value of $f_0 = \frac{(n-1)(n-2)}{n^2}$, Which is the necessary condition for purity of a density matrix. Let the set of n^2 vectors $\{\vec{p}_k\}$ form the SIC-POVM. Consider the subspace J_{n^2-2} generated by the vectors $\{\vec{p}_k\}$, which as shown in 2.2 is isomorphic to S^1. Based on our assumption, $f(\vec{x}) = f_0$ for all vector $\vec{x} \in J_{n^2-2}$. The subspace J_{n^2-2} contains the last 3 vectors of the set. Let the three density matrices be $\{\rho_a, \rho_b, \rho_c\}$, which correspond to the vectors $\{\vec{p}_{n^2-2}, \vec{p}_{n^2-1}, \vec{p}_{n^2}\}$ on the Bloch sphere, respectively.

Next, we will construct the circle J_{n^2-2} by using the vectors. For computational simplicity, we will use the Gell-Mann matrices as the basis vectors. This will allow us to write the vectors as matrices, where the dot product of two vectors is replaced with a trace.

The subspace J_{n^2-2} can be constructed by using the three vectors as follows. Let the three vectors $\vec{r}_1, \vec{r}_2, \vec{r}_3$ represent the vectors $\{\vec{p}_{n^2-2}, \vec{p}_{n^2-1}, \vec{p}_{n^2}\}$. Define the midpoint vector of the three vectors as $r_0 = \frac{1}{3}(\vec{r}_1 + \vec{r}_2 + \vec{r}_3)$ and the vectors connecting $\vec{r}_0$ to $\vec{r}_k$ as $\vec{v}_k$, i.e., $\vec{v}_k = \vec{r}_k - \vec{r}_0$. The subspace J_{n^2-1} can then be written as some linear combination of the basis vectors $\vec{e}_1$ and $\vec{e}_2$ given by the expressions

$$\begin{aligned} \vec{e}_1 &= \vec{v}_1 \ , \\ \vec{e}_2 &= \vec{v}_2 - \tfrac{\vec{v}_2.\vec{v}_1}{|\vec{v}_1|^2}\vec{v}_1 \ . \end{aligned} \tag{2.58}$$

After normalizing $\vec{e}_2$ to have the same magnitude as $\vec{e}_1$, we can define the circle as $\cos(\theta)\vec{e}_1 + \sin(\theta)\vec{e}_2$. First, we express the vectors $\vec{v}_k$ using the matrix representation by using the Gell-Mann matrices as $\vec{r}_k \to \vec{r}.\vec{\Lambda} = \rho_k - \frac{1}{n}\mathbb{I}$ as

$$\begin{aligned} \vec{v}_1 &\to \tfrac{2}{3}\rho_a - \tfrac{1}{3}(\rho_b + \rho_c) \ , \\ \vec{v}_2 &\to \tfrac{2}{3}\rho_b - \tfrac{1}{3}(\rho_a + \rho_c) \ , \\ \vec{v}_3 &\to \tfrac{2}{3}\rho_c - \tfrac{1}{3}(\rho_a + \rho_b) \ . \end{aligned} \tag{2.59}$$

We form the vectors $\vec{e}_1$ and $\vec{e}_2$ similarly, where $\vec{v}_2.\vec{v}_1 = \frac{1}{2}Tr\Big((\frac{2}{3}\rho_1 - \frac{1}{3}(\rho_2+\rho_3))(\frac{2}{3}\rho_2 - \frac{1}{3}(\rho_1+\rho_3))\Big)$ and $\vec{v}_1.\vec{v}_1 = \frac{1}{2}Tr\Big((\frac{2}{3}\rho_1 - \frac{1}{3}(\rho_2+\rho_3))^2\Big)$, which becomes

$$\begin{aligned} \vec{e}_1 &\to \tfrac{2}{3}\rho_a - \tfrac{1}{3}(\rho_b + \rho_c) \ , \\ \vec{e}_2 &\to \tfrac{1}{\sqrt{3}}(\rho_b - \rho_c) \ . \end{aligned} \tag{2.60}$$

Then, we write the circle J_{n^2-2} as $\cos(\theta)\vec{e}_1 + \sin(\theta)\vec{e}_2 + \vec{r}_0$, which has the following form in the matrix representation,

$$\begin{aligned} \Omega = &(\tfrac{2}{3}\cos(\theta) + \tfrac{1}{3})\rho_a + (-\tfrac{1}{3}\cos(\theta) + \tfrac{1}{\sqrt{3}}\sin(\theta) + \tfrac{1}{3})\rho_b \\ &+(-\tfrac{1}{3}\cos(\theta) - \tfrac{1}{\sqrt{3}}\sin(\theta) + \tfrac{1}{3})\rho_c - \tfrac{1}{n}\mathbb{I} \ . \end{aligned} \tag{2.61}$$

If $f(\vec{x}) = \frac{(n-1)(n-2)}{n^2}$ for all vectors in J_{n^2-2}, then the matrix shown in 2.61 must satisfy $Tr\Big((\frac{1}{n}\mathbb{I}+\Omega)^3\Big) = 1$ for all θ. We expand the trace of $(\frac{1}{n}\mathbb{I}+\Omega)^3$ as

$$\begin{aligned} Tr\Big((\tfrac{1}{n}\mathbb{I}+\Omega)^3\Big) = \tfrac{1}{9(n+1)^{3/2}} \quad &\Bigg(-4\alpha + 2\cos(3\theta)\left(2\alpha + \sqrt{n+1}n - 2\sqrt{n+1}\right) \\ &+7\sqrt{n+1}n + 13\sqrt{n+1}\Bigg) \ , \end{aligned} \tag{2.62}$$

where α is the cosine of the phase of the triple product $Tr(\rho_a\rho_b\rho_c)$. From 2.62, the

coefficient of $\cos(3\theta)$ vanishes for $\alpha = \frac{1}{2}(\sqrt{n+1}n - 2\sqrt{n+1})$. Since $-1 \leq \alpha \leq 1$, n can only be 3, where $\alpha = -1$. Therefore, for dimensions greater than 3, $f(\vec{x})$ takes a continuous value for $\vec{x} \in J_{n^2-2}$ and as a result, theorem 2.2 holds for a continuous value of f_0.

In dimension 3, we can use the identity presented in corollary 2 of the article Appleby et al. (2011),

$$\sum_{rst} Tr(\Pi_r \Pi_s \Pi_t) = n^4 \ , \tag{2.63}$$

to show that all the phases of the triple product can not be π. We can then choose three vectors of the SIC-POVMs that satisfy $Tr(\rho_a \rho_b \rho_c) \neq \pi$ to show that f_0 takes continuous values, i.e., for all $\vec{r} \in J_{n^2-2}$, $a \leq f(\vec{r}) \leq \frac{(n-1)(n-2)}{n^2}$ for some $a < \frac{(n-1)(n-2)}{n^2}$. Then, we can apply the orthogonal operators U_k sequentially to construct a set of vectors such that $f(\vec{p}_k)$ takes a continuous value, there by concluding the proof.

□

Theorem 2.3 can be extended to all $Tr(\rho^k)$ functions for $k > 3$. To show this, note that pure states can be identified by any one of the functions for powers $k \geq 3$, as shown in section 2.1.2. As a result, if a subspace J_{n^2-2} containing only pure states doesn't exist, then the functions $Tr(\rho^k)$ cannot be 1 for any subspace J_{n^2-1} as well. Consequently, continuous generalized SIC-POVMs must exist for any function $Tr(\rho^k)$.

In both dimensions, we searched for generalized SIC-POVMs, such that all of the elements have the same $Tr(\rho^3)$ or $Tr(\rho^4)$. In dimension 3, we generated 10^4 solutions with precision of $O(10^{-18})$ by starting from a known SIC-POVM and minimizing the function $\sum_k^{n^2} (f(\vec{p}_k) - f_0)^2$ for arbitrary values $f_0 \in [-\frac{2}{9}, \frac{2}{9}]$, where $f(\vec{r})$ is the polynomial

$$\begin{aligned} f(\vec{r}) \ &= 2\sqrt{3}r_1^2 r_8 + 6r_1 r_2 r_3 + 6r_1 r_5 r_6 + 3r_2^2 r_7 - \sqrt{3}r_2^2 r_8 \\ &-6r_2 r_4 r_6 - 3r_3^2 r_7 - \sqrt{3}r_3^2 r_8 + 6r_3 r_4 r_5 + 2\sqrt{3}r_4^2 r_8 \\ &+3r_5^2 r_7 - \sqrt{3}r_5^2 r_8 - 3r_6^2 r_7 - \sqrt{3}r_6^2 r_8 + 2\sqrt{3}r_7^2 r_8 - \frac{2r_8^3}{\sqrt{3}} \ . \end{aligned} \tag{2.64}$$

Similarly, we generated general SIC-POVMs $\{\Pi_k\}$ such that $Tr(\Pi_k^3) = f_0$ and $Tr(\Pi_k^4) = f_0$ separately. Such general SIC-POVMs have been constructed analyti-

cally in many dimensions Appleby (2007); Yoshida & Kimura (2022).

2.4 Symmetries of the Bloch Sphere and Invariant Theory

The SIC-POVM as shown in section 2.3 forms the vertices of a regular (n^2-1)-simplex in the Bloch sphere oriented such that each vertex satisfies $f(\vec{r}_k) = \frac{(n-1)(n-2)}{n^2}$. The unitary group connects SIC-POVM vectors continuously which define the unitarily equivalence class of SIC-POVM. We will now show that the only continuous transformation that connects different SIC-POVMs is the subset of $SO(n^2-1)$ shown in equation 2.25. Once we show that the equivalent classes are disconnected we will explore discrete symmetries of the Bloch sphere.

2.4.1 Continuous Symmetry of the Bloch Sphere

The geometry of the pure states on the Bloch sphere is entirely determined by the $Tr(\rho^3)$ function. Thus, a global symmetry in general can derived from the function,

$$f(\vec{r}) = \sum_{ijk} d_{ijk} r_i r_j r_k. \tag{2.65}$$

For a continuous symmetry over the transformations G, we can always define an infinitesimal transformation $\mathbb{I} + \eta\Omega$ by using the anti-symmetric generating matrix Ω.

$$G = \{M | M = exp\{\int_0^1 \Omega \, d\eta\} = \lim_{N\to\infty} (\mathbb{I} + \frac{1}{N}\Omega)^N, \Omega^T = -\Omega\} \tag{2.66}$$

If the function f is an invariant of a continuous transformation, then it must be fixed at the infinitesimal form of the transformation. Applying the transformation on the function $[\mathbb{I} + \delta\Omega](f) = f((\mathbb{I} + \delta\Omega).\vec{r})$, we generate the following expression.

$$f((\mathbb{I}+\delta\Omega).\vec{r}) = \sum_{ijk} d_{ijk}(\delta_{il}+d\eta\Omega_{il})r_l(\delta_{jm}+d\eta\Omega_{jm})r_m(\delta_{kn}+d\eta\Omega_{kn})r_n \tag{2.67}$$

$$\begin{aligned}(\mathbb{I}+\delta\Omega)(f(\vec{r})) = \sum_{ijk} d_{ijk}r_ir_jr_k + d\eta\sum_{ijk} d_{ijk}(\sum_l \Omega_{il}r_lr_jr_k + r_i\sum_m \Omega_{jm}r_mr_k \\ + r_lr_j\sum_n \Omega_{kn}r_n) + O(d\eta^2)\end{aligned} \tag{2.68}$$

For the transformation to be a symmetry of the function, the correction in the first order of η must vanish. This gives us a set of linear equations which we solve to get the explicit form of the transformation. For dimension 3 example, the general form of the matrix Ω is an anti-Hermitian matrix with $n^2(n^2-1)/2$ free parameters. After solving the linear equations, we generate the following generating matrix.

(2.69)

$$\Omega = \begin{pmatrix} 0 & m_{3,4}-m_{5,6} & m_{2,4} & -\frac{m_{6,8}}{\sqrt{3}} & -\frac{m_{3,8}}{\sqrt{3}} & -\frac{m_{4,8}}{\sqrt{3}} & -2m_{4,6} & 0 \\ m_{5,6}-m_{3,4} & 0 & \frac{m_{6,8}}{\sqrt{3}} & -\frac{m_{5,8}}{\sqrt{3}} & -\frac{m_{4,8}}{\sqrt{3}} & \frac{m_{3,8}}{\sqrt{3}} & -2m_{4,5} & 0 \\ -m_{2,4} & -\frac{m_{6,8}}{\sqrt{3}} & 0 & m_{3,4} & m_{4,6} & -m_{4,5} & \frac{m_{3,8}}{\sqrt{3}} & m_{3,8} \\ \frac{m_{6,8}}{\sqrt{3}} & \frac{m_{5,8}}{\sqrt{3}} & -m_{3,4} & 0 & m_{4,5} & m_{4,6} & \frac{m_{4,8}}{\sqrt{3}} & m_{4,8} \\ \frac{m_{3,8}}{\sqrt{3}} & \frac{m_{4,8}}{\sqrt{3}} & -m_{4,6} & -m_{4,5} & 0 & m_{5,6} & -\frac{m_{5,8}}{\sqrt{3}} & m_{5,8} \\ \frac{m_{4,8}}{\sqrt{3}} & -\frac{m_{3,8}}{\sqrt{3}} & m_{4,5} & -m_{4,6} & -m_{5,6} & 0 & -\frac{m_{6,8}}{\sqrt{3}} & m_{6,8} \\ 2m_{4,6} & 2m_{4,5} & -\frac{m_{3,8}}{\sqrt{3}} & -\frac{m_{4,8}}{\sqrt{3}} & \frac{m_{5,8}}{\sqrt{3}} & \frac{m_{6,8}}{\sqrt{3}} & 0 & 0 \\ 0 & 0 & -m_{3,8} & -m_{4,8} & -m_{5,8} & -m_{6,8} & 0 & 0 \end{pmatrix}$$

Notice that this has the same form as the matrix 2.78. Thus showing that the only continuous symmetry of the Bloch sphere is the symmetry to unitary transformations.

Conversely, If we take the matrix $\Omega = \sum_c f_{abc}t_c$ for some $\vec{t} \in \mathbb{R}^{n^2}$, the first order correction becomes,

$$
\begin{aligned}
&= \sum_{ijk} d_{ijk}(\sum_{l} \Omega_{il} r_l r_j r_k + r_i \sum_{m} \Omega_{jm} r_m r_k + r_i r_j \sum_{n} \Omega_{kn} r_n) \\
&= \sum_{ijk} d_{ijk}(\sum_{l} \sum_{a} f_{ila} t_a r_l r_j r_k + r_i \sum_{m} \sum_{a} f_{jma} t_a r_m r_k + r_i r_j \sum_{n} \sum_{a} f_{kna} t_a r_n \\
&= \sum_{jkla} \sum_{q} \Big(d_{qjk} f_{qla} + d_{jqk} f_{qla} + d_{jkq} f_{qla} \Big) t_a r_l r_j r_k \\
&= \sum_{jkla} \sum_{q} \Big(d_{jkq} f_{qla} + d_{klq} f_{qja} + d_{ljq} f_{qka} \Big) t_a r_l r_j r_k
\end{aligned}
\tag{2.70}
$$

Using the Jacobi identity $\sum_q (d_{jkq} f_{qla} + d_{klq} f_{qja} + d_{ljq} f_{qka}) = 0$, we show the first order correction is indeed zero, (for further detail check Borodulin, Slabospitsky & Rogalyov (1995)).

2.4.2 Surfaces Formed by the Trace Cube function in Dimension 3

The function $f_3(\vec{x}) = \sum d_{ijk} x_i x_j x_k$, where d_{ijk} is the trace of triple products of the Gell-Mann matrices together with $f_2(\vec{x}) = \sum \delta_{ij} x_i x_j$ form a 6 dimensional smooth non-singular (has a unique tangent everywhere) surface embedded in $\mathbb{R}^8$. To construct the surface we write the following two equations.

$$
f_2(\vec{x}) - \frac{1}{3} = 0 \tag{2.71}
$$

$$
f_3(\vec{x}) - \frac{2}{9} = 0 \tag{2.72}
$$

This forms a 6-manifold since one can construct the local tangent space at $\vec{x}_0 \in M^6$ by solving the following:

$$
(x_i - x_{0i}) \frac{\partial}{\partial x_i} f_2 = 0 \tag{2.73}
$$

$$
(x_i - x_{0i}) \frac{\partial}{\partial x_i} f_3 = 0 \tag{2.74}
$$

where the $rank[\frac{\partial}{\partial x_i} f_2, \frac{\partial}{\partial x_i} f_3] = 2$.

The functions f_2 and f_3 are invariants of the group $\Omega = \{exp(f_{ijk}c_k), \vec{c} \in \mathbb{R}^8, f_{ijk} = -\frac{i}{2}(d_{ijk} - d_{jik})\}$. Therefor we can alternatively generate manifolds using this transformation for any value of the functions f_2 and f_3.

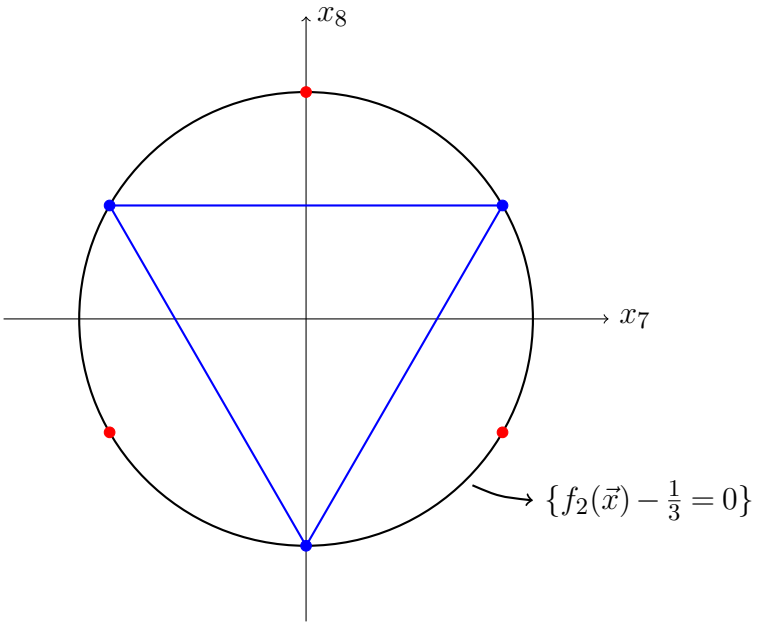

Figure 2.4 We have the diagonal subspace shown in the figure. The vertices of the triangle correspond to the three pure states. The three red dots belong to a manifold which is an inverse of the projective plane $\mathbb{CP}^3$ which contains all the pure states.

The proper definition of the manifolds we look at the local structure by using the group Ω. Let $u \in \Omega$, then we can write $u_{ij} = exp(f_{ijk}c_k)$ where $\vec{c} \in \mathbb{R}^8$ and let $\vec{r}$ be an element of the diagonal subspace where $|\vec{r}|^2 = \frac{1}{3}$. let's also define a surface M centered at $\vec{r}$ generated by the functions f_2 and f_3.

We can construct the tangent space applying infinitesimal transformations of Ω on the vector $\vec{r}$ since the polynomials f_2 and f_3 are invariants of the group ofΩ. I.e., We choose $u = \exp(f_{ijk}\delta c_k)$ where $\delta c_k \ll 1$.

$$u(\delta\vec{c}) = \exp(f_{ijk})\delta c_k \approx \mathbb{I} + f_{(ijk)}\delta c_k \tag{2.75}$$

Note that the operation $u(\delta\vec{c})$ fixes all vector belonging to the same basis subspace of $\vec{c}$, (I.e., $u(\delta\vec{c}).\vec{r} = \vec{r}$). This is easy to see if we think of the operations in the complex space, where if both the inverse map of $\delta\vec{c}$ and $\vec{r}$ commute the operation u fixes $\vec{r}$. This means we that the vector $\vec{c}$ must not be in the diagonal subspace since we chose the vector $\vec{r}$ to be in the diagonal subspace.

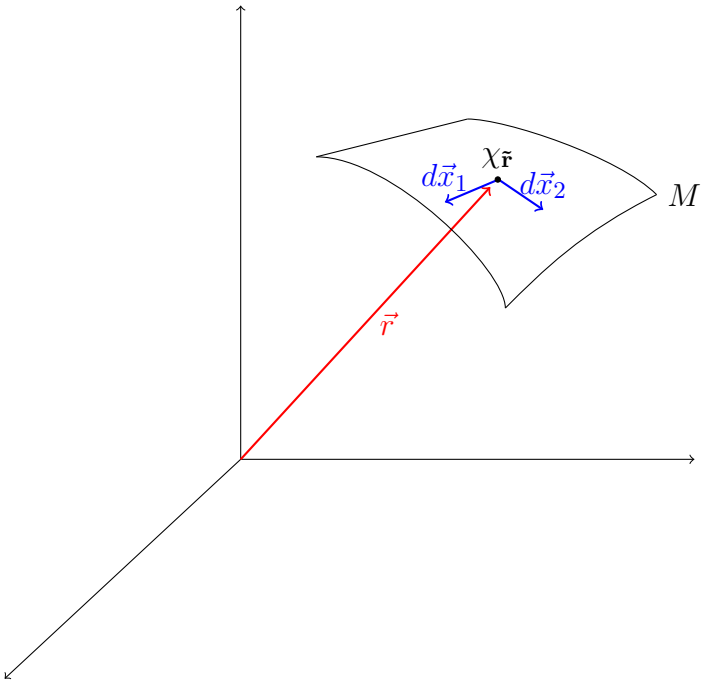

Figure 2.5 The vectors $d\vec{x}_k$ are the basis vectors of the tangent subspace $\chi_{\vec{r}} \in M$.

$$\vec{r} = (0,0,0,0,0,0,r_7,r_8) \tag{2.76}$$

$$\delta\vec{c} = (\delta c_1, \delta c_2, \delta c_3, \delta c_4, \delta c_5, \delta c_6, 0, 0) \tag{2.77}$$

By using the generating vector we create the orthogonal operation to the first order in $\delta\vec{c}$ as shown in equation (2.78). The first order approximation defines the tangent subspace $\chi_{\vec{r}} \in M$. By using $U(\delta\vec{c})$ we generate the tangent subspace $T_\chi M$ around the point $\vec{r}$ (2.79), from which we can form the basis vectors for the subspace.

(2.78)

$$U(\delta\vec{c}) \approx \begin{pmatrix} 1 & 0 & \delta c_6 & -\delta c_5 & \delta c_4 & -\delta c_3 & -2\delta c_2 & 0 \\ 0 & 1 & \delta c_5 & \delta c_6 & -\delta c_3 & -\delta c_4 & 2\delta c_1 & 0 \\ -\delta c_6 & -\delta c_5 & 1 & 0 & \delta c_2 & \delta c_1 & -\delta c_4 & -\sqrt{3}\delta c_4 \\ \delta c_5 & -\delta c_6 & 0 & 1 & -\delta c_1 & \delta c_2 & \delta c_3 & \sqrt{3}\delta c_3 \\ -\delta c_4 & \delta c_3 & -\delta c_2 & \delta c_1 & 1 & 0 & \delta c_6 & -\sqrt{3}\delta c_6 \\ \delta c_3 & \delta c_4 & -\delta c_1 & -\delta c_2 & 0 & 1 & -\delta c_5 & \sqrt{3}\delta c_5 \\ 2\delta c_2 & -2\delta c_1 & \delta c_4 & -\delta c_3 & -\delta c_6 & \delta c_5 & 1 & 0 \\ 0 & 0 & \sqrt{3}\delta c_4 & -\sqrt{3}\delta c_3 & \sqrt{3}\delta c_6 & -\sqrt{3}\delta c_5 & 0 & 1 \end{pmatrix}$$

$$U(\delta\vec{c}).\vec{r}-\vec{r}\approx\begin{pmatrix}-2\delta c_2 r_7\\ 2\delta c_1 r_7\\ -\delta c_4(r_7+\sqrt{3}r_8)\\ \delta c_3(r_7+\sqrt{3}r_8)\\ \delta c_6(r_7-\sqrt{3}r_8)\\ \delta c_5(-r_7+\sqrt{3}r_8)\\ 0\\ 0\end{pmatrix} \tag{2.79}$$

The tangent space shown in equation (2.79) is a 6 dimensional euclidean space given by $(d\tilde{x}_1, d\tilde{x}_2, d\tilde{x}_3, d\tilde{x}_4, d\tilde{x}_5, d\tilde{x}_6, 0, 0)^T$. However when the point $\vec{r}$ represents a pure state or the "inverse" of a pure state, i.e.,($\vec{r}_{pure}$ or $-\vec{r}_{pure}$) the tangent space is 4 dimensional. For example, if we take the point $\vec{r}=(0,\ldots,-\frac{1}{\sqrt{3}})^T$ the corresponding tangent space is $(0,0,\delta c_4,-\delta c_3,\delta c_6,-\delta c_5,0,0)^T$. For the given example, the tangent basis vectors are $(0,0,d\tilde{x}_3,d\tilde{x}_4,d\tilde{x}_5,d\tilde{x}_6,0,0)$. Since any point $\vec{r}$ can be constructed using an orthogonal transformation (which preserves norm) we can generate the tangent basis vectors at any point by simply applying the same operation to the basis vectors we generated for the diagonal subspace. From the we conclude that the equations $f_2-\frac{1}{3}=0$ and $f_3\pm\frac{2}{9}=0$ form a 4-manifold $\mathbf{M^4}$ and the equations $f_2-\frac{1}{3}=0$ and $f_3-a=0,-\frac{2}{9}<a<\frac{2}{9}$ form a 6-manifold $\mathbf{M^6}$.

Lemma 2.3. *The manifolds* $\mathbf{M^4}$ *and* $\mathbf{M^6}$ *are compact orientable manifolds.*

Proof. For a manifold to be compact means, the manifold is both bounded and closed. The equation $f_2-\frac{1}{3}=0$ shows that both $\mathbf{M^4}$ and $\mathbf{M^6}$ are bounded. That is to say all elements of the manifolds lie with in some finite distance from one another. The second equation $f_3-a=0$ defines a map from $\mathbb{S}^7$ to $\mathbb{R}$. This map is continuous and therefor the preimage of the closed set $f_3^{-1}(a)$ must be closed. This concludes the proof that the manifolds $\mathbf{M}^4$ and $\mathbf{M}^6$ are compact.

To prove the manifolds are orientable, we must find a chart for both manifolds. Define the coordinate charts $(\mathbf{M}^4,\varphi)$ and $(\mathbf{M}^6,\phi)$.

Let the vectors $\vec{r}_d$ and $\vec{r}'_d$ represent a vector belonging to the diagonal subspace of the Bloch sphere such that we can explicitly write down the manifolds as,

$$\mathbf{M}^4=\{U\cdot\vec{r}_d:\forall U\in\Omega\} \tag{2.80}$$

$$\mathbf{M}^6=\{U\cdot\vec{r}'_d:\forall U\in\Omega\} \tag{2.81}$$

Let the ordered basis for the tangent space $T_r M^4$ and $T_{r'} M^6$ as τ_d and τ'_d respectively.

$$\tau_d = \{dx^1, dx^2, dx^3, dx^4, dx^5, dx^6\} \tag{2.82}$$

$$\tau'_d = \{dx^3, dx^4, dx^5, dx^6\} \tag{2.83}$$

The two bases generate homeomorphisms describing the neighbourhood around the point r_d and r'_d. Therefore, the coordinate charts at the points $\vec{r}_d$ and $\vec{r}'_d$ are $(\vec{r}_d, \tau_d)$ and $(\vec{r}'_d, \tau'_d)$ respectively. For an arbitrary points $\vec{x} \in \mathbf{M}^4$ and $\vec{x}' \in \mathbf{M}^6$, the coordinate charts can be generated by using the orthogonal transformations $\in \Omega$.

$$\varphi_x = U_x \tau_d \text{ , and } \phi_{x'} = U_{x'} \tau'_d \tag{2.84}$$

where, $\vec{x} = U_x \vec{r}_d$ and $\vec{x}' = U_{x'} \vec{r}'_d$.

Because of the symmetries in the eigenvalues of the operations, U_x are not uniquely defined. Thus in its current form φ_x is ill-defined. To fix this, without explicitly showing how, we assign a single $\tilde{U}_x$ to define φ_x. I.e., $\tilde{U}_x \in \omega_x$ where $\omega_x = \{U_x : \forall U_x, U_x \cdot \vec{r}_d = x\}$. Then we define the chart,

$$\varphi_x = \tilde{U}_x \tau_d \tag{2.85}$$

which is well defined. Finally we have coordinate charts in $\mathbf{M}^4$ and $\mathbf{M}^6$ as

$$\{\mathbf{M}^4, \tilde{U}_x \tau_d\} \text{ , and } \{\mathbf{M}^6, \tilde{U}_{x'} \tau'_d\} \tag{2.86}$$

Being orientable for a manifold means, we can define charts for the manifold which have fixed orientations. To shown this, consider two points infinitesimally close to each other. We parametrize the transformation matrices that maps the charts to each other can be parameterized with an infinitesimal vector $\vec{c}$. For the two manifolds, the corresponding transformations to the first order in $\delta\vec{c}$ are as follows.

$$B^4 \cong \delta \begin{pmatrix} 1 & c^4 & 0 & c^1 \\ -c^4 & 1 & c^1 & 0 \\ 0 & -c^1 & 1 & c^4 \\ -c^1 & 0 & -c^4 & c^1 \end{pmatrix} \tag{2.87}$$

$$B^6 \cong \delta \begin{pmatrix} 1 & c^6 & c^5 & 0 & -c^3 & -c^2 \\ -c^6 & 1 & c^4 & -c^3 & 0 & c^1 \\ -c^3 & -c^4 & 1 & c^2 & c^1 & 0 \\ 0 & c^3 & -c^2 & 1 & c^6 & -c^5 \\ c^3 & 0 & -c^1 & -c^6 & 1 & c^4 \\ c^2 & -c^1 & 0 & c^5 & -c^4 & 1 \end{pmatrix} \tag{2.88}$$

Since the determinant of both transformations is 1 up to the first order in $\delta\vec{c}$, the transformation preserve the orientation of the charts.

$$\det(B^4) \approx 1 + \mathcal{O}(|\delta c|^2) \text{ , and } \det(B^6) \approx 1 + \mathcal{O}(|\delta c|^2) \tag{2.89}$$

To show that this extends to the hole of the manifolds, note that we can assign frames to the charts such that there is at least one continuous line connecting $\vec{x} \in \mathbf{M}$ and $\vec{r}_d \in \mathbf{M}$. For the case of $\mathbf{M}^6$, the map $\phi : \Omega \mapsto \mathbf{M}^6$, $\vec{x}' = U_{x'} \cdot \vec{r}'_d$ is a homeomorphism. Therefore the corresponding ordered frame $\tau'_x = U_{x'} \cdot \tau'_d$ forms a continuous differentiable vector field on $\mathbf{M}^6$. This shows that the manifold.

In the case of $\mathbf{M}^4$, the frames $\tau_x = \tilde{U}_x \tau_d$ may not form a differential vector field. This is because the elements of $\mathbf{M}^4$ do not belong to unique basis. consider the following continuous transformations to x such that we get two different frames at x, τ_x and $\tilde{\tau}_x$. We have two unitary operators such that $\vec{x} = U_x \cdot \vec{r}_d$ and $\vec{x} = \tilde{U}_x \cdot \vec{r}_d$. The difference between U_x and $\tilde{U}_x$ is that it maps the vector $\vec{r}_d$ to two different bases. Let the two bases be $b = \{\vec{a}, \vec{b}, \vec{c}\}$ and $\tilde{b} = \{\vec{\tilde{a}}, \vec{\tilde{b}}, \vec{\tilde{c}}\}$. We construct an operator $\hat{O}$ such that $\tilde{b} = \hat{O} b$, which has a matrix form shown below.

$$\begin{pmatrix} \alpha & \beta & 0 & \gamma \\ -\beta & \alpha & \gamma & 0 \\ 0 & -\gamma & \alpha & \beta \\ -\gamma & 0 & -\beta & \alpha \end{pmatrix} \tag{2.90}$$

where,

$$\alpha = \frac{1}{2} e^{\sqrt{-c1^2 - c4^2}} \left(1 + e^{2\sqrt{-c1^2 - c4^2}}\right) \tag{2.91}$$

$$\beta = \frac{c4 e^{-\sqrt{-c1^2 - c4^2}} \left(-1 + e^{2\sqrt{-c1^2 - c4^2}}\right)}{2\sqrt{-c1^2 - c4^2}} \tag{2.92}$$

$$\gamma = \frac{c1 e^{-\sqrt{-c1^2 - c4^2}} \left(-1 + e^{2\sqrt{-c1^2 - c4^2}}\right)}{2\sqrt{-c1^2 - c4^2}} \tag{2.93}$$

The matrix $\hat{O}$ has determinant 1, thus the operator preserves the orientation. This shows that even though the orthogonal matrices U_x are not uniquely defined for the point $\vec{x}$, they are all orientation preserving transformations. With that we conclude the proof that both manifolds $\mathbf{M}^4$ and $\mathbf{M}^6$ are compact orientable manifolds.

□

2.4.2.1 Euler Characteristics of $\mathbf{M}^4$ and $\mathbf{M}^6$

If ν is a smooth vector field with isolated singularities on a closed oriented differentiable manifold $\mathbf{M}^k$, then the sum of the indices of ν is the Euler characteristic of $\mathbf{M}^k$; that is,

$$\sum_m i_m = \chi(\mathbf{M}^k) \tag{2.94}$$

This is known as the Poincare-Hopf theorem.

Since both $\mathbf{M}^4$ and $\mathbf{M}^6$ are constructed using transformations $\Omega \cong SU(3)$ applied on the vector $\vec{r}_d$, The coordinate charts everywhere is similar to the chart on the point $\vec{r}_d$. This indicates that the manifolds have no boundary. In conclusion, the

manifolds are compact orientable manifolds with no boundary. I.e., they are closed orientable manifolds. Then, we can use the Poincare-Hopf theorem to compute the Euler characteristics of both manifolds.

To apply the theorem, we start by defining a vector field on the manifolds with isolated singularities. The infinitesimal transformation $U(\delta c)$ for a given $\vec{c}$ are ideal for this task, as the displacement vectors associated with the operations form tangent vectors fields on the manifolds. Define the vector field ν as,

$$\nu = \{U(\delta\vec{c}) \cdot \vec{x} - \vec{x} : \forall x \in \mathbf{M}, \delta\vec{c} = \delta(0,0,0,0,0,0,c_7,c_8)\}. \tag{2.95}$$

In order for ν to have isolated singularities we require that $\delta\vec{c}$ uniquely belongs to a basis. One such $\delta\vec{c}$ can be $\delta\vec{c} = \epsilon(0,\ldots,0,\sin(\pi/6),\cos(\pi/6)$ where $\epsilon \ll 1$. The vector can be written in its matrix form as below, where we see that it is not degenerate.

$$\delta\vec{c} \rightarrow \begin{pmatrix} \frac{1}{3} & 0 & 0 \\ 0 & \frac{1}{3} - \epsilon & 0 \\ 0 & 0 & \frac{1}{3} + \epsilon \end{pmatrix} \tag{2.96}$$

Expanding $U(\delta\vec{c})$ to the first order in $\vec{c}$ we get the matrix O_{jk} where $O_{13} = -O_{24} = -O_{31} = O_{42} = \epsilon$, $-O_{35} = O_{53} = 2\epsilon$ and all others terms are zero. We can then simplify the vector field explicitly as,

$$\nu = \{\epsilon(x_4, -x_5, -2x_6, -x_1, x_2, 2x_3, 0, 0); \forall\vec{x} \in \mathbf{M}\} \tag{2.97}$$

where $\mathbf{M}$ can be $\mathbf{M}^4$ or $\mathbf{M}^4$. The only singularities of the vector field are found in the diagonal subspace. The 3 blue points and 3 red points in the figure 2.6, generate the $\mathbf{M}^4$ manifolds one for each color. All other vectors form a $\mathbf{M}^6$ manifold under the operations Ω. In other words, each color corresponds to the intersection of $\mathbf{M}$ and the diagonal subspace. Thus, to $\mathbf{M}^4$ has 3 singularities and the manifold $\mathbf{M}^6$ has 6 singularities.

The index of the vector field ν around a singularity is equal to the degree of the map $\mu : \partial D \mapsto S^k$ where D is an infinitesimal closed ball around the singularity and,

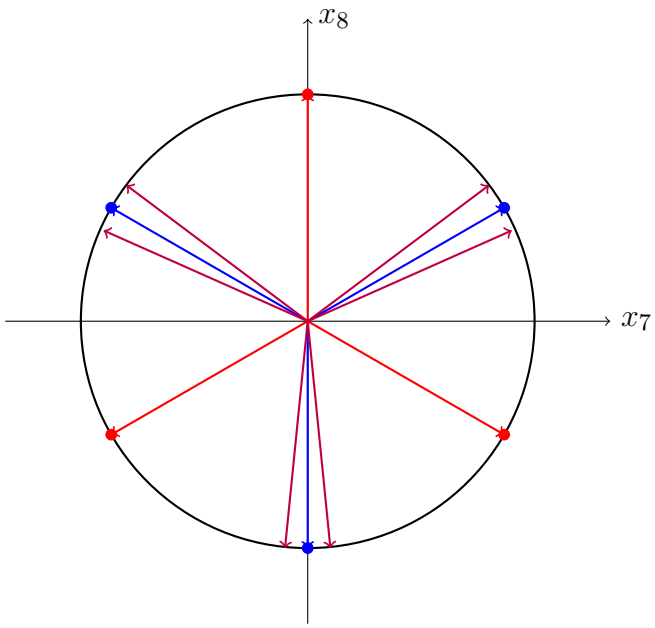

Figure 2.6 The intersection of the diagonal subspace and 2 $\mathbf{M}^4$ manifolds formed by the pure state and its inverse on the Bloch vectors, depicted with colors blue and red. The purple colored vectors are the intersection with $\mathbf{M}^6$ manifold.

$$\mu(\vec{Y}) = \frac{\nu(\vec{Y})}{|\nu(\vec{Y})|}, \text{ where } |Y| = 1. \tag{2.98}$$

In the case of $\mathbf{M}^4$, the map is $\mu : \partial D \mapsto S^3$ and in the case of $\mathbf{M}^6$, $\mu : \partial D \mapsto S^5$. Applying the expression of $\nu(\vec{Y})$, for the vector $\vec{r}_d = (0,0,0,0,0,0,0,-\frac{1}{\sqrt{3}})$ in $\mathbf{M}^4$ we get,

$$\mu(\vec{Y}) = \frac{(-y_5, -2y_6, y_2, 2y_3)}{\sqrt{1+3(y_3^2+y_6^2)}}. \tag{2.99}$$

Similarly for $\mathbf{M}^6$ we get,

$$\mu(\vec{Y}) = \frac{(y_4, -y_5, -2y_6, -y_1, y_2, 2y_3)}{\sqrt{1+3(y_3^2+y_6^2)}}. \tag{2.100}$$

Both maps are orientation preserving homeomorphisms, since the transformations matrices $Y \to \mu(Y)$ excluding the normalization has a positive determinant. The degree of an orientation preserving homeomorphism is $+1$, and noting that all singular

points on the diagonal subspace have the same index we conclude,

$$\chi(\mathbf{M}^4) = 3 \text{ , and } \chi(\mathbf{M}^6) = 6 \tag{2.101}$$

We can generalize these results to higher dimensions where the Euler characteristic is determined by the degeneracy of the operators. For dimensions 4, we get the manifolds $\mathbf{M}^6$, $\mathbf{M}^1 1$ and $\mathbf{M}^{24}$, with the Euler characteristics $4, 6$ in the first two types of manifolds, and in the third type manifold there are surfaces with Euler characteristics of 12 and 24. The vectors that satisfy 2.2 form an generalized SIC-POVM (without the rank restriction) exist on these manifolds.

2.4.3 General Symmetries of the Bloch Sphere

The discrete symmetry of a Bloch sphere generates all the disjoint equivalent classes of SIC-POVMs. First, lets consider trivial symmetries of the trace cube function. We will once again take dimension 3 to demonstrate the trivial discrete symmetries. The trivial transformations that fix equation (2.64) are reflection operations. We can easily identify these transformations by looking reflections that would fix $r_1 r_3 r_5 + r_2 r_4 r_5 - r_2 r_3 r_6 + r_1 r_4 r_6$. We present these $[a,b,c] = \{Diag(x_1, x_2, ..., x_8) |\ \forall k \in \{a,b,c\}, x_k = -1 \text{ and } \forall k \notin \{a,b,c\}, x_k = 1\}$. The reflection operations are $\{[126],[135],[234],[456],[2356],[1346],[1245]\}$. If we include the identity operation to the list, these set forms a group generated by $< [136],[145],[235],[246] >$.

In general, to find the discrete symmetries of the polynomial (2.64), We need to find linear transformations for which the polynomial is invariant to. The study of the transformations that fix a polynomial is known as Invariant Theory, (check the book Derksen & Kemper (2015) for more detail on invariant theory). Invariant theory allows us to write the problem in its most general and complete form. Let's solve a simple example for dimension 3 before we write the problem in its complete form.

Example 2.1. *consider the simpler case where* $\vec{r} = \{0,0,0,0,0,0,r_7,r_8\}$. *Then the trace cube equation reduces to* $f(r_7,r_8) = -\frac{2r_8^3}{\sqrt{3}} + 2\sqrt{3} r_7^2 r_8$. *we first write the complete polynomial with two parameters* $f(r_7,r_8) = c_1 r_7^3 + c_2 r_7^2 r_8 + c_3 r_7 r_8^2 + c_4 r_8^3$ *where* $\vec{c} = \{0, 2\sqrt{3}, 0, -\frac{2}{\sqrt{3}}\}$. *A* 2×2 *orthogonal matrix* O *acts on* f *as* $O(f) \mapsto f(O\vec{r})$.

(2.102) $$O = \{\begin{pmatrix} a & b \\ -b & a \end{pmatrix}, \begin{pmatrix} a & b \\ b & -a \end{pmatrix}\}, a^2 + b^2 = 1$$

we can rewrite the transformation as 4×4 *transformations applied on the coefficients of the vector* $\vec{c}$*. If the function* f *is an invariant of an operation* O*, then* $\vec{c}$ *will be an eigenvector to the matrix* $\tilde{O}$*. The two types matrices of* O *have determinant 1 and -1 respectively.*

(2.103)
$$\tilde{O} = \{\begin{pmatrix} a^3 & -a^2b & ab^2 & -b^3 \\ 3a^2b & (a^3 - 2ab^2) & b^3 - 2a^2b & 3ab^2 \\ 3ab^2 & (2a^2b - b^3) & a^3 - 2ab^2 & -3a^2b \\ b^3 & ab^2 & a^2b & a^3 \end{pmatrix}, \begin{pmatrix} a^3 & a^2b & ab^2 & b^3 \\ 3a^2b & -(a^3 - 2ab^2) & b^3 - 2a^2b & -3ab^2 \\ 3ab^2 & -(2a^2b - b^3) & a^3 - 2ab^2 & 3a^2b \\ b^3 & -ab^2 & a^2b & -a^3 \end{pmatrix}\}$$
$$, a^2 + b^2 = 1$$

(2.104) $$\begin{pmatrix} 0 \\ 2\sqrt{3} \\ 0 \\ -\frac{2}{\sqrt{3}} \end{pmatrix} = \begin{pmatrix} a^3 & \mp a^2b & ab^2 & \mp b^3 \\ 3a^2b & \pm(a^3 - 2ab^2) & b^3 - 2a^2b & \pm 3ab^2 \\ 3ab^2 & \pm(2a^2b - b^3) & a^3 - 2ab^2 & \mp 3a^2b \\ b^3 & \pm ab^2 & a^2b & \pm a^3 \end{pmatrix} \begin{pmatrix} 0 \\ 2\sqrt{3} \\ 0 \\ -\frac{2}{\sqrt{3}} \end{pmatrix}$$

This gives 6 solutions which forms a dihedral group of order 6, which is obvious when we look at the plot of $f(r_7, r_8)$ *shown in figure 2.7.*

(2.105)
$$\{\begin{pmatrix} 1 & 0 \\ 0 & 1 \end{pmatrix}, \begin{pmatrix} -\frac{1}{2} & -\frac{\sqrt{3}}{2} \\ \frac{\sqrt{3}}{2} & -\frac{1}{2} \end{pmatrix}, \begin{pmatrix} -\frac{1}{2} & \frac{\sqrt{3}}{2} \\ -\frac{\sqrt{3}}{2} & -\frac{1}{2} \end{pmatrix}, \begin{pmatrix} -1 & 0 \\ 0 & 1 \end{pmatrix}, \begin{pmatrix} \frac{1}{2} & -\frac{\sqrt{3}}{2} \\ -\frac{\sqrt{3}}{2} & -\frac{1}{2} \end{pmatrix}, \begin{pmatrix} \frac{1}{2} & \frac{\sqrt{3}}{2} \\ \frac{\sqrt{3}}{2} & -\frac{1}{2} \end{pmatrix}\}$$

For the complete polynomial, the vector $\vec{c}$ corresponds to the structure factor of the Gell-Mann matrices d_{ijk}. The dimension of the vector is equal to the number of order-3 monomias with $n^2 - 1$ variables given by the $n^2 - 1$ multi-combination 3.

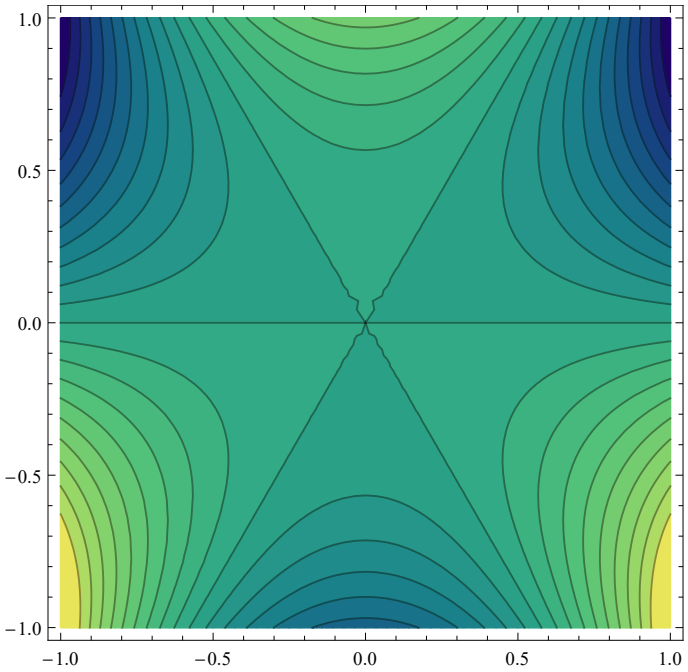

Figure 2.7 The x-axis is r_7 and the y-axis is r_8. The D_6 symmetry is apparent from the contour plot of $f(r_7, r_8)$.

$$\left(\binom{n^2-1}{3}\right) = \binom{(n^2-1)+3-1}{3} = \binom{n^2+1}{3} \tag{2.106}$$

The corresponding matrix O is the union of the $(n^2-1)\times(n^2-1)$ orthogonal matrices with determinants $+1$ and -1. We transform the matrix O to the space of $\vec{c}$ in similar manner to the example to form a $\binom{n^2+1}{3}\times\binom{n^2+1}{3}$ matrix. The elements are polynomials of the 3rd order and even for the simplest dimension of interest, i.e., dimension 3 where the matrix $\tilde{O}$ is 120×120, the number of variables is too large for a general solution. We can derive the continuous symmetry from the expression by approximating the operator O to the first order in its generator. For a discrete symmetry however, we must rely on numerical solutions of the equation:

$$\vec{c} = \tilde{O}\cdot\vec{c} \tag{2.107}$$

We can rely on matrices O which can be written as finite sum of their generates to generate group structures with in the symmetry of the Bloch sphere. Without any constraint on the generators, we will have to guess different symmetries and attempt to construct explicit solutions.

It is worth noting that the global invariant of the trace cube equation gives us the smallest set of equivalence classes. We may still have symmetries of SIC-POVMs that are not shared by the Bloch sphere. To adders the complexity of the solving (2.107) and to exploring the complete symmetries of the SIC-POVM, We need to formulate a numerical method to construct and characterise general solutions.

3. Structure and Construction of Group Covariant SIC-POVMs

Since the work by Zauner, it has been known that we can construct SIC-POVMs using the Weyl-Heisenberg group. Group covariance reduces the search of SIC-POVMs to a search of a fiducail vector. Group covariant SIC-POVMs have been constructed in all dimensions 2-151 and some higher dimensions, reaching as high as 1151 Fuchs (2010). We will cover the essentials of the known construction of SIC-POVMs before we proceed with general approach to the equivalence classes.

3.1 Group Covariant SIC-POVMs

SIC-POVMs are formed by a set of n^2 equiangular vectors in an n-dimensional Hilbert space. The only restriction on these vectors is that the modulus square of the inner products of the vectors must be $\frac{1}{n+1}$ (see definition (2.3)). Applying the condition on the $2n^2(n-1)$ free parameters gives us a set of polynomials, which has no general solution. If we assume that our solution is group covariant, meaning that all the SIC-POVM elements can be generated as the orbit of a special vector on a group, the problem simplifies significantly and in the dimensions 2-4 can be easily solved by hand (see Appendix A). The group proposed by Zauner and independently by Renes et.al. Renes et al. (2004) was the Weyl-Heisenberg group.

3.1.1 The Weyl-Heisenberg Group

The Weyl-Heisenberg group is a generalization of the Pauli group in dimensions > 2. The group is isomorphic to $\mathbb{Z}_n \times \mathbb{Z}_n$ for a given dimension n. The group is generated by the phase operators $\hat{Z} = \sum_{k=0}^{n-1} e^{i\frac{2\pi k}{n}} |k\rangle\langle k|$ and the shift operator

$\hat{X} = \sum_{k=0}^{n-1} |(k+1) \mathrm{mod} n\rangle\langle k|$.

Definition 3.1. *In n-dimensional Hilbert space, the Weyl-Heisenberg group is a set of unitary operators* $\{\hat{D}_{\boldsymbol{p}}\}$*. The elements of the group are defined as,*

$$\hat{D}_{\boldsymbol{p}} = \tau^{p_1 p_2} \hat{X}^{p_1} \hat{Z}^{p_2} \tag{3.1}$$

where $\boldsymbol{p} = \begin{pmatrix} p_1 \\ p_2 \end{pmatrix}, p_1, p_2 \in \mathbb{Z}_n$ *and* $\tau = -e^{i\frac{\pi}{n}}$*. The product of the group elements gives us,*

$$\hat{D}_{\boldsymbol{p}} \hat{D}_{\boldsymbol{q}} = \tau^{<\boldsymbol{p},\boldsymbol{q}>} \hat{D}_{\boldsymbol{p}+\boldsymbol{q}} \tag{3.2}$$

where $<\boldsymbol{p},\boldsymbol{q}> = p_2 q_1 - p_1 q_2 \hat{D}_{\boldsymbol{p}+\boldsymbol{q}}$.

Note that the Weyl-Heisenberg group forms a proper group under the equivalence relation $\{e^{i\theta} D_{\boldsymbol{p}} \sim \hat{D}_{\boldsymbol{p}} : \forall \theta \in [0, 2\pi]\}$. This is not an issue to the construction of SIC-POVMs since global phase of the vectors does not appear in the POVM elements. The particular form of the group elements was chosen to simplify the product of the elements.

From the definition, one can easily prove that $\hat{D}_{\boldsymbol{p}}^{\dagger} = \hat{D}_{-\boldsymbol{p}}$ and $Tr(\hat{D}_{\boldsymbol{p}}) = \delta_{0,\boldsymbol{p}} n$. The Weyl-Heisenberg group, being the generalization of the Pauli group, spans the Hilbert space and thus quantum states or density operators can be expanded using the group ,Appleby, Bengtsson, Flammia & Goyeneche (2019). For a given density operators $\hat{\rho}$,

$$\hat{\rho} = \frac{\mathbb{I}}{n} + \frac{1}{n\sqrt{n+1}} \sum_{\boldsymbol{p}} e^{i\theta_{\boldsymbol{p}}} \hat{D}_{\boldsymbol{p}} \tag{3.3}$$

where

$$e^{i\theta_{\boldsymbol{p}}} = \begin{cases} 1 & \boldsymbol{p}=\boldsymbol{0} \mathrm{mod} n \\ \sqrt{n+1} Tr(\hat{D}_{\boldsymbol{p}}^{\dagger} \hat{\rho}) & \text{else} \end{cases}. \tag{3.4}$$

To generate a SIC-POVM, one must find vector $|\psi_0\rangle$ such that the set of vectors $\{\hat{D}_{\boldsymbol{p}} |\psi_0\rangle\}$ are all equiangular. Such vector is known as a "fiducial" vector. This reduces the construction of SIC-POVMs to only $2n-2$ variables. The general solution to dimension 3 and 4 can be found in Appendix A. Renes et al. (2004) presented a list of fiducial vectors constructed numerically (see Table 3.1). These fiducial vectors all formed SIC-POVMs as orbits on the standard Weyl-Heisenberg group defined

above. The connection between the fiducial vectors comes from the Clifford group. Starting from 2005 by Appleby (2005) later by Zhu (2010) and Scott (2017); Scott & Grassl (2010), the fiducial vectors were computed studied extensively studies using the Clifford group.

n	Number of SIC-POVMs
2	2
3	∞(uncountable)
4	16
5	80

Table 3.1 Renes presented the number of fiducial vector for dimensions 2-7 though exhaustive numerical search. The complete list can be found in Renes et al. (2004)

3.1.2 The Clifford Group

The Clifford group $C(n)$ is a group of unitary operations that maps the Weyl-Heisenberg group onto its self. In a mathematical language, it is a normalizer of the Weyl-Heisenberg group. In quantum information, the Clifford group is used in the stabilizer formalism for quantum error correction code Nielsen & Chuang (2010). We will define the Clifford group using the indexing of Appleby from Appleby (2005).

Let the $\bar{n}$ be n for odd dimensions and $2n$ for even dimensions. Then define the group $SL(2,\mathbb{Z}_{\bar{n}})$ as a group of 2×2 matrices with determinant $1(\text{mod } \bar{n})$. For every Clifford unitary $U \in C(n)$, there exists a matrix $F \in SL(2,\mathbb{Z}_{\bar{n}})$ and a vector $\chi \in \mathbb{Z}_n \times \mathbb{Z}_n$ such that,

$$U\hat{D}_{\boldsymbol{p}}U^{\dagger} = \tau^{2<\chi,F\boldsymbol{p}>}\hat{D}_{F\boldsymbol{p}} \tag{3.5}$$

For all $\boldsymbol{p} \in \mathbb{Z}_n \times \mathbb{Z}_n$.

The Clifford unitaries are commonly represented by the pair (F,χ). Given a matrix $F \in SL(2,\mathbb{Z}_{\bar{n}})$,

$$F = \begin{pmatrix} a & b \\ c & d \end{pmatrix} \tag{3.6}$$

The matrix form of the Clifford unitary is given by,

$$(F, \boldsymbol{\chi}) = \hat{D}_{\boldsymbol{\chi}} V_F \tag{3.7}$$

where $\langle j|V_F|k\rangle = \frac{1}{\sqrt{n}}\tau^{b^{-1}(ak^2-2jk+dj^2)}$ and $b^{-1}b = 1 \bmod \bar{n}$. The product of two Clifford unitaries (F_1, χ_1) and (F_2, χ_2) is given by $(F_1F_2, \chi_1 + F_1\chi_2)$. By definition, the Weyl-Heisenberg matrices are also elements of the Clifford group, since $\hat{D}_{\boldsymbol{q}}\hat{D}_{\boldsymbol{p}}\hat{D}_{\boldsymbol{q}}^{\dagger} = \hat{D}_{\boldsymbol{q}}\hat{D}_{\boldsymbol{p}}\hat{D}_{-\boldsymbol{q}} = \tau^{2<\boldsymbol{q},\boldsymbol{p}>}\hat{D}_{\boldsymbol{p}}$. The generating operators of the Weyl-Heisenberg group can also be represented in using the symplectic matrix and a vector as follows.

$$\hat{X} = \left[\begin{pmatrix} 1 & 0 \\ 0 & 1 \end{pmatrix}, \begin{pmatrix} 1 \\ 0 \end{pmatrix}\right], \hat{Z} = \left[\begin{pmatrix} 1 & 0 \\ 0 & 1 \end{pmatrix}, \begin{pmatrix} 0 \\ 1 \end{pmatrix}\right] \tag{3.8}$$

As shown above, given a fiducial vector $|\psi_0\rangle$, the SIC-POVM is given by the set,

$$\Pi_{\boldsymbol{p}} = \frac{1}{n}\hat{D}_{\boldsymbol{p}}|\psi_0\rangle\langle\psi_0|\hat{D}_{\boldsymbol{p}}^{\dagger}. \tag{3.9}$$

When we apply a Clifford unitary $U_{(F,\chi)}$ on the SIC-POVM operators, we simply generate another SIC-POVM.

$$U_{(F,\chi)}\Pi_{\boldsymbol{p}}U_{(F,\chi)}^{\dagger} = \frac{1}{n}U_{(F,\chi)}\hat{D}_{\boldsymbol{p}}|\psi_0\rangle\langle\psi_0|\hat{D}_{\boldsymbol{p}}^{\dagger}U_{(F,\chi)}^{\dagger} \tag{3.10}$$

$$= \frac{1}{n}U_{(F,\chi)}\hat{D}_{\boldsymbol{p}}U_{(F,\chi)}^{\dagger}U_{(F,\chi)}|\psi_0\rangle\langle\psi_0|U_{(F,\chi)}^{\dagger}U_{(F,\chi)}\hat{D}_{\boldsymbol{p}}^{\dagger}U_{(F,\chi)}^{\dagger} \tag{3.11}$$

Since $U_{(F,\chi)}\hat{D}_{\boldsymbol{p}}U_{(F,\chi)}^{\dagger} = \tau^{2<\chi,F\boldsymbol{p}>}\hat{D}_{F\boldsymbol{p}}$, which is just another Weyl-Heisenberg operator $\tau^{2<\chi,F\boldsymbol{p}>}\hat{D}_{F\boldsymbol{p}}$, the vector $U_{(F,\chi)}|\psi_0\rangle$ must be a fiducial vector. The orbit of the fiducial vector on the Clifford group gives us all the possible fiducial vectors of the Weyl-Heisenberg group covariant SIC-POVMs.

The complete set of fiducial vectors also includes the complex conjugate of the vectors. This is generalized in the Extended Clifford group $EC(n)$, which is the group $C(n) \cup \hat{K}C(n)\hat{K}^{\dagger}$ where $\hat{K}$ is the anti-unitary operator. The Extended Clifford

group has $2n^5\Pi_{p|n}(1-\frac{1}{p^2})$ elements where p goes over all the primes that divide n. Immediately, we see that the number of fiducial vectors listed in 3.1 is less than the order of the extended Clifford group $|EC(n)|$, for example, in dimension 4 $|EC(n)| = 1536$ and in dimension 5 $|EC(n)| = 6000$. The difference indicates that the fiducial vectors are eigenvectors of the Clifford unitaries. This symmetry of the fiducial vectors is of vital importance in the construction of SIC-POVMs, since it reduces the number of free parameters. The next question would be, which Clifford unitaries contain the fiducial vectors in their eigenbasis? This will be the next topic of discussion.

3.1.3 Zauner Symmetry and Order-3 Unitaries and the Analytic Construction of the Fiducial Vector

When constructing SIC-POVMs, even though group covariance reduces the difficulty significantly, as dimensions grow we are faced with the inescapable challenge of solving polynomial equations. Further reduction of the free parameters comes from the symmetries of the fiducial vectors in the extended Clifford group as discussed above. Zauner conjectured that a fiducial vector exists which is an eigenvector for the matrix shown in (3.12). The matrix is now known as Zauner matrix.

$$\hat{\mathcal{Z}} = \frac{e^{i\pi\frac{n-1}{12}}}{\sqrt{n}} \sum_{jk}^{n} \tau^{2jk+j^2} |j\rangle\langle k| \tag{3.12}$$

The eigenvalues of $\hat{\mathcal{Z}}$ are simply the cube roots of unities $e^{ik\pi/3}$ for $k \in \{0,1,2\}$, each with the dimension of the degenerate subspace $\dim(\hat{\mathcal{Z}}_k) = \lfloor (n+3-2k)/3 \rfloor$. Consider a 4-dimensional fiducial vector $|\psi_0\rangle$ that is an eigenvector of $\hat{\mathcal{Z}}$, which means

$$\hat{\mathcal{Z}}|\psi_0\rangle = |\psi_0\rangle, \tag{3.13}$$

where the eigenvalue is 1. Then, we can expand the vector $|\psi\rangle$ in the degenerate subspace of dimension 2 spanned by $\{\alpha_0|\xi_0\rangle, \alpha_1|\xi_1\rangle\}$.

$$|\psi_0\rangle = \alpha_1|\xi_1\rangle + \alpha_s|\xi_2\rangle \tag{3.14}$$

We have reduced the number of free variables to just 2 which simplifies to construction. The other two eigenbasis have just one vector which we can simply check if they are fiducial vectors.

The Zauner matrix is not the only symmetry that exists. Appleby et.al. Appleby (2005) generalized the symmetry and showed that in all the dimensions SIC-POVMs are known, the fiducial vectors are eigenvectors of order-3 Clifford unitaries. This included the Zauner matrix which is an order-3 Clifford unitary, i.e., $\hat{\mathcal{Z}}^3 = \mathcal{I}$. The results were further expanded and classified in Scott & Grassl (2010) and later Scott (2017). The standard representation of the order-3 Clifford unitaries F_z for Zauner matrix which stabilizes SIC-POVMs in most dimensions known, F_a in dimensions $n = 9k + 3$. Order-2 Clifford unitaries also have been found that stabilize fiducial vectors in dimensions $n = k^2 - 1$ and $n = (3k \pm 1)^2 + 3$ labeled as F_b and F_c respectively.

With all the simplifications we have described, the task of analytic solutions is very challenging. In many dimensions, we rely on numerical methods to construct fiducial vectors.

3.2 Numerical Construction of SIC-POVMs

The numerical construction of SIC-POVMs can in principle be done by solving the n^2 polynomial equations,

$$|\langle\psi_0|\hat{D}_{\boldsymbol{q}}^{\dagger}\hat{D}_{\boldsymbol{p}}|\psi_0\rangle|^2 = \frac{1}{n+1}. \tag{3.15}$$

This would unnecessarily complicate the calculation. Instead, we rely on a property of tight frames, which the SIC-POVMs are, to define a single function and where the fiducial solution is found by minimizing the functions. Before we introduce the numerical method, we will describe the SIC-POVMs as a special type of a frames

and the resulting bounds satisfied by tight frames. The concept of frames is a familiar topic in mathematics and engineering with applications in signal processing, Kovacevic & Chebira (2007a,0). We will restrict our discussion of frames to just the SIC-POVMs and only introduce the relevant properties of frames.

3.2.1 Tight Frames

Frames are a generalization of bases for a vector space. Let the set of vectors $\{|\xi_k\rangle\}$ be a frame spanning the vector space V. Then for any vector $|\psi\rangle \in V$ we have the inequality,

$$A\langle\psi|\psi\rangle \leq \sum_k |\langle\psi|\xi_k\rangle|^2 \leq B\langle\psi|\psi\rangle \tag{3.16}$$

where $0 < A \leq B < \infty$, Waldron (2018). If $A = B$ the frame becomes a tight frame. Examples of tight frames include, any orthogonal basis for the real vector space and a eigenbasis of a quantum observable or a complete quantum measurement such as the SIC-POVM and MUBs. Consider the SIC-POVM $\{\Pi_k = \frac{1}{n}|\psi_k\rangle\langle\psi_k|\}$. Due to the completeness condition $\sum_k \Pi_k = \mathbb{I}$. Then for an arbitrary state $|\phi\rangle$ we have,

$$\langle\phi|\mathbb{I}|\phi\rangle = \sum_k \frac{1}{n}|\langle\phi|\psi_k\rangle|^2 \tag{3.17}$$

The constants become $A = B = n$ proving that the SIC-POVMs are tight frames. More precisely, the SIC-POVM forms an equiangular tight frame. The approach to the SIC-POVMs from the frame point of view allows us to write constraints on the fiducial vectors such as the Welch bound, which is instrumental in the construction of the operators.

3.2.2 The Welch Bounds

Consider the n^2 normalized tight frame $|\xi_k\rangle$, where $\sum_k |\xi_k\rangle\langle\xi_k| = \mathbb{I}$. We can describe the frame up to a unitary equivalence by using the matrix P, where $\langle j|P|k\rangle = \langle\xi_j|\xi_k\rangle$, Appleby et al. (2019).

$$P \circ P = \begin{pmatrix} \langle\xi_1|\xi_1\rangle^2 & \langle\xi_1|\xi_2\rangle^2 & \dots \\ \langle\xi_2|\xi_1\rangle^2 & \langle\xi_2|\xi_2\rangle^2 & \dots \\ \vdots & \vdots & \ddots \end{pmatrix} \tag{3.18}$$

The matrix P is known as the Gram matrix. The Gram matrix of SIC-POVMs will be discussed in more detail in the next chapter. For now we only need it show the emergence of the bound briefly for one of the bounds before we give the full form. The matrix $P \circ P$

From the triangle inequality $|\vec{u}|^2|\vec{v}|^2 \geq (\vec{u}\cdot\vec{v})^2$, we form the identity,

$$m\sum_k u_k^2 \geq (\sum_k u_k)^2 \tag{3.19}$$

Where we took $\vec{v} = \{\underbrace{1,\dots,1}_{m},0,\dots,0\}$ and m is the number of non-zero elements of $\vec{u}$. We will apply the inequality on the eigenvalues of the matrix $P \circ P$ as follows.

$$Tr(P \circ P) = \sum_k \lambda_k = n^2 \tag{3.20}$$

$$Tr((P \circ P)^2) = \sum_k \lambda_k^2 = \sum_{jk} |\langle\xi_j|\xi_k\rangle|^4 \tag{3.21}$$

Let $u_k = \lambda_k$, then m is the rank of $P \circ P$ and the inequality can be written as,

$$\sum_{jk} |\langle\xi_j|\xi_k\rangle|^4 \geq \frac{n^4}{\text{Rank}(P \circ P)} \tag{3.22}$$

By absolute maximum of the rank of $P \circ P$ is $\frac{n(n+1)}{2}$. To show this, consider the

$n \times n^2$ matrix $V = (\xi_1, \ldots, \xi_{n^2})$. By definition the Gram matrix is formed by $P = V^\dagger V$. Define the set of n vectors $\{\langle \nu_k|\}$ as the column vectors of $V = \begin{pmatrix} \langle \nu_1| \\ \langle \nu_2| \\ \vdots \end{pmatrix}$. Then, we can equivalently write the Gram matrix as $P = \sum_k^n |\nu_k\rangle\langle\nu_k|$. We can then expand the $P \circ P$ into rank-1 operators and compute the maximum bound.

$$P \circ P = \sum_k |\nu_k \circ \nu_k\rangle\langle\nu_k \circ \nu_k| + 2\sum_{j\neq k} |\nu_j \circ \nu_k\rangle\langle\nu_j \circ \nu_k| \tag{3.23}$$

since $\text{rank}(A+B) \leq \text{rank}(A) + \text{rank}(B)$, the rank of $P \circ P$ is at most $\frac{n(n+1)}{2}$. Finally we find the Welch bound of index 2.

$$\sum_{jk} |\langle \xi_j | \xi_k \rangle|^4 \geq \frac{2n^3}{n+1} \tag{3.24}$$

A tight frame that satisfies the bound (3.24) is known as a spherical-2 design. Renes eq al. Renes et al. (2004) proved that the SIC-POVMs are a only equiangular tight frames that saturate the bound (3.24). The general Welch bound is given by the equation , and a frame satisfying the bound for a given t forms a Spherical-t design Delsarte, Goethals & Seidel (1991). The Spherical designs have applications in experimental design, geometry and in our case quantum state tomography.

$$\sum_{j,k}^{N} |\langle \psi_j | \psi_k \rangle|^{2t} \geq N^2 \binom{n+t-1}{t}^{-1} \text{, where } t \in \mathbb{Z}^+ \tag{3.25}$$

3.2.3 Numerical Construction of the Fiducial Vector

The SIC-POVMs are spherical-2 design, so they satisfy the bound (3.24). For Weyl-Heisenberg group covariant SIC-POVMs, we write the equation,

$$\sum_{\boldsymbol{q},\boldsymbol{p}} |\langle \psi_0 | \hat{D}_{\boldsymbol{q}}^\dagger \hat{D}_{\boldsymbol{p}} | \psi_0 \rangle|^4 \geq \frac{2n^3}{n+1} \tag{3.26}$$

in low dimensions, it is possible to directly search for global minima of the sum. Even though the convergence rate is fast, the function has local minima and the main time consuming part is to find a suitable initial point. In higher dimensions, we must us the symmetries described in 3.1.3. So far, numerical solutions are known in all dimensions up to 151 and some higher dimensions, the highest being 19603 Appleby, Bengtsson, Grassl, Harrison & McConnell (2022). In our research into general equivalent classes of SIC-POVMs, the Weyl-Heisenberg solutions are restrictive. We need to have a means of generating solutions with out the restriction of group covariance if we are to make general statement about the SIC-POVMs. This will be the focus of our analysis in the next chapter.

4. Symmetries of the SIC Gram Matrix in Dimensions 4-7

Identifying the symmetry of the physical state on the Bloch sphere proved to be a complicated task as discussed in 2.3.2. One of the challenges with the approach of invariant theory was that we were searching for a symmetry of the entire physical states, while the symmetry of SIC-POVMs need not be a symmetry of the Bloch sphere. To further our understanding and to be able to move forward with our analysis, we need a way of capturing the SIC-POVM vectors in a compact form. Since the SIC-POVM is a tight frame, the Gram matrix achieves this takes perfectly. As shown in chapter 2, the Gram matrix has been central in understanding the group covariant SIC-POVMs. In our case, we want to apply it in its most general form in order to generalize the geometry of SIC-POVMs.

4.1 Generalized Numerical Construction of SIC Gram Matrices

The Gram matrix of the SIC-POVMs uniquely represents the tight frame up to unitary transformation. Thus, it is possible to reconstruct the SIC-POVM given a Gram matrix. Instead of solving the series of polynomials (3.15), we generate a valid Gram matrix. The Welch bound can also be used to generate a general SIC-POVMs, however, because (3.24) have local minima that correspond to informationally complete POVMs it is impractical to search for a general SIC-POVM. The number of free parameters in (3.24) is $2n^2(n-1)$. We found that generating the Gram matrix directly, which has $\frac{n^2(n^2-1)}{2}$ converges much faster in dimensions 3-7. We will generate solutions on these dimensions to explore the property of general SIC-POVMs.

Let's first introduce the Gram matrix for SIC-POVMs and its properties in detail. Then we can derive a method for constructing SIC-POVM Gram matrix. The Gram matrices have both continuous and discrete symmetry groups. we will first explore

the trivial symmetry groups.

4.1.1 The Gram Matrix

Let the set of projective operators $E_k = \frac{|\psi_k\rangle\langle\psi_k|}{n}$ form a SIC-POVM, then the Gram matrix P is the Hermitian matrix where $P_{jk} = \frac{1}{n}\langle\psi_j|\psi_k\rangle$. The SIC-POVMs are a tight frame and consequent the Gram matrix become a projective matrix. To show this, let's first define an $n^2 \times n$ matrix V as shown below.

$$V = \frac{1}{\sqrt{n}} \begin{pmatrix} \langle\psi_1| \\ \langle\psi_2| \\ \vdots \\ \langle\psi_{n^2}| \end{pmatrix} \tag{4.1}$$

Using the matrix V, we write the Gram matrix as $P = VV^\dagger$ and the completeness relations as,

$$V^\dagger V = \sum_k |\phi_k\rangle\langle\psi_k| = \mathbb{I}. \tag{4.2}$$

The completeness condition of the POVM shows that all generalized quantum measurements form tight frames whether equiangular or not. The Gram matrix is hermitian since $(VV^\dagger)^\dagger = VV^\dagger$. Now consider the square of the Gram matrix,

$$\begin{aligned} P^2 &= VV^\dagger VV^\dagger \\ &= V(V^\dagger V)V^\dagger \\ &= V(\mathbb{I}_{n\times n})V^\dagger = VV^\dagger \\ &= P \end{aligned} \tag{4.3}$$

Proving that the gram matrix of a tight frame a projective matrix. We can immediately deduce that the eigenvalues of the Gram matrix are either 0 or 1, and the trace of the Gram matrix gives us the rank. The trace of the Gram matrix

is $Tr(P) = \sum_k^{n^2} \frac{1}{n}\langle\psi_k|\psi_k\rangle$. Since the vectors of the SIC-POVM are normalized, $Tr(P) = n$ and rank $(P) = n$.

Once we generate a Gram matrix, we need to reconstruct the SIC-POVM vectors up to some unitary transformation. We can do this if we can construct the matrix V from a Gram matrix. Let's re-write the matrix $V = (|\omega_1\rangle, |\omega_2\rangle, \ldots, |\omega_n\rangle)$ where the vectors $|\omega_k\rangle \in \mathbb{C}^{n^2}$ are the column vectors of V. By applying the completeness relation, we can show that $\langle\omega_j|\omega_k\rangle = \delta_{jk}$.

$$V^\dagger V = \sum_{jk} \langle\omega_j|\omega_k\rangle |j\rangle\langle k| = \mathbb{I} \tag{4.4}$$

In order to get an identity the vectors $|\omega_k\rangle$ must be orthogonal. Similarly the Gram matrix can be constructed using the vectors $|\omega_k\rangle$.

$$P = VV^\dagger = \sum_k^n |\omega_k\rangle\langle\omega_k| \tag{4.5}$$

The expression above is just the expansion of the Gram matrix using the basis vectors $|\omega_k\rangle$, meaning that the vectors $|\omega_k\rangle$ are the eigenvectors of the Gram matrix with the eigenvalue of 1. We can then simply generate the vectors by solving for its n eigenvectors, and construct the matrix V.

Based on the definition of the SIC-POVMs, the Gram matrix elements take the form in equation (4.6). Lets define the space of $n^2 \times n^2$ hermitian matrices $\mathcal{B} = \{B : \phi_{jk} \in [0, 2\pi]\}$ that contains all Gram matrices by letting ϕ_{jk} be free parameters.

$$B_{jk} = \begin{cases} \frac{e^{i\phi_{jk}}}{n\sqrt{n+1}} & , j < k \\ \frac{e^{-i\phi_{jk}}}{n\sqrt{n+1}} & , j > k \\ \frac{1}{n} & , j = k \end{cases} \tag{4.6}$$

If any matrix $B \in \mathcal{B}$ is a rank-n projective matrix, then B is a valid Gram matrix of a SIC-POVM. Now, we just need to derive an equation to identify projective matrices which are elements of $\mathcal{B}$. Notice the similarity of identifying projective matrices in $\mathbb{C}^{n^2} \times \mathbb{C}^{n^2}$ and identifying the pure states, which are rank-1 projective matrices, on the Bloch sphere. Thus, we will use to the trace of the Gram matrix

to generate scalar function that we may use for numerical method. By definition, $Tr(P) = n$ and since the Gram matrix is a projective matrix, $Tr(P^k) = n$ for all positive integers k. All matrices $\in \mathcal{B}$ satisfy $Tr(B) = n$ and $Tr(B^2) = n$.

$$Tr(B^2) = Tr(\sum_k b_{ij} b_{jk} |j\rangle\langle k|) \tag{4.7}$$

$$= \sum_{jk} b_{kj} b_{jk} = \sum_{jk} b^*_{jk} b_{jk} \tag{4.8}$$

$$= n^2 \left(\frac{1}{n^2} + \frac{(n^2-1)}{n^2(n+1)} \right) = n \tag{4.9}$$

In theorem 4.1, we show that we only need to show $Tr(P^3) = n$ and $Tr(P^4) = n$ to identify a projective matrix within the space $\mathcal{B}$.

Theorem 4.1. *Given a matrix $B \in \mathcal{B}$, the equations $Tr(B^3) = n$ and $Tr(B^4) = n$ are sufficient and enough conditions to show that the matrix B is a projective matrix.*

Proof. lets define two functions $f(x)$ and $g(x)$ as below, where $\lambda_k (\in \mathbb{R})$ are the eigenvalues of the matrix.

$$g(x) = \sum_k \lambda_k^x \tag{4.10}$$

$$f(x) = \sum_k |\lambda_k|^x \tag{4.11}$$

We derive the following results from the definitions of the functions.

- $\forall x \in \mathbb{R}^+, g(x) = Tr(P^x)$.
- $\forall x = 2m, m \in \mathbb{N}, f(x) = g(x)$.
- $f(x) \geq \mathfrak{Re}[g(x)]$, Since $\forall \lambda_k \in \mathbb{R}, \mathfrak{Re}[\lambda_k^x] \leq |\lambda_k|^x$.

The function $f(x)$ is a convex function since $\frac{d^2}{dx^2} f = \sum_k (ln|\lambda_k|)^2 |\lambda_k|^x \geq 0$. therefore, $f(a) = f(b) = f(c) \iff |\lambda_k| \in \{0, 1\}$.

For even powers, $Tr(B^2) = g(2) = f(2) = n$ and $Tr(B^4) = g(4) = f(4) = n$. For odd powers, since $f(x)$ is an upper bound to $g(x)$ and is a convex function, $g(3) \leq f(3) \leq n$. Therefore, if $g(3) = n$, then $f(3) = g(3)$. This shows that λ_ks are either 0 or 1. Finally we conclude that if $Tr(B^3) = n$ and $Tr(B^4) = n$ for a matrix $B \in \mathcal{B}$ if and only if P is a projective matrix. □

4.1.2 Construction of SIC Gram Matrices with out the Constraint of Group Covariance

We can now expand the equations $Tr(B^3) = n$ and $Tr(B^4) = n$, which we will use to construct SIC-POVMs without the assumption of group covariance. By directly expanding the functions $Tr(B^3)$ and $Tr(B^4)$, where the matrix B takes the form shown in (4.6), we define the functions $\mathbf{f}_n(\Phi) = Tr(B^3)$ and $\mathbf{g}_n(\Phi) = Tr(B^4)$, where Φ corresponds to phase parameters as follows:

$$\mathbf{f}_n(\Phi) = \frac{3n-2}{n} + \frac{6}{n^3(n+1)^{\frac{3}{2}}} \sum_{a<b<c}^{n^2} \cos\left(\phi_{ab} + \phi_{bc} - \phi_{ac}\right) \tag{4.12}$$

$$\begin{aligned} \mathbf{g}_n(\Phi) = {} & \frac{2(n^3+2n^2-n-1)}{n^2(n+1)} + \frac{24}{n^4(n+1)^{\frac{3}{2}}} \sum_{a<b<c}^{n^2} \cos\left(\phi_{ab} + \phi_{bc} - \phi_{ac}\right) \\ & + \frac{8}{n^4(n+1)^2} \sum_{a<b<c<d}^{n^2} \Big[\cos\left(\phi_{ab} + \phi_{bc} + \phi_{cd} - \phi_{ad}\right) + \cos\left(\phi_{ab} + \phi_{bd} - \phi_{cd} - \phi_{ac}\right) \\ & \qquad + \cos\left(\phi_{ac} - \phi_{bc} + \phi_{bd} - \phi_{ad}\right) \Big] \end{aligned} \tag{4.13}$$

We can think of the phase variables as elements of a $\frac{n^2(n^2-1)}{2}$ dimensional vector, and represent each element of $\mathcal{B}$ by a unique vector up to mod(2π). We will refer to the set of phases as the phase vector of the Gram matrix. For the vector representation of the phase variables, we define a single index $\chi(a,b) = (a-1)n^2 - \frac{1}{2}a(a+1) + b$ where the indices a and b correspond to the index in the upper triangle of the Gram matrix. After this point, the phase vector Φ is represented using the index $\chi(a,b)$ where the value ranges from 1 to $n^2(n^2-1)/2$.

The equations $\mathbf{f}_n(\Phi)$ and $\mathbf{g}_n(\Phi)$ are presented in a way that makes some symmetries of the Gram matrices obvious. That includes the continuous symmetry of n^2-1 dimension and the discrete symmetry to the permutation operation. These symmetries are needed to identify and characterize general SIC-POVM solutions generated using the functions $\mathbf{f}_n$ and $\mathbf{g}_n$.

4.2 Local Structure of SIC Gram Matrices

4.2.1 Continuity Conditions of SICs

To identifying the continuous symmetry of the functions $\mathbf{f}_n(\Phi)$ and $\mathbf{g}_n(\Phi)$, let's first define the vectors $\vec{K}_{rst}$ such that the phases inside the cosine functions can be written as a dot product $\vec{K}_{rst} \cdot \Phi$. In the function $\mathbf{f}_n$, the vectors $\vec{K}_{rst}$ have 3 non zero elements. For example, consider the first cosine functions in $\mathbf{f}_n$ which is $\cos(\phi_1 + \phi_2 - \phi_3)$, then $\vec{K}_{1,2,3} = (1, -1, 0, \ldots, 0, 1, 0, \ldots, 0)$ has elements 1 at indices $\chi(1,2)$ and $\chi(2,3)$, -1 at the index $\chi(1,3)$ and 0 everywhere else. We can then write the cosine function as $\cos(\vec{K}_{1,2,3}.\Phi)$. Similarly, we rewrite $\mathbf{f}_n$ as,

$$\mathbf{f}_n(\Phi) = \frac{3n-2}{n} + \frac{6}{n^3(n+1)^{\frac{3}{2}}} \sum_{r,s,t} \cos(\vec{K}_{rst}.\Phi) \tag{4.14}$$

The simplest symmetry one would expect from the equations is one where all the cosine functions in the sum remain fixed, and we can check for such a symmetry by simply checking for the linear independence of the vectors $\vec{K}_{rst}$. Since the vectors are $n^2(n^2-1)/2$ dimensional, it suffices to take $n^2(n^2-1)/2$ vectors, which we will prove next.

Proposition 4.1. *The vectors $\vec{K}_{rst}$ which are conjugate to the phase vectors $\mathbf{\Phi}$ span a $(n^2-1)(n^2-2)/2$ vector space.*

Proof. The continuous symmetry of the functions $\mathbf{f}_n(\Phi)$ and $\mathbf{g}_n(\Phi)$ corresponds to the invariance of individual cosine functions in the functions $\mathbf{f}_n(\Phi)$ and $\mathbf{g}_n(\Phi)$ to a translation on the phase vector Φ. Lets define the vectors $\vec{K}_{abc}$ for $a < b < c$ such that $\cos(\vec{K}_{abc}.\Phi) = \cos(\phi_{ab} + \phi_{bc} - \phi_{ac})$. The continuous symmetry appears because the vectors K_{abc} do not span a $n^2(n^2-1)/2$ dimensional space.

Let's define a basis formed with the vectors $\mathbf{K} = \{K_{ijk} : i < j < k, j = i+1\}$. We will then show that any vector $\vec{K}_{abc}$ belongs to the space spanned by $\mathbf{K}$. For simplicity of further calculations, the vector $\vec{K}_{abc}$ is presented with its non zero indices as $(a,b) - (a,c) + (b,c)$.

Given indices a, b and c the phases $(\phi_{ab}, \phi_{bc}, \phi_{ac})$, we will start by adding elements of the basis $\mathbf{K}$ incrementally until we generate $\vec{K}_{abc}$.

$$(4.15)\quad (a,b)-(a,c)+(b,c) \to -((a,a+1)-(-a,b)+(a+1,b)) \\ +((a,a+1)-(-a,c)+(a+1,c))+(b,c)$$

Notice that the indices $(a+1,b)$ and $(a+1,c)$ are not part of the $\vec{K}_{abc}$, so we will add vectors from $\mathbf{K}$ to cancel the two elements. which will leave two terms, $(a+2,b)$ and $(a+2,c)$ that we need to removed. We repeat the process until $a+m=b-1$, as shown below.

$$\begin{aligned}(4.16)\quad (a,b)-(a,c)+(b,c) \to &-\Big((a,a+1)-(a,b)+(a+1,b)\Big) \\ &+\Big((a,a+1)-(a,c)+(a+1,c)\Big) \\ &-\Big((a+1,a+2)-(a+1,b)+(a+2,b)\Big) \\ &+\Big((a+1,a+2)-(a+1,c)+(a+2,c)\Big) \\ &\vdots \\ &+\Big((b-1,b)-(b-1,c)+(b,c)\Big)\end{aligned}$$

Note that every index is canceled out in equation (4.16), and only the term $(a,b)-(a,c)+(b,c)$ remains. This shows that, for arbitrary indices a,b, and c, the vector $\vec{K}_{abc}$ is an element of the space spanned by $\mathbf{K}$.

The phases in the function $\mathbf{g}_n$ can be broken down into sums of the vectors $\vec{K}_{ijk}$ as well. As shown above, all such vectors are elements of the space spanned by $\mathbf{K}$.

$$(4.17)\quad (a,b)-(a,d)+(b,c)+(c,d) \to \Big((a,b)-(a,c)+(a,d)\Big) \\ +\Big((a,c)-(a,d)+(c,d)\Big)$$

$$(4.18)\quad (a,b)-(a,c)+(b,d)-(c,d)\rightarrow\Big((a,b)-(a,c)+(b,c)\Big)-\Big((b,c)-(b,d)+(c,d)\Big)$$

$$(4.19)\quad (a,c)-(a,d)-(b,c)+(b,d)\rightarrow\Big((a,b)-(a,d)+(b,d)\Big)-\Big((a,b)-(a,c)+(b,c)\Big)$$

The orthogonal vectors to the space spanned by $\mathbf{K}$, form the continuous symmetry of the functions $\mathbf{f}_n(\Phi)$ and $\mathbf{g}_n(\Phi)$. We can then show the dimension pf the symmetry as the difference in the dimension of the space $\vec{\Phi}$ and the space spanned by $\mathbf{K}$ as, $n^2(n^2-1)/2-(n^2-1)(n^2-2)/2$ which is (n^2-1). □

This means, the functions $\mathbf{f}_n(\Phi)$ and $\mathbf{g}_n(\Phi)$ are invariant in the orthogonal space of the vectors $\vec{K}_{rst}$. We may also understand the continuous symmetry by noting that a unitary operation conserves all trace values and the only continuous unitary operations that form automorphism of $\mathcal{B}$ are $\Gamma=\{e^{i\Omega},\Omega=\mathrm{diag}(x_1,x_2,\ldots,x_{n^2}),x_k\in[0,2\pi]\}$. The unitary operations have n^2 parameters and equivalent to a (n^2-1)-dimensional subspace of $\mathcal{B}$.

*The second trivial symmetry we observe is the permutation symmetry. It is obvious the permutation operation is an automorphism of $\mathcal{B}$, and thus will be an invariant of the functions $\mathbf{f}_n(\Phi)$ and $\mathbf{g}_n(\Phi)$. We will represent the permutation operations with a permutation matrix X_σ. For a Gram matrix of a SIC-POVM, the permutation operations are equivalent to the reordering of the SIC-POVMs. The permutation group generates a large set of Gram matrices which will become important in classifying numerical SIC-POVMs.

4.2.2 Isolated Islands of SIC-POVM Gram Matrices

The two trivial transformations described above are both symmetries of the functions and they map the space of matrices $\mathcal{B}$ to its self. For the purpose of generating

general SIC-POVMs however, we don't need the transformations to be automorphism of the entire matrix space $\mathcal{B}$. We only need the transformation to map one SIC Gram matrix to another. One such a transformation we can search for is a continuous transformation that preserves the functions $\mathbf{f}_n(\Phi) = n$ and $\mathbf{g}_n(\Phi) = n$. In other words we ask: are the SIC-POVM Gram matrices path connected in the space of $\vec{\Phi}$? Based on the Weyl-Heisenberg group solutions, Bruzda et al. Bruzda et al. (2017) showed that in dimensions $4-16$, the SIC-POVMs are isolated and free parameters can not be introduce. Since we are working with the Gram matrix in the space $\mathcal{B}$, we will re-derive the results using the functions $\mathbf{f}_n(\Phi)$ and $\mathbf{g}_n(\Phi)$.

As shown in the previous section, a matrix $B \in \mathcal{B}$ is a SIC-POVM Gram matrix if and only if $\mathbf{f}_n(\Phi) = n$ and $\mathbf{g}_n(\Phi) = n$. Another way to look at the equations is, the two functions define two $n^2(n^2-1)/2-1$ dimensional surfaces in the vector space of $\vec{\Phi}$ and the SIC-POVM Gram matrices exist on the intersection of the two surfaces. To characterize the intersection of the two surfaces we need to understand the local structure of the surfaces. Both surfaces are smooth since the functions are differentiable, C^∞. We can thus explore the local structure by expanding the functions around a solution point $\vec{\Phi}_0$. The first property we find is that all Gram matrices exist on critical point of both functions. In theorem 4.2, we show that this is a general result that holds in arbitrary dimensions.

Theorem 4.2. *SIC-POVM Gram matrices are located at the common critical points of the surfaces* $\mathbf{f}_n(\Phi) = n$ *and* $\mathbf{g}_n(\Phi) = n$.

Proof. The straightforward method to prove the theorem would be to construct the gradients of the two functions and confirm that both gradients are 0. However, this would be an unnecessarily long method. Instead, we will reconstruct the functions by considering an infinitesimal shift of the vector $\vec{\Phi}$.

Let G be the Gram matrix of a SIC-POVM of n-dimensional Hilbert space, and the shift on $\vec{\Phi}$ be $\vec{v}$. We can then write the new Gram matrix as,

$$g_{jk}(\vec{\Phi}+\vec{v}) = \frac{e^{i\phi_{jk}+i\lambda v_{jk}}}{n\sqrt{n+1}}. \tag{4.20}$$

For $|\vec{v}| << 1$, we expand the exponential to the first order in $\vec{v}$ and approximate the Gram matrix as follows.

$$g_{jk}(\vec{\Phi}+\vec{v}) \simeq \frac{e^{i\phi_{jk}}}{n\sqrt{n+1}} + iv_{jk}\frac{e^{i\phi_{jk}}}{n\sqrt{n+1}} \tag{4.21}$$

$$G(\vec{\Phi}+\vec{v}) \simeq G(\vec{\Phi}) + \Delta \tag{4.22}$$

We can now compute the trace cube and fourth power and approximate it to the first order in the shift $\vec{v}$. Since the Gram matrices of SIC-POVMs are projective matrices, we can reduce all powers of $G(\vec{\Phi})^k$ to $G(\vec{\Phi})$ greatly reducing the calculation.

$$\begin{aligned} Tr(G(\vec{\Phi}+\vec{v})^3) &\simeq Tr(G(\vec{\Phi})^3 + 3G^2\Delta + O(\Delta^2)) \\ &\simeq Tr(G(\vec{\Phi}) + 3G\Delta + O(\Delta^2)) \\ &\simeq n + 3Tr(G(\vec{\Phi})\Delta) \end{aligned} \tag{4.23}$$

Similarly,

$$\begin{aligned} Tr(G(\vec{\Phi}+\vec{\delta})^4) &\simeq Tr(G(\vec{\Phi})^4 + 4G^2\Delta + O(\Delta^2)) \\ &\simeq n + 4Tr(G(\vec{\Phi})\Delta) \end{aligned} \tag{4.24}$$

Note that the first order correction on both functions depends on the term $Tr(G(\vec{\Phi})\Delta)$. This shows that if the first order correction of both functions vanishes simultaneously. We then expand the first order correction in to its elements and group the terms based on δ_{jk}.

$$\begin{aligned} Tr(G(\vec{\Phi})\Delta) &= \sum_{ab} i\frac{e^{i\phi_{ab}}}{n\sqrt{n+1}} v_{ba} \frac{e^{i\phi_{ba}}}{n\sqrt{n+1}}, \text{ where } a \neq b \\ &= \frac{i}{n^2(n+1)} \sum_{ab} e^{i(\phi_{ab}+\phi_{ba})} v_{ba} \\ &= 0 \end{aligned} \tag{4.25}$$

Since the first order correction in equations (4.23) and (4.24) is equal to $\vec{v}\cdot\nabla\mathbf{f}_n$ and $\vec{v}\cdot\nabla\mathbf{g}_n$ respectively, and vanished for both functions, all SIC-POVM Gram matrices exist on critical points of both functions.

□

The fact that the Gram matrices exist on critical points means the continuous space of solutions may be dimension less than $n^2(n^2-1)/2-2$, which is the typical intersections of two $n^2(n^2-1)/2-1$ dimensional surfaces. But, this isn't enough to say that the solutions are isolated sets. For this, we need to explicitly use the Hessian matrix of the functions. The Hessian matrix of a function at a given point is the matrix $H_{jk} = \frac{\partial^2}{\partial\phi_j\partial\phi_k} f\Big|_{\vec{\Phi}}$. On critical points, the null space of the Hessian matrix shows the continuous symmetry of the functions.

$$f(\Phi+\delta\Phi) = f(\Phi) + \delta\vec{\Phi}\cdot\nabla f\Big|_{\Phi} + \frac{1}{2}(\delta\vec{\Phi}^{T}\cdot H\cdot\delta\vec{\Phi}) + \mathcal{O}(\delta\Phi^3) \tag{4.26}$$

For a SIC-POVMs Gram matrix, we compute the Hessian matrix by expanding the Gram matrix to the second order. The trace functions to the second order correction take form $G(\vec{\Phi}+\vec{v}) \simeq G(\vec{\Phi}) + G^2\Delta^{(1)} + G\Delta^{(2)} + O(\Delta^2))$, where $\Delta^{(1)} = ie^{i\phi_{ab}}v_{ab}/n\sqrt{n+1}$ and $\Delta^{(2)} = -e^{i\phi_{ab}}v_{ab}^2/n\sqrt{n+1}$. Then the trace of $\mathbf{f}_n(\Phi)$ and $\mathbf{g}_n(\Phi)$ can be expanded to the second order, from which we generate the Hessian matrices.

$$Tr(G(\vec{\Phi}+\vec{v})^3) \simeq n+3(Tr(G\Delta^{(2)}) + Tr(G\Delta^{(1)}\Delta^{(1)})) + O(\Delta^3)) \tag{4.27}$$

$$\begin{aligned} Tr(G(\vec{\Phi}+\vec{v})^4) \simeq n+4(&Tr(G\Delta^{(2)}) + Tr(G\Delta^{(1)}\Delta^{(1)})) \\ &+ 2Tr(G\Delta^{(1)}G\Delta^{(1)}) + O(\Delta^3)) \end{aligned} \tag{4.28}$$

The second order correction of a functions is given by the Hessian matrix as $\frac{1}{2}H_{jk}x_jx_k$. In equations (4.27) and (4.28), the variables are the vector elements v_{ab}, and by extracting the terms of the sum based on the vector elements, we generate the Hessian matrices of the two functions. Unlike the gradient case, the Hessian matrices are difficult to simplify, and generating a general result of continuity is challenging. As is evident from expressions, the Hessian matrices involve the triple products of the SIC-POVM, and general proof of continuity requires further restrictions on these products. However, numerically, we can still use the expression to explore local structure of the surfaces defined by $\mathbf{f}_n(\Phi)$ and $\mathbf{g}_n(\Phi)$. In dimension 3, the intersection of the null spaces of the two matrices form a 10-dimensional space. This means that two free parameters exist which describe the continuous fiducial vectors that have been constructed in dimension 3. In dimensions $4-7$, the in-

tersection of the null space of the two Hessian matrices form a n^2-1 dimensional space, which is the continuous symmetry Γ introduced above. We explore the local structures of general solutions by using the numerical solutions in the next section.

4.3 Group Structure of SIC Gram Matrices

4.3.1 Generating Sets of the Gram Matrix

The Bargmann invariants of the SIC-POVMs are the ideal tools to check if two SIC-POVMs Appleby et al. (2011) belong to the same island. Let's explain the structure of these islands and briefly discuss how to group solutions using the Bargmann invariants. The islands of solutions are formed by the diagonal unitary operations on the n^2 dimensional Hilbert space. Since the Gram matrices of two SIC-POVMs equivalent up to a unitary operator are identical, a global phase shift on all the SIC-POVMs does not generate a different Gram matrix. This means that the islands are generated by unitary operators which are elements of $SU(n^2)$. Thus, the operators can be represented by a set of n^2-1 free parameters. Let the diagonal unitary operator U be $U=e^{i\Omega}$ where $\Omega=\mathrm{diag}(c_1,c_2,\ldots,c_{n^2})$, and $\sum_k c_k=0$. Applying the operator on a $P\in\mathcal{B}$ as $P'=U^\dagger PU$, we generate a different Gram matrix in the same island as P.

$$P'_{jk}=\frac{1}{n\sqrt{n+1}}\begin{cases}e^{i(\phi_{jk}-c_j+c_k)} & ,j<k\\ e^{-i(\phi_{jk}-c_j+c_k)} & ,j>k\\ \sqrt{n+1} & ,j=k\end{cases} \tag{4.29}$$

This corresponds to a shift in the phase vector as $\phi_{jk}\mapsto\phi_{jk}-c_j+c_k$, forming the n^2-1-dimensional plane. The Bargmann invariants of a SIC-POVM are given by the trace of triple products of the $T_{ijk}=n^3Tr(E_i,E_j,E_k)$. If we generate the Bargmann invariant of the Gram matrix P', we see that the variables c_k disappear, and the entire island has unique T_{ijk}'s. Conversely, if two SIC-POVMs have identical Bargmann invariants, then fixing one of the indices gives us two identical

Gram matrices, which indicates that the two SIC-POVMs belong to the same island Appleby et al. (2011). By using the Bargmann invariants, we filter all generated solutions so that all belong to different islands.

The second symmetry of the functions $\mathbf{f}_n(\Phi)$ and $\mathbf{g}_n(\Phi)$ is due to the permutation operations σ. Not all permutation operations however connect different islands as shown in theorem 4.3. Compared to the total number of permutations possible, the number of automorphisms is much less, and the total number of islands is ($\approx n^2!$).

Theorem 4.3. *A permutation operation X_σ that form an automorphism of an island of Gram matrices if and only if there exists a projective unitary operations V and SIC-POVM vectors $\{|\psi_k\rangle\}$ such that,*

$$V|\psi_k\rangle \mapsto |\psi_{\sigma(k)}\rangle \ , \ \forall k \in \mathbb{Z}_n \times \mathbb{Z}_n \tag{4.30}$$

where σ is the permutation of indices.

Proof. Let P and P' be SIC-POVM Gram matrices, where $P' = X_\sigma^\dagger P X_\sigma$ and the two Gram matrices belong to the same island of solutions. We then construct two sets of SIC-POVMs $|\psi_k\rangle$ and $|\psi'_k\rangle$ from the Gram matrices, respectively. Since both Gram matrices belong to the same island of solutions, there necessarily exist projective unitary matrix that maps one to the other.

$$|\psi'_k\rangle = U|\psi_k\rangle \tag{4.31}$$

On the other hand, we can reconstruct the Gram matrix we have by simply applying the permutation on the SIC-POVM: $|\psi_k\rangle \mapsto |\psi_{\sigma(k)}\rangle$. At this point, we have two SIC-POVMs that generate an identical Gram matrix and hence are unitarily equivalent to each other as $|\psi_{\sigma(k)}\rangle = C|\psi'_k\rangle$, where $C \in U(n)$.

We can then construct a projective unitary operation that maps the $|\psi_k\rangle$ to $|\psi_{\sigma(k)}\rangle$.

$$|\psi_{\sigma(k)}\rangle = V|\psi_k\rangle \ , \text{ where } V = CU \tag{4.32}$$

□

Permutations that generate automorphisms indicate the symmetries possessed by the SIC-POVMs in a given island. For the purpose of describing the group-covariant

SIC-POVM islands, we will focus on automorphisms that have fixed points in a given island of SIC-POVM Gram matrices.

The Gram matrices constructed with the functions $\mathbf{f}_n(\Phi)$ and $\mathbf{g}_n(\Phi)$ can be an element of any island of solution, and checking the equivalence of any two Gram matrices is difficult due to the large number of possible permutations. All permutations that do not form an automorphism of a given island, generate SIC-POVMs that are not unitarily equivalent to the initial SIC-POVMs. To identify if two Gram matrices are equivalent, one can use the Gram matrices. Before explicitly constructing the permutation operations connecting two islands, we will define the generating set of the Bargmann invariant.

Definition 4.1. *The generating set of the Bargmann invariant gen*$[T_{ijk}]$ *is a set containing all the phases that appear in the tensor of the Bargmann invariants i.e.,* $T_{ijk} = Tr(\Pi_i \Pi_j \Pi_k)$.

If two SIC-POVMs have different generating set, then the two Gram matrices are not equivalent up to unitary operation. This is because two SIC-POVMs are equivalent up to a projective unitary transformation if and only if their Bargmann invariants are identical Appleby et al. (2011). The generating set is the first criteria to determine equivalence of two SIC-POVMs. However, if the generating set of two SIC-POVMs is the same, the two SIC-POVMs are not necessarily equivalent. therefore, for solutions that do have a common generating set, we need to explicitly construct the permutation operation in order to show their equivalence. We will use the Gram matrix instead of the tensor of Bargmann invariants for the construction of the permutation operations.

In order to compare the Gram matrices belonging to different island of solutions, we first define a means of identifying the islands in a way that allows us to construct a permutation operations between solutions. The best choice for this is to shift the phases of a given row and column to 0. We can do this by using the continuous symmetry of the islands.

4.3.2 Construction of Symmetry Group from the Gram Matrices

The numerical solutions we generate have a generating set much smaller than the $n^2(n^2-1)/2$. This is an indication that the islands are not invariant to all permutations and as a result have a nontrivial symmetry group. To compute the symmetry group we must first reduce the phase matrix by $mod(2\pi)$. This will allow us to

easily construct fixed points of specific automorphism, i.e., Gram matrices that are invariant to the automorphism. This is guarantied by the fact that any transformation with a stationary point in a given island of SIC-POVM is automorphism of the island if the island is isolated. In dimensions > 3 we can construct automorphisms by searching fixed points of permutation operations with in the island of Gram matrices. The actual construction of the symmetry matrix is a long processes that require checking for permutations that fix the matrix. To simplify the search, we start with the element with the lowest frequency and work our way up. We will describe the generating sets for the dimensions 4-7, and demonstrate the construction of the symmetry group.

All the numerical solutions were generated on the Sabanci universities TOSUN HPC cluster with the Mathematica software. We used the conjugate gradient method to find global minima of the function $\sqrt{(\mathbf{f}_n(\Phi)-n)^2+(\mathbf{g}_n(\Phi)-n)^2}$. In dimensions 4 and 5, the search converges at a reasonable time all searches reach global minima. This is not the case for dimensions 6 and 7, where we encounter some local minima, where 43% and 13.5% of the searches yield a solution respectively.

n	Gram Matrix (s)
4	~ 3.76
5	~ 71
6	~ 725
7	~ 5300

Table 4.1 The table shows the average time it took to generate the solutions for dimensions 4-7.

4.3.2.1 Dimension 4

In dimension 4, the functions $\mathbf{f}_n(\Phi)$ and $\mathbf{g}_n(\Phi)$ yield general solutions very quickly despite the large number of parameters. From the numerical solutions, we observe that all generated solutions have the generating set (4.33), indicating that all the solutions may be equivalent up to permutation. Notice that the generating set is the same if we multiply all the phases by -1, which means the set also characterizes anti-unitarily equivalent SIC-POVMs.

(4.33)

$$gen[T_{ijk}] = \{0, 0.33312, 0.571437, 0.666239, 0.904557, 0.999359, 1.5708, 1.90392,$$
$$2.47535, 3.80783, 4.37927, 4.71239, 5.28383, 5.37863, 5.61695, 5.71175, 5.95007\}$$

After projecting the Gram matrices onto a unique point in their respective island, the generating phases are distributed in the matrices with the respective frequencies given below.

(4.34) $\{49, 18, 9, 18, 9, 18, 18, 9, 9, 18, 18, 18, 18, 6, 6, 6, 6\}$

For example, the matrix in equation (4.35) is a numerical phase matrix reduced to the in the first index, where the coefficients $\{a, b, \ldots, q\}$ corresponds to the generating set (4.33) respectively.

(4.35)

$$\begin{pmatrix}
a & a & a & a & a & a & a & a & a & a & a & a & a & a & a \\
a & a & q & e & h & g & e & l & c & k & q & m & i & o & k & b \\
a & b & a & g & l & i & c & q & m & k & h & e & e & k & o & q \\
a & n & l & a & g & a & e & n & o & i & d & l & a & e & g & j \\
a & k & g & l & a & o & q & h & q & c & k & i & e & m & e & b \\
a & l & j & a & d & a & l & g & e & e & n & o & a & g & i & n \\
a & n & p & n & b & g & a & j & k & h & b & h & d & l & q & f \\
a & g & b & e & k & l & i & a & q & m & h & q & o & e & c & k \\
a & p & f & d & b & n & h & b & a & l & j & k & g & q & h & n \\
a & h & h & j & p & n & k & f & g & a & n & b & l & b & q & d \\
a & b & k & o & h & e & q & k & i & e & a & q & l & c & m & g \\
a & f & n & g & j & d & k & b & h & q & b & a & n & h & l & p \\
a & j & n & a & n & a & o & d & l & g & g & e & a & i & e & l \\
a & d & h & n & f & l & g & n & b & q & p & k & j & a & b & h \\
a & h & d & l & n & j & b & p & k & b & f & g & n & q & a & h \\
a & q & b & i & q & e & m & h & e & o & l & c & g & k & k & a
\end{pmatrix}$$

By starting from the elements with the lowest frequencies which are the last 4 elements, i.e.,$\{c, f, m, p\}$. The corresponding indices for the four elements are,

(4.36)

$$\begin{aligned}
(c) &\to \{(2,9), (3,7), (5,10), (8,15), (11,14), (16,12)\} \\
(f) &\to \{(7,16), (9,3), (10,8), (12,2), (14,5), (15,11)\} \\
(m) &\to \{(2,12), (3,9), (5,14), (8,10), (11,15), (16,7)\} \\
(p) &\to \{(7,3), (9,2), (10,5), (12,16), (14,11), (15,8)\}
\end{aligned}$$

The simplest symmetry to construct is one that has a fixed point. Thus we start by

choosing a fixed index and reducing the matrix to the chosen index. For the matrix above, the fixed index would be 1. We do this because, any symmetry permutation that exist need not require reducing the matrix for confirmation.

The next step is to check possible permutations one by one. Notice that any permutation we form based of the list (4.36) will contain 12 indices. Meaning the remaining 3 indices, excluding the fixed one, must be mapped to each other. We can easily verify, the indices $(4, 6, 13)$ are missing from the list. Thus we start our construction with permutations of the 3 elements which is just 6 different possibilities. For every possible permutation that we try, we check it against higher frequency elements. Ultimately, we find the permutation shown in the diagram 4.1.

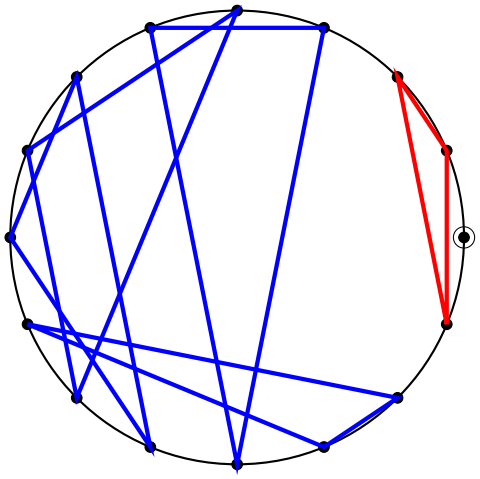

Figure 4.1 The blue orbits are clockwise and the red orbits are counter-clockwise, where the indices follow the angels $2\pi k/16$ for $k \in \mathbb{Z}_{16}$

One can see easily that the symmetry operation is an order-3 matrix, i.e., $\sigma^3 = \mathbb{I}$. We proceed by changing the fixed index through all 16 possibilities. Finally we find 16 distinct permutation operations that fix the island of solutions. Together with their square we have 36 matrices forming an automorphism of the island. At last, the symmetry group $Aut(P)$ is generates by including all products of the order-3 permutations we constructed. The products generate 16 more permutations including the identity. Of these, 15 of which are order-4 permutations, one example is shown in diagram 4.2. In total the size of the symmetry group becomes $|Aut(P)| = 48$.

Important to note that the fixed points in dimension 4 are not isolated, meaning they are not unique. For the order3 permutations, if we shift the phases of each triple of indices by a constant value, the resulting Gram matrix remains a fixed point to the automorphism. Thus, the fixed Gram matrices to the order-3 permutations form a 5-dimensional plane.

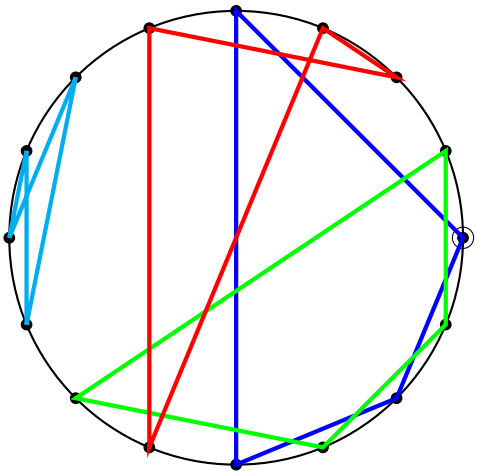

Figure 4.2 The permutation set shown in the diagram is $\{(1,15,13,5),(2,16,14,11),(3,4,12,6),(7,10,8,9)\}$, where the indices follow the angels $2\pi k/16$ for $k \in \mathbb{Z}_{16}$

In dimension 4, we constructed 7.55×10^5 numerical Gram matrices. For every solution we construct the generating set and the corresponding symmetry group $\mathrm{Aut}(P)$. The corresponding symmetry group we find for all numerical solutions has 48 elements, where 32 of the elements fix a single index and are order-3 permutations, the remaining matrices excluding the identity operation have no fixed index.

4.3.2.2 Dimension 5

In dimension 5, the numerical solutions converge relatively fast without for all arbitrary initial search points used. This allowed us to generate 4.8×10^4 numerical solutions. Similar to dimension 4, all solutions constructed have the generating set (4.37) with 73 elements.

(4.37)

$$gen[T_{ijk}] = \{0, 0.00220427, 0.00903612, 0.0460726, 0.123129, 0.23881, 0.295211,$$
$$0.321435, 0.434237, 0.487521, 0.498761, 0.536226, 0.675251, 0.720412, 0.757876,$$
$$0.885633, 0.905025, 1.02595, 1.10858, 1.11982, 1.24631, 1.25884, 1.30271, 1.37977, 1.45798,$$
$$1.48732, 1.55185, 1.60825, 1.62764, 1.63447, 1.93189, 2.02575, 2.07904, 2.13544, 2.36521,$$
$$2.6501, 2.75208, 3.5311, 3.63309, 3.91797, 4.14775, 4.20415, 4.25743, 4.3513, 4.64871,$$
$$4.65554, 4.67494, 4.73134, 4.79586, 4.8252, 4.90342, 4.98048, 5.02434, 5.03688,$$
$$5.16337, 5.17461, 5.25723, 5.37816, 5.39755, 5.52531, 5.56277, 5.60793, 5.74696,$$
$$5.78442, 5.79566, 5.84895, 5.96175, 5.98797, 6.04437, 6.16006, 6.23711, 6.27415, 6.28098\}$$

The corresponding frequency is given in (4.38). Similar to the case of dimension 4, we generating permutation matrices by starting with the lowest frequency and work our way up. For all constructed Gram matrices, we were able to construct a unique permutation that maps the numerical solutions to a Weyl-Heisenberg group covariant SIC-POVM Gram matrix.

(4.38)

$$\{73, 9, 9, 3, 3, 9, 9, 9, 9, 3, 9, 9, 9, 9, 9, 3, 9, 9, 9, 9, 9, 9, 3, 3, 9, 9, 9, 9, 3, 9, 9, 3, 9, 9, 9, 9, 9, 9,$$
$$9, 9, 9, 9, 9, 3, 9, 9, 3, 9, 9, 9, 9, 3, 3, 9, 9, 9, 9, 9, 9, 3, 9, 9, 9, 9, 9, 3, 9, 9, 9, 9, 3, 3, 9, 9\}$$

We construct the automorphisms using similar approach to dimension 4. With the Key difference being that the lowest frequencies of the generating set is 3, which corresponds to a 2 pairs of 3 indices that must map to on another. For example, we constructed a gram matrix reduced in the index, where the indices of the lowest frequencies form the following groups of set of indices we can permute.

(4.39)

$$\{(13, 2), (15, 21), (23, 17)\}$$
$$\{(4, 24), (5, 16), (6, 12)\}$$
$$\{(7, 20), (8, 9), (25, 18)\}$$
$$\{(10, 3), (11, 14), (22, 19)\}$$

The only permutation that can be constructed that fixes the reduced Gram matrix, is

the permutation $\{(2,17,21),(3,14,19),(4,5,6),(7,8,25),(9,18,20),(10,11,22)\}$. Figure 4.3 shows these permutation. In total we find 50 order-3 permutation operations that map the island of Gram matrices to its self. To generate the group $\mathrm{Aut}(P)$, we multiply the permutations matrices generating a group of 75 permutation operations, which also contains 24 order-5 permutations.

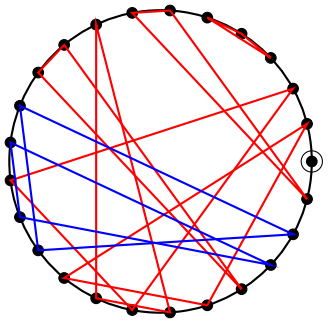

Figure 4.3 The blue orbits are clockwise and the red orbits are counter-clockwise, where the indices follow the angels $2\pi k/25$ for $k \in \mathbb{Z}_{25}$

The fixed points in dimension 5, like the case of dimension 4, are not isolated. For the order-3 operators, the fixed Gram matrices form a 8-dimensional plane within the island.

4.3.2.3 Dimensions 6 and 7

In dimensions 6 and 7, in addition to the difficulty of obtaining numerical solutions due to the large number of free parameters, we also encounter local minima. This makes the time needed to generate a numerical solution long. As a result, we constructed 162 solutions in dimension 6 and 50 solutions in dimension 7. The Gram matrices in dimension 6 found all have a single generating set. The Gram matrices generated in dimension 7, however, belonged to two different generating sets, corresponding to two unitarily in-equivalent classes of SIC-POVMs. The generating set in these dimensions can be found in Appendix A. The exact form of these generating sets can be constructed the analytic solutions in Scott (2017).

Using the generating set of dimension 6, which can be found in Appendix A, we construct permutations that have fixed points.The automorphisms of the islands in dimension 6, unlike the previous two dimensions are not n^2 in number. In dimensions $n = 0 \ mod \ 3$, automorphisms with a single fixed index can not be formed. Instead we have matrices that fix 3 indices for each order-3 permutation, forming 12 distinct elements. The $\mathrm{Aut}(P)$ group has 36 elements with where 12 of the permutations do

not fix any index.

In Dimension 7, for both generating sets, we get 98 permutations each fixing a single index. The total Aut(P) group has 147 elements with the 48 elements being order-7. The generating set of dimension 7 can be found in Appendix A.

4.3.3 Analysis of the Symmetry Group and Connection to the W-H group

In all 4 cases presented above, the group Aut(P) contains elements that fix a single index, with exception of dimension 6 where 3 indices are fixed by the order-3 automorphisms. Let X be a permutation which is an order-3 automorphism for an Island of SIC-POVM in a given dimension n. By definition, $X^3 = \mathbb{I}$. Since the permutation maps the island to it self, the SIC-POVMs the operator connects are equivalent up to a projective unitary operator. For a SIC-POVM operators, this means equivalence up to a unitary operator. For a given X such that $P' = XPX^\dagger$, we can define a unitary matrix U_x such that $\{\Pi'_k\} = \{U_x \Pi'_k U_x^\dagger\}$. We can easily see that $U_x^3 = \mathbb{I}$. If P is a fixed Gram matrix of the permutation X for $n = \{4, 5, 7\}$, there exists a vector elements of the corresponding SIC-POVM where,

$$U|\psi_k\rangle = e^{i\theta}|\psi_k\rangle \tag{4.40}$$

The remaining n^2 elements of Aut(P) in dimensions $4, 5, 7$ do not fix any index as described in previous section. Let Y represent the permutations of order-n where $Y^n = \mathbb{I}$. Since Y maps the island to it self, we can again define a unitary matrix U_y where $U_y^n = \mathbb{I}$.

The permutation matrices Y in the dimensions $4, 5$ and 7 form a group $\cong \mathbb{Z}_n \times \mathbb{Z}_n$, which means that the corresponding unitary matrices U_y also form a group, up to a phase equivalence. Since applying the set Y on the Gram matrix rotates the indices, the unitary U_y must map the SIC-POVM vectors to each other up to a phase factor. Thus, we can write the SIC-POVM as the orbit of the unitary group $\{U_y|\phi_k\rangle\}$.

$$X \begin{pmatrix} |\phi_1\rangle \\ |\phi_2\rangle \\ \vdots \\ |\phi_{n^2}\rangle \end{pmatrix} = \begin{pmatrix} |\phi_{\sigma_1}\rangle \\ |\phi_{\sigma_2}\rangle \\ \vdots \\ |\phi_{\sigma_{n^2}}\rangle \end{pmatrix} \tag{4.41}$$

This makes the SIC-POVM a group covariant SIC-POVM. As discussed in chapter 2, for a Weyl-Heisenberg group covariant SIC-POVMs the set of unitaries U_y corresponds to $D_{\boldsymbol{p}}$. The other elements of the $\mathrm{Aut}(P)$ fix a single index in the dimensions $4, 5$ and 7, which means that there exists a vector that is an eigenvector of the unitaries U_x such that the its orbit on the matrices $\{U_y\}$ forms a SIC-POVM. In other words, the $|\psi\rangle$ is a fiducial vector. In the Weyl-Heisenberg group covariant solutions, the unitary matrices U_x correspond the the order-3 unitaries such as Zauner's matrix. The automorphism of the islands show a close relation between the group $\cong \mathbb{Z}_n \times \mathbb{Z}_n$ and order-3 unitaries. In dimension 6, we still get order-3 unitaries which fix a fiducial state. We don't generate the entire order-6 permutations which are similar to the Weyl-Heisenberg group, but the remaining set can obtained once the equivalence of the two groups is established.

All solutions we computed exhibit the group covariant property in all 4 dimensions. Zhu Zhu (2010) showed that in prime dimensions, group covariant SIC-POVMs are covariant to the Weyl-Heisenberg group. To confirm that the numerical solutions we constructed are covariant with respect to the Weyl-Heisenberg group, we explicitly generated transformations matrices that map each solutions to a known Weyl-Heisenberg solutions for all $4-7$ dimensions. The result we find is that, all the numerical islands constructed are equivalent to islands of Weyl-Heisenberg group covariant SIC-POVMs up to a permutation operation.

5. Conclusion And Discussion

The Weyl-Heisenberg group covariant SIC-POVMs have been shown to have symmetries which allowed us to simplify the construction of fiducial vectors. These fiducial vectors define equivalent classes defined by the orbit they form on the Clifford group. In dimension 3, it is known that all SIC-POVMs are equivalent to a Weyl-Heisenberg solution. In Higher dimensions, the only solutions we know are Weyl-Heisenberg solutions with the exception of dimension 8. To further understand the structure of general SIC-POVMs, we explored general solutions by starting from the geometrical properties of the SIC-POVMs in the real space and continuing with numerical solutions to classify general SIC-POVMs in dimensions $4-7$.

In our geometrical approach to the SIC-POVM problem, we showed that the n^2-1 vertices of a regular simplex can be oriented such that $Tr(\rho^3)$ of all the points is equal. We showed that the existence of SIC-POVMs is equivalent to showing the solution satisfying the modified Kakutani's theorem can be achieved for the extreme values of the $Tr(\rho^3)$ function. We further analyzed quantum states on the Bloch sphere, by defining a set of manifolds of different topology on the Bloch sphere. The manifolds have continuous symmetry, which is the special unitary group. The global symmetry, however, was much more complicated due to the non-linear nature of the characteristic polynomial of the Bloch sphere.

We continued our analysis by generating SIC-POVM Gram matrices without using the Weyl-Heisenberg group. The characteristic equations for general SIC-POVM Gram matrix involve two trace functions. The solutions are found on the critical points of the functions, allowing the solutions to form a disjoint islands of solutions. Each solution forming an equivalent class. Using similar methods as the Bloch sphere, we showed that the islands of solutions can be related by a permutation operation.

We generated $\sim 10^5$ solutions in dimension 4 and $\sim 10^4$ in dimension 5, where we found that all constructed solutions are equivalent to the Weyl-Heisenberg solutions up to a permutation operation. We expected to find solutions which are not covariant

to any group, which due to the lack of any symmetry group, should be much larger in number compared to the group covariant solutions. For the solutions we have generated, in addition to the $3n^3$ elements of symmetry group we formed, exists $2n^5 \prod_{p|n}(1-p^{-2})$ Clifford unitaries, where p goes over all prime numbers that divide n. This reduces the number of distinct islands by a factor of $\sim 10^3$. despite this difference in number, we did not find any Gram matrix with less symmetry group than $\mathbb{Z}_n \times \mathbb{Z}_n$. This strongly indicates that the group structure of SIC-POVM Gram matrices can only exist with the aforementioned symmetry group. From a purely probabilistic point of view, the chances of not finding a non-group covariant Gram matrix for N solutions is $(\sim 10^{-3N})$. Since the symmetries of the Bloch sphere are also symmetries of the SIC-POVM, the lack of nontrivial symmetry of the Gram matrices indicate that the only symmetry of the Bloch sphere is the unitary and anti-unitary groups.

Even though the numerical results may provide a strong reason to expect group covariance property in SIC-POVMs, an analytic proof is still needed. One possible approach to an analytic proof is to use the surfaces $\mathbf{f}_n(\Phi) = a$ and $\mathbf{g}_n(\Phi) = b$. Numerical solutions show that the intersection of the two surfaces is continuous and connected. This allows us to characterize the intersection as a manifold.

The methods used in exploring the general SIC-POVMs are not unique to these frames, and can be extended to mutually unbiased bases. MUBs form a tight frame, and consequently, their Gram matrices is a projective. We can apply the numerical methods to the MUBs to explore group covariant properties in those frames. In particular, the problem of dimension 6 can be explored using similar approach to both search for a solution and classify the symmetries of the solutions.

BIBLIOGRAPHY

(1947). PROBLÈMES vol. 1, fasc. 1. volume 1. *Colloquium Mathematicae*.

Appleby, D. (2007). Symmetric informationally complete measurements of arbitrary rank. volume 103. Springer, *Optics and Spectroscopy*.

Appleby, D., Flammia, S. T., & Fuchs, C. A. (2011). The lie algebraic significance of symmetric informationally complete measurements. volume 52. American Institute of Physics, *Journal of Mathematical Physics*.

Appleby, D. M. (2005). Symmetric informationally complete–positive operator valued measures and the extended Clifford group. volume 46. American Institute of Physics, *Journal of Mathematical Physics*.

Appleby, M., Bengtsson, I., Flammia, S., & Goyeneche, D. (2019). Tight frames, hadamard matrices and zauner's conjecture. volume 52. IOP Publishing, *Journal of Physics A: Mathematical and Theoretical*.

Appleby, M., Bengtsson, I., Grassl, M., Harrison, M., & McConnell, G. (2022). Sic-povms from stark units: Prime dimensions n2+ 3. volume 63. AIP Publishing, *Journal of Mathematical Physics*.

Bertlmann, R. A. & Krammer, P. (2008). Bloch vectors for qudits. volume 41. IOP Publishing, *Journal of Physics A: Mathematical and Theoretical*.

Bloch, F. (1946). Nuclear induction. volume 70. American Physical Society, *Physical Review*.

Borodulin, V., Slabospitsky, S., & Rogalyov, R. (1995). Core compendium of relations: version 2.1. Technical report, SCAN-9606079.

Borsuk, K. (1933). Drei sätze über die n-dimensionale euklidische sphäre. volume 20. Polska Akademia Nauk. Instytut Matematyczny PAN, *Fundamenta Mathematicae*.

Bruzda, W., Goyeneche, D., & Życzkowski, K. (2017). Quantum measurements with prescribed symmetry. volume 96. APS, *Physical Review A*.

Busch, P. (1991). Informationally complete sets of physical quantities. volume 30. Springer, *International Journal of Theoretical Physics*.

Delsarte, P., Goethals, J.-M., & Seidel, J. J. (1991). Spherical codes and designs. In *Geometry and Combinatorics* (pp. 68–93). Elsevier.

Derksen, H. & Kemper, G. (2015). *Computational invariant theory*. Springer.

Duda, R. (1987). Life and work of bronislaw knaster (1893–1980). volume 51. *Colloquium Mathematicae*.

Durt, T., Kurtsiefer, C., Lamas-Linares, A., & Ling, A. (2008). Wigner tomography of two-qubit states and quantum cryptography. volume 78. APS, *Physical Review A*.

Dyson, F. J. (1951). Continuous functions defined on spheres. JSTOR, *Annals of Mathematics*.

Fuchs, C. A. (2010). QBism, the perimeter of quantum Bayesianism. *arXiv preprint arXiv:1003.5209*.

Fuchs, C. A., Hoang, M. C., & Stacey, B. C. (2017). The SIC question: History and state of play. volume 6. MDPI, *Axioms*.

Haantjes, J. (1948). Equilateral point-sets in elliptic two-and three-dimensional spaces. volume 22. *Nieuw Arch. Wiskunde (2)*.

Hoggar, S. G. (1981). Two quaternionic 4-polytopes. In *The Geometric Vein: The Coxeter Festschrift* (pp. 219–230). Springer.

Hughston, L. P. & Salamon, S. M. (2016). Surveying points in the complex projective plane. volume 286. Elsevier, *Advances in Mathematics*.

Kakutani, S. (1942). A proof that there exists a circumscribing cube around any bounded closed convex set in r 3. JSTOR, *Annals of Mathematics*.

Kovacevic, J. & Chebira, A. (2007a). Life beyond bases: The advent of frames (part i). volume 24. IEEE, *IEEE Signal Processing Magazine*.

Kovacevic, J. & Chebira, A. (2007b). Life beyond bases: The advent of frames (part ii). volume 24. IEEE, *IEEE Signal Processing Magazine*.

Landau, L. D. & Lifshitz, E. M. (1977). *Quantum mechanics: non-relativistic theory*, volume 3. Pergamon Press.

Nielsen, M. A. & Chuang, I. L. (2010). *Quantum computation and quantum information*. Cambridge university press.

Prugovečki, E. (1977). Information-Theoretical aspects of quantum measurement. volume 16. Springer, *International Journal of Theoretical Physics*.

Renes, J. M., Blume-Kohout, R., Scott, A. J., & Caves, C. M. (2004). Symmetric informationally complete quantum measurements. volume 45. American Institute of Physics, *Journal of Mathematical Physics*.

Sakurai, J. J. & Commins, E. D. (1995). *Modern quantum mechanics, revised edition*. American Association of Physics Teachers.

Scott, A. J. (2006). Tight informationally complete quantum measurements. volume 39. IOP Publishing, *Journal of Physics A: Mathematical and General*.

Scott, A. J. (2017). SICs: Extending the list of solutions. *arXiv preprint arXiv:1703.03993*.

Scott, A. J. & Grassl, M. (2010). Symmetric informationally complete positive-operator-valued measures: A new computer study. volume 51. American Institute of Physics, *Journal of Mathematical Physics*.

van Lint, J. H. & Seidel, J. J. (1966). Equilateral point sets in elliptic geometry. volume 69. *Proceedings of the Koninklijke Nederlandse Akademie van Wetenschappen: Series A: Mathematical Sciences*.

Waldron, S. F. (2018). *An introduction to finite tight frames*. Springer.

Yamabe, H. & Yujobô, Z. (1950). On the continuous function defined on a sphere.

Yoshida, M. & Kimura, G. (2022). Construction of general symmetric-informationally-complete–positive-operator-valued measures by using a complete orthogonal basis. volume 106. APS, *Physical Review A*.

Zauner, G. (2011). Quantum designs: Foundations of a noncommutative design theory. volume 9. World Scientific, *International Journal of Quantum Information*.

Zhu, H. (2010). SIC POVMs and Clifford groups in prime dimensions. volume 43. IOP Publishing, *Journal of Physics A: Mathematical and Theoretical*.

APPENDIX A

Eigenvalues of Density operators

Given a density matrix ρ of an n-dimensional quantum system, with eigenvalues $\{\lambda_1, \ldots, \lambda_n\}$. We write the trace functions using the eigenvalues as follow.

$$Tr(\rho^m) = \sum_{k=1}^{n} \lambda_k^m \tag{A.1}$$

We can immediately write the bounds of the trace functions, since the eigenvalues of a density matrix are all positive and adds up to 1.

$$\frac{1}{n^{k-1}} \leq \sum_{k} \lambda_k^m \leq 1 \tag{A.2}$$

The eigenvalues of the density matrix are solutions to the equation $\mathrm{Det}(\lambda\mathbb{I} - \rho) = 0$. Using newton's identity we expand the determinant in to a sum of the trace functions.

$$\mathrm{Det}(\lambda\mathbb{I} - \rho) = c_0\lambda^n + c_1\lambda^{n-1} + \ldots + c_{n-1}\Lambda + c_n \tag{A.3}$$

where c_m's are the elementary symmetric polynomials formed by $(\lambda - \lambda_k)$'s. The real solution of the polynomial corresponds to the eigenvalue of the density matrix.

purity condition of a density matrix

If a given density matrix represents a pure state, then $\rho = \rho^2$.since density matrices by definition satisfy $Tr(\rho) = 1$, pure state density matrices satisfy the equalities $Tr(\rho^m) = 1$ where $m \epsilon N$. It's can be shown that three of this trace equalities can be used to check if a density matrix represents a pure state or not. Taking the equalities $Tr(\rho) = 1$, $Tr(\rho^{2n}) = 1$ and $Tr(\rho^m) = 1$ where $m, n\ \epsilon N$ and $m \neq 2n$. These give us the following expressions respectively.

$$\sum_i \lambda_i = 1 \tag{A.4}$$

$$\sum_i \lambda_i^{2n} = 1 \tag{A.5}$$

$$\sum_i \lambda_i^{m} = 1 \tag{A.6}$$

where λ_i are eigenvalues of the density matrix. From equation 1 and 2 we conclude that $-1 \leq \lambda_i \leq 1$.

$$\sum_i \lambda_i^{m} - \sum_i \lambda_i^{2n} = 0 \tag{A.7}$$

$$\sum_i (\lambda_i^{m-2n} - 1)\lambda_i^{2n} = 0 \tag{A.8}$$

This is possible only for $\lambda_i = 0, 1$. This with the condition of equation 1 gives us a pure state condition.

Gell-Mann expansion of density matrix

A given d dimensional density matrix ρ can be expanded using generalized Gell-Mann matrices by the following equation.

$$\rho = \frac{\mathbb{I}}{n} + \Lambda_k r_k \tag{A.9}$$

where $r_k \, \epsilon \, R^{n^2-1}$ and Λ_k are the generalized Gell-Mann matrices.

The generalized Gell-Mann as defined in (2.1), are $n^2 - 1$,$n \times n$ symmetric matrices

given as follows.

$$\lambda_m = |j\rangle\langle k| + |k\rangle\langle j| \ , \ 1 \leq m \leq \frac{n(n-1)}{2} \ , \ 0 \leq k < j \leq n-1 \tag{A.10}$$

$$\lambda_m = -i(|j\rangle\langle k| - |k\rangle\langle j|) \ , \ \frac{n(n-1)}{2} + 1 \leq m \leq n(n-1) \ , \ 0 \leq k < j \leq n-1 \tag{A.11}$$

$$\Lambda_m = \sqrt{\frac{2}{l(l+1)}} \left(\sum_{k=1}^{l} |k\rangle\langle k| + l|l+1\rangle\langle l+1| \right) \ , \ n(n-1) \leq m \leq n^2 - 1 \ , \ 0 \leq l \leq n-1 \tag{A.12}$$

the Gell-Mann matrices satisfy the following,

$$Tr(\Lambda_n) = 0 \tag{A.13}$$

$$Tr(\Lambda_n \Lambda_m) = 2\delta_{nm} \tag{A.14}$$

Defining $d_{ijk} = Tr(\Lambda_i \Lambda_j \Lambda_k)$ we can write the product of two gellmann matrices

$$\Lambda_n \Lambda_m = \frac{2}{d}\delta_{nm} I + \frac{d_{nmk}}{2}\Lambda_k \tag{A.15}$$

using this we can write,

$$\Lambda_i \Lambda_j \Lambda_k \Lambda_l = \frac{2}{d}\delta_{ij}\Lambda_k \Lambda_l + \frac{d_{ijx}}{2}\Lambda_x \Lambda_k \Lambda_l \tag{A.16}$$

$$\Lambda_i \Lambda_j \Lambda_k \Lambda_l \Lambda_n = \frac{2}{d}\delta_{ij}\Lambda_k \Lambda_l \Lambda_n + \frac{d_{ijx}}{2}\Lambda_x \Lambda_k \Lambda_l \Lambda_n \tag{A.17}$$

$$\Lambda_i \Lambda_j \Lambda_k ... \Lambda_z = \frac{2}{d}\delta_{ij}\Lambda_k ... \Lambda_z + \frac{d_{ijx}}{2}\Lambda_x \Lambda_k ... \Lambda_z \tag{A.18}$$

using this relations we can write $d^n_{a_1a_2...a_n} = Tr(\Lambda_{a_1}\Lambda_{a_2}...\Lambda_{a_n})$ in-terms of d_{ijk} tensor,

$$d^n_{a_1a_2...a_n} = \frac{2}{d}\delta_{a_1a_2}d^{n-2}_{a_3a_4...a_n} + \frac{d_{a_1a_2x}}{2}d^{n-1}_{xa_3a_4...a_n} \tag{A.19}$$

here $d^0 = d$ and $d^1_{a_1} = 0$, then the recursion relation gives us all traces of multiples of Gell-Mann matrices. $d^3_{a_1a_2a_3} = d_{a_1a_2a_3}$

purity conditions $Tr(\rho^m)$ in dimension 3

the purity conditions for $d \times d$ density matrices can be checked by taking $Tr(\rho) = 1$, $Tr(\rho^2) = 1$ and $Tr(\rho^m) = 1$ for any $m \geq 3$. the first equation is a given, the second equation restricts us to the surface of a (d^2-1)-sphere of radius $\sqrt{\frac{d-1}{2d}}$. the third equation can be written for any m as,

$$Tr(\rho^m) = Tr\left(\left(\frac{I}{d} + \Lambda_k r_k\right)^m\right) \tag{A.20}$$

$$Tr(\rho^m) = \left(\frac{1}{d}\right)^{m-1} + \sum_{i=1}^{m}\binom{m}{i}\left(\frac{1}{d}\right)^{m-i}\sum_{a_1a_2...a_i} d^i_{a_1a_2...a_i}r_{a1}r_{a2}..r_{ai} \tag{A.21}$$

for the case of $d = 3$ the purity condition with $m = 3$ and $m = 4$ are,

(A.22)
$$Tr(\rho^3) = \frac{1}{9} + \binom{3}{1}\frac{1}{9}\sum_{a_1} d^1_{a_1}r_{a_1} + \binom{3}{2}\frac{1}{3}\sum_{a_1a_2} d^2_{a_1a_2}r_{a_1}r_{a_2} + \binom{3}{3}\sum_{a_1a_2a_3} d^3_{a_1a_2a_3}r_{a_1}r_{a_2}r_{a_3}$$

$$\frac{1}{9} + \frac{6}{9} + \sum_{a_1a_2a_3} d^3_{a_1a_2a_3}r_{a_1}r_{a_2}r_{a_3} = 1 \tag{A.23}$$

(A.24) $$\sum_{a_1 a_2 a_3} d^3_{a_1 a_2 a_3} r_{a_1} r_{a_2} r_{a_3} = \frac{2}{9}$$

in the diagonal basis $(0, ..., 0, r_7, r_8)$,

(A.25) $$\sum_{a_1 a_2 a_3} d^3_{a_1 a_2 a_3} r_{a_1} r_{a_2} r_{a_3} = 2\sqrt{3} r_7^2 r_8 - \frac{2r_8^3}{\sqrt{3}}$$

similarly for $m = 4$,

(A.26) $$Tr(\rho^4) = \frac{13}{27} + \frac{4}{3}\left(2\sqrt{3} r_7^2 r_8 - \frac{2r_8^3}{\sqrt{3}}\right) + 2(r_7^2 + r_8^2)^2$$

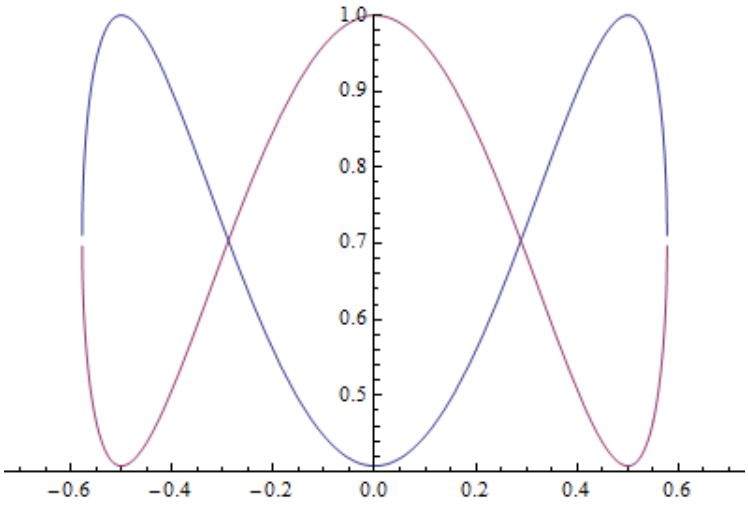

Figure A.1 $Tr(\rho^4)$ plotted against r_7 on the circle $r_7^2 + r_8^2 = \frac{1}{3}$

Quantum States in Dimension 3 Gell-Mann space

By using the Gell-Mann matrices, we map density matrices to the real space as $\rho = \frac{\mathbb{I}}{3} + \sum_{k=1}^{8} \Lambda_k r_k$, where the Gell-Mann matrices Λ in dimension three are given as,

$$\Lambda = \{ \begin{pmatrix} 0 & 1 & 0 \\ 1 & 0 & 0 \\ 0 & 0 & 0 \end{pmatrix}, \begin{pmatrix} 0 & 0 & 1 \\ 0 & 0 & 0 \\ 1 & 0 & 0 \end{pmatrix}, \begin{pmatrix} 0 & 0 & 0 \\ 0 & 0 & 1 \\ 0 & 1 & 0 \end{pmatrix},$$

$$\begin{pmatrix} 0 & -i & 0 \\ i & 0 & 0 \\ 0 & 0 & 0 \end{pmatrix}, \begin{pmatrix} 0 & 0 & -i \\ 0 & 0 & 0 \\ i & 0 & 0 \end{pmatrix}, \begin{pmatrix} 0 & 0 & 0 \\ 0 & 0 & -i \\ 0 & i & 0 \end{pmatrix}, \tag{A.27}$$

$$\begin{pmatrix} 1 & 0 & 0 \\ 0 & -1 & 0 \\ 0 & 0 & 0 \end{pmatrix}, \begin{pmatrix} \frac{1}{\sqrt{3}} & 0 & 0 \\ 0 & \frac{1}{\sqrt{3}} & 0 \\ 0 & 0 & -\frac{2}{\sqrt{3}} \end{pmatrix} \}.$$

These matrices span the space of three dimensional trace one symmetric matrices and allow us to represent quantum states with vectors in the space $\mathbb{R}^{n^2-1}$. However, the Gell-Mann space is a larger space that the space of density matrices (i.e. $\rho^\dagger = \rho$, $tr(\rho) = 1$ and all eigenvalues of ρ are positive). We therefor need the equations $tr(\rho^2), tr(\rho^3), ..., tr(\rho^n)$ to check if a matrix represents a quantum state. The number of equations reduces with the degeneracy of the state we are interested in. In the case of the pure state density matrix (i.e. one of the eigenvalues is one and all the rest are zero), we only requires two trace equations, as is proven in lemma A.1.

If a given density matrix represents a pure state, then $\rho = \rho^2$. Since density matrices by definition satisfy $tr(\rho) = 1$, pure state density matrices satisfy the equalities $tr(\rho^m) = 1$ for all $m \epsilon N$. It can be shown that we only need two of such equalities to check if a density matrix represents a pure state or not. We now prove that, $tr(\rho^{2n}) = 1$ and $tr(\rho^m) = 1$ where $m, n\ \epsilon N$ and $m \neq 2n$ are sufficient conditions to identify pure state density matrices in the Gell-Mann space.

Lemma A.1. *If ρ is a density matrix where $tr(\rho^{2n}) = 1$ and $tr(\rho^m) = 1$ where $m, n\ \epsilon N$ and $m \neq 2n$, then ρ is a pure state density matrix, i.e. $\rho = |\phi\rangle\langle\phi|$ for some $\phi \in \mathbb{C}^n$.*

Proof. The two equalities in the diagonal basis give the following equations.

$$\sum_i \lambda_i^{2n} = 1 \tag{A.28}$$

$$\sum_i \lambda_i^{m} = 1 \tag{A.29}$$

where λ_i are eigenvalues of the density matrix ρ. From equation (A.28) we conclude that $-1 \leq \lambda_i \leq 1$. Then by subtracting the (A.28) from (A.29) we write the following.

$$\sum_i \lambda_i^m - \sum_i \lambda_i^{2n} = 0 \tag{A.30}$$

$$\sum_i (\lambda_i^{m-2n} - 1)\lambda_i^{2n} = 0 \tag{A.31}$$

This is possible only for $\lambda_i = 0, 1$, and by equation (A.28) only one of the eigenvalues can be one and the rest must be zero. This implies that ρ is a pure state density matrix. □

Equations (A.28) and (A.29) form polynomial equations that classify a subspace of pure states in the real space of the Gell-Mann space. We then choose $m = 3$ and $n = 1$ to get the simplest of the polynomial equations.

$$Tr(\rho^m) = \left(\frac{1}{d}\right)^{m-1} + \sum_{i=1}^{m} \binom{m}{i} \left(\frac{1}{d}\right)^{m-i} \sum_{a_1 a_2 \ldots a_i} d^i_{a_1 a_2 \ldots a_i} r_{a1} r_{a2} \ldots r_{ai} \tag{A.32}$$

Where $d^i_{a_1 a_2 \ldots a_i} = tr(\underbrace{\Lambda_{a_1} \Lambda_{a_2} \ldots \Lambda_{a_i}}_{i})$.

$$Tr(\rho^2) = \frac{1}{3} + \binom{2}{1} \frac{1}{3} \sum_{a_1} d^1_{a_1} r_{a_1} + \sum_{a_1 a_2} d^2_{a_1 a_2} r_{a_1} r_{a_2} \tag{A.33}$$

(A.34)

$$Tr(\rho^3) = \frac{1}{9} + \binom{3}{1} \frac{1}{9} \sum_{a_1} d^1_{a_1} r_{a_1} + \binom{3}{2} \frac{1}{3} \sum_{a_1 a_2} d^2_{a_1 a_2} r_{a_1} r_{a_2} + \binom{3}{3} \sum_{a_1 a_2 a_3} d^3_{a_1 a_2 a_3} r_{a_1} r_{a_2} r_{a_3}$$

After few simplifications we get the following two equations for $m = 2$ and $m = 3$ respectively.

$$\sum_{k=1}^{8} r_k^2 = \frac{1}{3} \tag{A.35}$$

(A.36)

$$\sum_{a_1a_2a_3} d^3_{a_1a_2a_3} r_{a_1} r_{a_2} r_{a_3} = 2\sqrt{3}r_1^2 r_8 + 6r_1 r_2 r_3 + 6r_1 r_5 r_6 + 3r_2^2 r_7 - \sqrt{3}r_2^2 r_8 - 6r_2 r_4 r_6 - 3r_3^2 r_7$$
$$- \sqrt{3}r_3^2 r_8 + 6r_3 r_4 r_5 + 2\sqrt{3}r_4^2 r_8 + 3r_5^2 r_7 - \sqrt{3}r_5^2 r_8 - 3r_6^2 r_7 - \sqrt{3}r_6^2 r_8 + 2\sqrt{3}r_7^2 r_8 - \frac{2r_8^3}{\sqrt{3}} = \frac{2}{9}$$

It is worth to mention that on the sphere defined by equation (A.35), equation (A.36) maps points on the sphere to the real space, $f : \vec{r} \mapsto \mathbb{R}, f(\vec{r}) = \sum_{a_1a_2a_3} d^3_{a_1a_2a_3} r_{a_1} r_{a_2} r_{a_3}$ where $-\frac{2}{9} \leq f(\vec{r}) \leq \frac{2}{9}$.

fiducial Vectors in Dimension 3

If the vector $|\psi\rangle$ is a fiducial vector, then the set $\{\hat{D}_{\boldsymbol{p}}|\psi\rangle, (p_1, p_2) \in \mathbb{Z}_3 \times \mathbb{Z}_3\}$ is a SIC-POVM. I.e. for every element of the SIC set, $|\langle\psi|\hat{D}_{\boldsymbol{p}}|\psi\rangle|^2 = \frac{1}{4}$ is satisfied. This gives us nine equations to solve, but since we only have four free parameters in our vectors solving four must suffice. We re-write this equations in the Gell-Mann space by using the density matrix formalism $\rho = |\psi\rangle\langle\psi| = \frac{\mathbb{I}}{3} + \Lambda.\vec{r}$.

(A.37)
$$tr(\rho \hat{D}_{\boldsymbol{p}} \rho \hat{D}^\dagger_{\boldsymbol{p}}) = \frac{1}{4}$$

(A.38)
$$\sum_{\alpha=1,\beta=1}^{8} M_{\alpha\beta}(\boldsymbol{p}) r_\alpha r_\beta = -\frac{1}{24}$$

After Solving equation (A.38), we get the following four equations for each $\boldsymbol{p} = (p_1, p_2)$.

(A.39)
$$(10), (20) : -\frac{1}{2}\sum_{k=1}^{6} r_k^2 + r_7^2 + r_8^2 = -\frac{1}{24}$$

$$(A.40)\quad (0,1),(0,2): r_1r_2 + r_2r_3 + r_1r_3 - (r_4r_5 + r_5r_6 - r_4r_6) - \frac{1}{2}(r_7^2 + r_8^2) = -\frac{1}{24}$$

$$(A.41)\quad (1,1),(2,2): -\frac{1}{2}(r_1r_2 + r_2r_3 + r_1r_3) + \frac{1}{2}(r_4r_5 + r_5r_6 - r_4r_6) - \frac{1}{2}(r_7^2 + r_8^2) + \frac{\sqrt{3}}{2}(r_2r_4 - r_3r_4 + r_1r_5 - r_3r_5 + r_1r_6 - r_2r_6) = -\frac{1}{24}$$

$$(A.42)\quad (2,1),(1,2): -\frac{1}{2}(r_1r_2 + r_2r_3 + r_1r_3) + \frac{1}{2}(r_4r_5 + r_5r_6 - r_4r_6) - \frac{1}{2}(r_7^2 + r_8^2) - \frac{\sqrt{3}}{2}(r_2r_4 - r_3r_4 + r_1r_5 - r_3r_5 + r_1r_6 - r_2r_6) = -\frac{1}{24}$$

This equations reduce in to three equations (A.43),(A.44) and (A.45) as expected, and since we have four free parameters this is an indication that we have a continuous solutions.

$$(A.43)\qquad r_7^2 + r_8^2 = \frac{1}{12}$$

$$(A.44)\qquad r_2r_4 - r_3r_4 + r_1r_5 - r_3r_5 + r_1r_6 - r_2r_6 = 0$$

$$(A.45)\qquad r_1r_2 + r_2r_3 + r_1r_3 - (r_4r_5 + r_5r_6 - r_4r_6) = 0$$

The three equations together with equations (A.35) and (A.36) define the fiducial vectors in the Gell-Mann space. The first trivial solutions to the three equations are the sets $\{r_1, 0, 0, r_4, 0, 0, r_7, r_8\}$,
$\{0, r_2, 0, r_5, 0, r_7, r_8\}$ and $\{0, 0, r_3, 0, 0, r_6, r_7, r_8\}$, and by applying equations (A.35) and (A.36) we get the following solutions.

$$\{\begin{pmatrix}\frac{\cos\theta}{2}\\0\\0\\\frac{\sin\theta}{2}\\0\\0\\0\\\frac{1}{\sqrt{12}}\end{pmatrix},\begin{pmatrix}0\\\frac{\cos\theta}{2}\\0\\0\\\frac{\sin\theta}{2}\\0\\\frac{1}{4}\\-\frac{1}{4\sqrt{3}}\end{pmatrix},\begin{pmatrix}0\\0\\\frac{\cos\theta}{2}\\0\\0\\\frac{\sin\theta}{2}\\-\frac{1}{4}\\-\frac{1}{4\sqrt{3}}\end{pmatrix}\} \tag{A.46}$$

We then use a little trick to get the other fiducial solutions. Note that the operators X and Z are equivalent up to a unitary operator, and the fact that all three circles above are generated by phase operators. This indicates to the existence of more solutions. We calculate the additional solutions by a change of basis to the basis of X.

$$\{\begin{pmatrix}\frac{1}{12}-\frac{\cos\theta}{6}\\\frac{1}{12}+\frac{\cos\theta}{12}+\frac{\sin\theta}{4\sqrt{3}}\\\frac{1}{12}+\frac{\cos\theta}{12}-\frac{\sin\theta}{4\sqrt{3}}\\-\frac{1}{4\sqrt{3}}+\frac{\cos\theta}{2\sqrt{3}}\\\frac{1}{4\sqrt{3}}+\frac{\cos\theta}{4\sqrt{3}}+\frac{\sin\theta}{4}\\-\frac{1}{4\sqrt{3}}-\frac{\cos\theta}{4\sqrt{3}}+\frac{\sin\theta}{4}\\\frac{\sin\theta}{2\sqrt{3}}\\-\frac{\cos\theta}{2\sqrt{3}}\end{pmatrix},\begin{pmatrix}\frac{1}{12}-\frac{\cos\theta}{6}\\\frac{1}{12}+\frac{\cos\theta}{12}-\frac{\sin\theta}{4\sqrt{3}}\\\frac{1}{12}+\frac{\cos\theta}{12}+\frac{\sin\theta}{4\sqrt{3}}\\\frac{1}{4\sqrt{3}}-\frac{\cos\theta}{2\sqrt{3}}\\-\frac{1}{4\sqrt{3}}-\frac{\cos\theta}{4\sqrt{3}}+\frac{\sin\theta}{4}\\\frac{1}{4\sqrt{3}}+\frac{\cos\theta}{4\sqrt{3}}+\frac{\sin\theta}{4}\\-\frac{\sin\theta}{2\sqrt{3}}\\-\frac{\cos\theta}{2\sqrt{3}}\end{pmatrix},\begin{pmatrix}-\frac{1}{6}-\frac{\cos\theta}{6}\\-\frac{1}{6}+\frac{\cos\theta}{12}-\frac{\sin\theta}{4\sqrt{3}}\\-\frac{1}{6}+\frac{\cos\theta}{12}+\frac{\sin\theta}{4\sqrt{3}}\\-\frac{\cos\theta}{2\sqrt{3}}\\-\frac{\cos\theta}{4\sqrt{3}}+\frac{\sin\theta}{4}\\\frac{\cos\theta}{4\sqrt{3}}+\frac{\sin\theta}{4}\\-\frac{\sin\theta}{2\sqrt{3}}\\-\frac{\cos\theta}{2\sqrt{3}}\end{pmatrix}\} \tag{A.47}$$

This six continuous solutions contain the entire fiducial vectors in dimension three in agreement with **?**. Note that the the thee first three solutions have intersections with each with each of the second three solutions, showing that the fiducial vectors form a connected subspace.

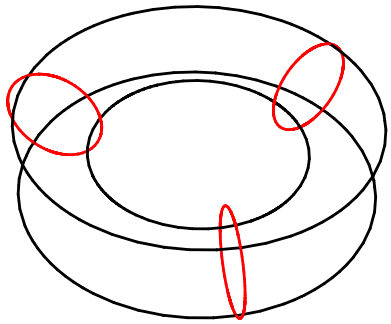

Figure A.2 The geometry of fiducial vectors in dimension three. the colors correspond to the two sets (A.46) and (A.47).

Fiducial Vectors in Dimension 4

Similar to dimension three, we can calculate the fiducial solutions in dimension four by using the W-H group. We have fifteen equations and six variables, but for a fiducial solution the equations reduce to six and we end up with a finite set of SIC solutions.

The W-H group in dimension four is generated by the phase shift operator $Z = |k\rangle\langle k|e^{i\frac{\pi k}{2}}$ and the shift operator $X = |k+1\rangle\langle k|$. The Weyl-Heisenberg group elements are defined as $\hat{D}_{\boldsymbol{p}} = \tau^{p_1 p_2} X^{p_1} Z^{p_2}$ up to phase equivalency. Lets consider the unit vector $|\psi\rangle = [z_0, z_1, z_2, z_3]$. If the vector is a fiducial vector, then for all $\boldsymbol{p}$ we have $|\langle\psi|\hat{D}_{\boldsymbol{p}}|\psi\rangle|^2 = \frac{1}{5}$.

Starting with the equations $|\langle\psi|Z^k|\psi\rangle|^2 = \frac{1}{5}$. In its diagonal basis the operators Z^k is presented as follows.

(A.48)
$$Z^k = \begin{bmatrix} 1 & 0 & 0 & 0 \\ 0 & e^{i\frac{\pi k}{2}} & 0 & \\ 0 & 0 & e^{i\pi k} & 0 \\ 0 & 0 & 0 & e^{i\frac{\pi 3k}{2}} \end{bmatrix}$$

Then the corresponding square of the expectation value of Z^k gives us three equations for each k.

$$|\langle\psi|Z^k|\psi\rangle|^2 = \left||z_0|^2 + e^{i\frac{\pi k}{2}}|z_1|^2 + e^{i\pi k}|z_2|^2 + e^{i\frac{\pi 3k}{2}}|z_3|^2\right|^2 = \frac{1}{5}, k \in \{1,2,3\} \tag{A.49}$$

After expanding equation (A.49), we solve for $|z_k|$ with a parameter χ. Here we only take the positive values of the solutions since any phase information will be included in to the phases of the vectors.

$$|z_0| = \sqrt{\frac{1}{4}\left(1+\frac{1}{\sqrt{5}}\right) + \frac{1}{2\sqrt{5}}\cos(\chi)} \tag{A.50}$$

$$|z_1| = \sqrt{\frac{1}{4}\left(1-\frac{1}{\sqrt{5}}\right) + \frac{1}{2\sqrt{5}}\sin(\chi)} \tag{A.51}$$

$$|z_2| = \sqrt{\frac{1}{4}\left(1+\frac{1}{\sqrt{5}}\right) - \frac{1}{2\sqrt{5}}\cos(\chi)} \tag{A.52}$$

$$|z_3| = \sqrt{\frac{1}{4}\left(1-\frac{1}{\sqrt{5}}\right) - \frac{1}{2\sqrt{5}}\sin(\chi)} \tag{A.53}$$

At this point we have to apply the X operator in our equations, but which ones of the equations should we solve? We approached this by noting that the number of must drop to six in order to find a solution. I.e. there must be some symmetries in the equations that would reduce the number of equations. With this idea we reduce our equations to three, $|\langle\psi|\hat{D}_{10}|\psi\rangle|^2 = \frac{1}{5}$,$|\langle\psi|\hat{D}_{11}|\psi\rangle|^2 = \frac{1}{5}$ and $|\langle\psi|\hat{D}_{22}|\psi\rangle|^2 = \frac{1}{5}$ Where $|\psi\rangle = [|z_0|, |z_1|e^{i\phi_1}, |z_2|e^{i\phi_2}, -i|z_3|e^{i\phi_1}]$. Finding the solution is a matter of finding the correct χ so the lines expressed by the three equations intersect at a single point as shown on figure A.3.

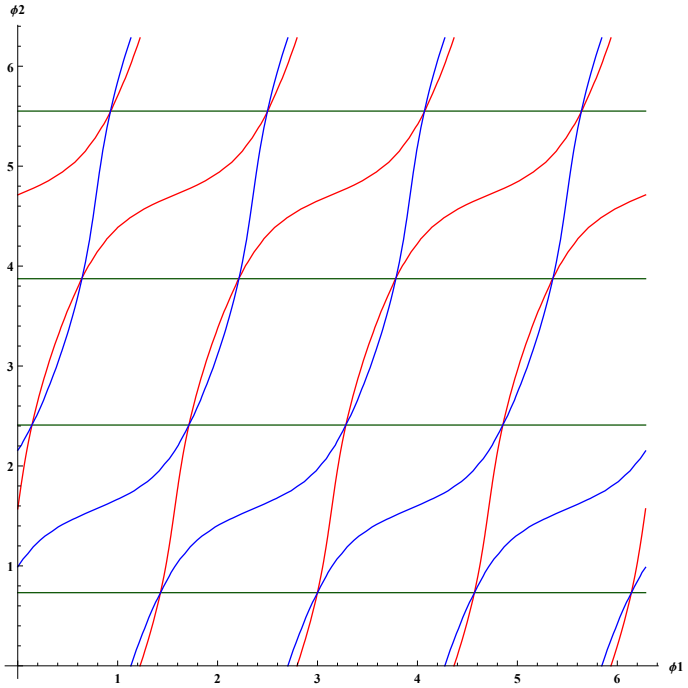

Figure A.3 plots of $|\langle\psi|\hat{D}_{10}|\psi\rangle|^2 = \frac{1}{5}$,$|\langle\psi|\hat{D}_{11}|\psi\rangle|^2 = \frac{1}{5}$ and $|\langle\psi|\hat{D}_{22}|\psi\rangle|^2 = \frac{1}{5}$ equations. Each intersection represents a solution.

After solving the three equations arrive at a single solution for $\chi = \arccos\frac{\sqrt{1+\sqrt{5}}}{2}$, and 4 solutions for ϕ_2 and 16 solutions for ϕ_1, thereby finding all the intersection points on figure A.3.

$$|z_0| = \frac{1}{2}\sqrt{\sqrt{\frac{1}{5}+\frac{1}{\sqrt{5}}}+\frac{1}{\sqrt{5}}+1} \tag{A.54}$$

$$|z_1| = \frac{1}{2}\sqrt{\sqrt{\frac{3}{5}-\frac{1}{\sqrt{5}}}-\frac{1}{\sqrt{5}}+1} \tag{A.55}$$

$$|z_2| = \frac{1}{2}\sqrt{-\sqrt{\frac{1}{5}+\frac{1}{\sqrt{5}}}+\frac{1}{\sqrt{5}}+1} \tag{A.56}$$

$$|z_3| = \frac{1}{2}\sqrt{\frac{1}{5}(-\sqrt{15-5\sqrt{5}}-\sqrt{5}+5)} \tag{A.57}$$

$$\phi_2 = \frac{1}{2}\cos^{-1}\left(\frac{3-\sqrt{5}}{5+\sqrt{5}}\right) \tag{A.58}$$

$$\phi_1 = \frac{1}{2}\tan^{-1}\left(\frac{\sqrt{5+3\sqrt{5}}-2\sqrt{5+2\sqrt{5}}}{\sqrt{4\sqrt{55+25\sqrt{5}}+9\sqrt{5}+25}}\right)+k\pi,\ k=\{0,1,2,3\}$$

$$\text{(A.59)}\quad \phi_2 = \pi - \frac{1}{2}\cos^{-1}\left(\frac{3-\sqrt{5}}{5+\sqrt{5}}\right)$$
$$\phi_1 = \frac{1}{2}\tan^{-1}\left(-\frac{(1+\sqrt{5})(\sqrt{\sqrt{5}-1}-2)}{2\sqrt{2(2\sqrt{2(2+\sqrt{5})}+\sqrt{5}+4)}}\right)+k\pi,\ k=\{0,1,2,3\}$$

$$\text{(A.60)}\quad \phi_2 = \pi + \frac{1}{2}\cos^{-1}\left(\frac{3-\sqrt{5}}{5+\sqrt{5}}\right)$$
$$\phi_1 = \frac{1}{2}\tan^{-1}\left(-\frac{\sqrt{1+\sqrt{5}}+\sqrt{5}-1}{\sqrt{\sqrt{5}-1}-2}\right)+k\pi,\ k=\{0,1,2,3\}$$

$$\text{(A.61)}\quad \phi_2 = 2\pi - \frac{1}{2}\cos^{-1}\left(\frac{3-\sqrt{5}}{5+\sqrt{5}}\right)$$
$$\phi_1 = \frac{1}{2}\tan^{-1}\left(-\frac{\sqrt{5(\sqrt{5}-1)}+3\sqrt{5}-5}{\sqrt{10-20\sqrt{5\sqrt{5}-11}}}\right)+k\pi,\ k=\{0,1,2,3\}$$

And Finally, the numerical values of the sixteen fiducial vectors is presented bellow.

(A.62)

$$\begin{pmatrix}
0.750285 & 0.06891+0.480799i & 0.298029+0.268063i & 0.199154-0.0285434i \\
0.750285 & -0.480799+0.06891i & 0.298029+0.268063i & 0.0285434+0.199154i \\
0.750285 & -0.06891-0.480799i & 0.298029+0.268063i & -0.199154+0.0285434i \\
0.750285 & 0.480799-0.06891i & 0.298029+0.268063i & -0.0285434-0.199154i \\
0.750285 & 0.480799+0.06891i & -0.298029+0.268063i & 0.0285434-0.199154i \\
0.750285 & 0.06891-0.480799i & -0.298029+0.268063i & -0.199154-0.0285434i \\
0.750285 & -0.06891+0.480799i & -0.298029+0.268063i & 0.199154+0.0285434i \\
0.750285 & -0.480799-0.06891i & -0.298029+0.268063i & -0.0285434+0.199154i \\
0.750285 & -0.29125+0.388703i & -0.298029-0.268063i & 0.161006+0.12064i \\
0.750285 & 0.388703+0.29125i & -0.298029-0.268063i & 0.12064-0.161006i \\
0.750285 & -0.388703-0.29125i & -0.298029-0.268063i & -0.12064+0.161006i \\
0.750285 & 0.29125-0.388703i & -0.298029-0.268063i & -0.161006-0.12064i \\
0.750285 & 0.29125+0.388703i & 0.298029-0.268063i & 0.161006-0.12064i \\
0.750285 & -0.388703+0.29125i & 0.298029-0.268063i & 0.12064+0.161006i \\
0.750285 & -0.29125-0.388703i & 0.298029-0.268063i & -0.161006+0.12064i \\
0.750285 & 0.388703-0.29125i & 0.298029-0.268063i & -0.12064-0.161006i
\end{pmatrix}$$

Generating Set of D=6

The generating set of the Gram matrix in dimension 7 is given below.

(A.63)

$$\{0, 0.00813836, 0.0446798, 0.0626793, 0.136054, 0.167773, 0.188038, 0.204613, 0.219766, 0.290583, 0.295695, 0.366512, 0.413095, 0.418499, 0.503337, 0.634103, 0.668086, 0.680387, 0.717227, 0.720073, 0.788044, 0.790891, 0.866819, 0.876862, 0.913701, 0.984518, 1.00252, 1.02106, 1.07049, 1.10988, 1.21753, 1.34034, 1.37717, 1.41371, 1.42631, 1.49998, 1.5708, 1.65677, 1.681, 1.7987, 1.83524, 1.91402, 1.92662, 1.95834, 2.03172, 2.0657, 2.0711, 2.08626, 2.12309, 2.26217, 2.29901, 2.42152, 2.70396, 2.92183, 2.95355, 3.0081, 3.27509, 3.32963, 3.36136, 3.57922, 3.86167, 3.98418, 4.02102, 4.16009, 4.19693, 4.21208, 4.21749, 4.25147, 4.32484, 4.35656, 4.36917, 4.44794, 4.48448, 4.60218, 4.62642, 4.71239, 4.78321, 4.85688, 4.86948, 4.90602, 4.94285, 5.06565, 5.17331, 5.2127, 5.26213, 5.28067, 5.29867, 5.36948, 5.40632, 5.41637, 5.49229, 5.49514, 5.56311, 5.56596, 5.6028, 5.6151, 5.64908, 5.77985, 5.86469, 5.87009, 5.91667, 5.98749, 5.9926, 6.06342, 6.07857, 6.09515, 6.11541, 6.14713, 6.22051, 6.23851, 6.27505\}$$

The corresponding frequency is given below.

(A.64)

$$\{106, 18, 36, 9, 18, 9, 36, 9, 9, 9, 9, 3, 9, 18, 9, 9, 18, 9, 9, 36, 18, 9, 18, 9, 9, 9, 9, 9, 36, 3, 18, 18, 9, 9, 9, 18, 9, 3, 9, 9, 9, 9, 9, 18, 9, 3, 9, 9, 9, 9, 9, 18, 9, 18, 21, 21, 9, 3, 3, 9, 18, 9, 9, 9, 12, 12, 9, 12, 9, 18, 9, 12, 18, 9, 3, 9, 9, 9, 9, 1, 9, 9, 9, 9, 18, 1, 9, 9, 18, 9, 18, 3, 3, 9, 9, 3, 3, 3, 9, 9, 18, 3, 18, 9, 9, 9, 3, 3, 3, 3, 3\}$$

Generating Set of D=7

The generating set of the Gram matrix in dimension 7 is given below.

(A.65)

$$\{0, 0.0262707, 0.0371246, 0.0785547, 0.0916918, 0.0965666, 0.112387, 0.122846, 0.143147,$$
$$0.177678, 0.193142, 0.20097, 0.216661, 0.24742, 0.26626, 0.266655, 0.293199, 0.331247,$$
$$0.336556, 0.367239, 0.368539, 0.396932, 0.401543, 0.41468, 0.415772, 0.417233, 0.429441,$$
$$0.436073, 0.456374, 0.481825, 0.486976, 0.585191, 0.592631, 0.605334, 0.610642, 0.630943,$$
$$0.633232, 0.652073, 0.657223, 0.679043, 0.688766, 0.704456, 0.716665, 0.73046, 0.73415,$$
$$0.746357, 0.760154, 0.773291, 0.774751, 0.858184, 0.871327, 0.878485, 0.884728, 0.903568,$$
$$0.908178, 0.910732, 0.923869, 0.934722, 0.949451, 0.976153, 0.98929, 0.993742, 0.994165,$$
$$1.02191, 1.06474, 1.14026, 1.14312, 1.14502, 1.16425, 1.18986, 1.1908, 1.20257, 1.23455,$$
$$1.2517, 1.2543, 1.28644, 1.30822, 1.31228, 1.33882, 1.36575, 1.39365, 1.42481, 1.42796,$$
$$1.45825, 1.45864, 1.46395, 1.47894, 1.50293, 1.50824, 1.52854, 1.52894, 1.53083, 1.64396,$$
$$1.65965, 1.71664, 1.75847, 1.78233, 1.78462, 1.80117, 1.80807, 1.82147, 1.83193, 1.86805,$$
$$1.89134, 1.97613, 1.99617, 2.00174, 2.00403, 2.03557, 2.03786, 2.1076, 2.11145, 2.16558,$$
$$2.19213, 2.23642, 2.25157, 2.25672, 2.32425, 2.47613, 2.48625, 2.54965, 2.55535, 2.55724,$$
$$2.58216, 2.61424, 2.65338, 2.67966, 2.70566, 2.85624, 2.87047, 2.98506, 3.29813, 3.41271,$$
$$3.42694, 3.57752, 3.60353, 3.62981, 3.66895, 3.70103, 3.72594, 3.72784, 3.73354, 3.79693,$$
$$3.80705, 3.95893, 4.02646, 4.03162, 4.04677, 4.09106, 4.1176, 4.17173, 4.17558, 4.24532,$$
$$4.24761, 4.27916, 4.28145, 4.28702, 4.30706, 4.39185, 4.41514, 4.45126, 4.46172, 4.47512,$$
$$4.48202, 4.49857, 4.50086, 4.52472, 4.56654, 4.62354, 4.63923, 4.75236, 4.75425, 4.75464,$$
$$4.77495, 4.78025, 4.80424, 4.81924, 4.82454, 4.82494, 4.85523, 4.85838, 4.88953, 4.91743,$$
$$4.94436, 4.97091, 4.97497, 4.99675, 5.02889, 5.03149, 5.04864, 5.08062, 5.09239, 5.09332,$$
$$5.11893, 5.13817, 5.14006, 5.14292, 5.21845, 5.26128, 5.28902, 5.28944, 5.2939, 5.30703,$$
$$5.33373, 5.34846, 5.35932, 5.37245, 5.37501, 5.37962, 5.39846, 5.4047, 5.41186, 5.425, 5.50843,$$
$$5.50989, 5.52303, 5.53683, 5.54904, 5.55272, 5.56652, 5.57873, 5.59442, 5.60414, 5.62596,$$
$$5.63111, 5.64995, 5.65224, 5.67254, 5.67785, 5.69055, 5.69799, 5.79621, 5.80136, 5.82681,$$
$$5.84711, 5.85374, 5.86595, 5.86741, 5.86851, 5.88164, 5.88625, 5.91465, 5.91595, 5.94663,$$
$$5.95194, 5.98999, 6.01653, 6.01693, 6.03576, 6.06652, 6.08222, 6.09004, 6.10551, 6.14004,$$
$$6.16034, 6.1708, 6.18662, 6.19149, 6.20463, 6.24606, 6.25691\}$$

The corresponding frequency is given below.

$$\{145,9,9,9,45,9,9,9,9,9,9,9,9,9,9,9,9,9,9,9,9,9,9,9,9,9,9,9,3,9,$$
$$9,9,9,9,9,9,9,9,9,9,3,9,9,9,9,9,9,9,9,9,9,9,45,9,9,9,9,9,9,9,9,9,9,$$
$$9,9,9,9,9,9,9,9,9,3,9,9,9,9,9,9,9,9,9,9,3,9,9,9,9,9,9,3,9,9,9,9,9,9,$$
$$9,9,9,9,9,9,9,9,9,9,9,9,9,9,9,9,9,3,9,9,9,9,9,9,9,9,9,9,9,9,9,9,9,$$
$$9,9,9,9,9,3,9,9,9,9,3,9,9,9,9,9,9,3,9,9,9,9,9,9,9,9,9,9,9,9,9,9,3,$$
$$9,9,9,9,9,9,9,9,9,9,9,9,9,9,9,9,9,6,9,9,9,9,9,9,9,3,9,9,9,9,9,9,9,$$
$$9,9,9,9,9,9,3,9,3,9,9,9,9,9,9,9,9,9,3,9,9,9,9,9,9,9,3,3,9,9,9,9,9,$$
$$9,9,6,9,9,9,9,6,9,9,9,9,6,9,9,9,9,3,3,9,3,3,3,9,3,3,3\} \tag{A.66}$$